Deltares

Rapid assessment study on the Geul river basin

Appendices with background material

With contributions from:

TUDelft   RWTH AACHEN UNIVERSITY   KU LEUVEN   LUXEMBOURG INSTITUTE OF SCIENCE AND TECHNOLOGY | LIST

This document provides a collection of contributions with background material supporting the main report on therapid assessment study on the Geul river basin. In this study, we assessed the hydrological response of the basin to heavy rainfall, the associated floodings and their consequences in order to find measures that are potentially suitable for the prevention of future floods impacts. We made extensively use of three recently published reports from Klein, Natuurmonumenten and Deltares related to this flood event on the Geul basin and extended this knowledge base with an assessment based on a set of computer flood simulations, covering the entire basin of the Geul river. Further, insights and experiences from different universities in neighboring countries are included, as well. The studies done so far in the Netherlands concentrated on the Dutch part of the Geul basin or on specific interests; with this rapid assessment we focus on the difference between the main Belgian and Dutch basin parts and their contributions to the flood peak discharges observed in the city of Valkenburg a/d Geul.

Appendix 1: Limburg 2021 Research Projects (TU Delft)

Overview of the current student research projects nearing completion considering the Geul (Rutten, M. and J. van der Steen, 2022)

Appendix 2: Extreme discharge estimates for the river Geul (TU Delft)

Memo describing the extreme discharge estimates for the Geul that were made in a larger study focusing on estimating extreme discharges for the Meuse river. (Rongen, G., 2022)

Appendix 3: Land cover assessment Geul catchment (Deltares)

As part of the rapid assessment study on the response of the Geul basin to extreme rainfall (Slager, K., 2022)

Appendix 4: W-flow model setup and runs (Deltares)

Technical model documentation describing hydrological model setup and results (Bouaziz, L., 2022)

Appendix 5: Explanatory hydro-dynamic modelling notes (Deltares)

A short memo describing modelling assumptions and choices and some detailed results (Becker, A. 2022)

Appendix 6: Overview of flood protection measures in Cologne district (RWTH Aachen)

Technical appendix report by IWW at RWTH Aachen University (Klopries, 2022)

Appendix 7: Hydrological assessment on upper Geul basin: comparison between model results and explanatory notes on potential floodplain storage (KU Leuven)

Rapid assessment of the July 2021 flood for the Geul basin. (Moustakas and Willems, 2022)

2   Appendix 1: Limburg 2021 Research Projects (TU Delft)

Overview of the current student research projects nearing completion considering the Geul (Rutten, M. and J. van der Steen, 2022)
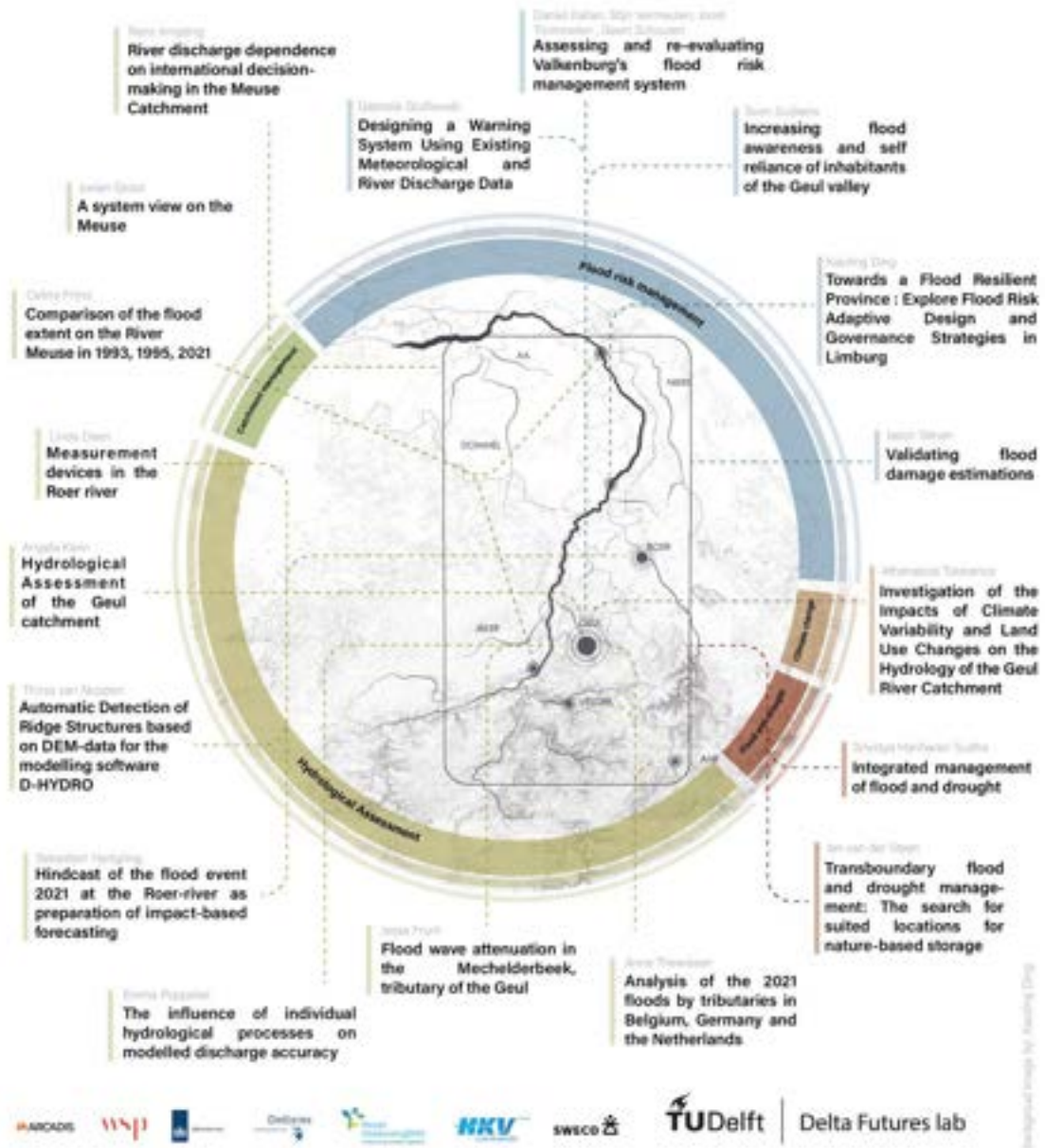
Limburg 2021 - Research Projects

Overview of current student research projects nearing completion considering the Geul.
Martine Rutten and Jan van der Steen, June 2022

Limburg 2021

In July 2021, large areas in Western Europe were hit by extreme rainfall. For example, in the Geul catchment, maximum precipitation amounts of up to 180 mm were recorded. The Waterboard of Limburg estimated that the damage was around 1.8 billion euros in the Netherlands, while the total international damage is more than tenfold that amount. The thematic working group Limburg 2021 of the Delta Futures Lab in Delft works on a variety of research topics to add to the knowledge about the event and to investigate how such large damages can be avoided in case of future events. These investigations include topics on flood risk management, climate change, flood damage estimates, hydrological assessments of several areas, and a comparison of the effects of this flood to the effects of historic events.

River discharge dependence on international decision-making in the Meuse Catchment

Assessing and re-evaluating Valkenburg's flood risk management system

Designing a Warning System Using Existing Meteorological and River Discharge Data

Increasing flood awareness and self reliance of inhabitants of the Geul valley

A system view on the Meuse

Towards a Flood Resilient Province : Explore Flood Risk Adaptive Design and Governance Strategies in Limburg

Comparison of the flood extent on the River Meuse in 1993, 1995, 2021

Validating flood damage estimations

Measurement devices in the Roer river

Hydrological Assessment of the Geul catchment

Investigation of the Impacts of Climate Variability and Land Use Changes on the Hydrology of the Geul River Catchment

Automatic Detection of Ridge Structures based on DEM-data for the modelling software D-HYDRO

Integrated management of flood and drought

Hindcast of the flood event 2021 at the Roer-river as preparation of impact-based forecasting

Transboundary flood and drought management: The search for suited locations for nature-based storage

Flood wave attenuation in the Mechelderbeek, tributary of the Geul

Analysis of the 2021 floods by tributaries in Belgium, Germany and the Netherlands

The influence of individual hydrological processes on modelled discharge accuracy

TUDelft | Delta Futures lab

TUDelft | Delta Futures Lab

Abstract

Introduction

On the front page is an overview of the Delta Futures lab Limburg 2021 research topics.In this memo the projects that are most relevant for the Geul and (almost) finished are summarized according to the research questions of the Rapid Assessment lead by Deltares with the main question.

What can we learn from the July 2021 floods in the Geul river catchment about its hydrological response to heavy rainfall, the associated floodings and their consequences in order to find measures that are potentially suitable to prevent impacts of future floods?

The memo is structured in two sections:

Section I: Geul Characteristics and Climate Change

    i.   *How do the physical characteristics of the Geul river catchment determine its response to heavy rainfall?*

    ii.   *How were the flooded areas at the July 2021 flood event distributed and what were the impacts of the flooding?*

Section 2: Risk Reduction Strategies

    iii.   *What types of measures are potentially suitable and effective at short and long-term to mitigate the (most severe) consequences*

Models Used within the Delta Futures Lab

Angela Klein	WFLOW SBM
Jesse Frunt	ArcMap
Athanasios Tsiokanos	No model, data analysis
Gabriela Godlewski	Delft FEWS (Consisting of HBV model and SOBEK1DFLOW-Rural model) and Coupled SOBEK1D2D model
Sven Suijkens	SOBEK event map of 2021 floods, SSM-2017
Multidisciplinary Project	No hydraulic or hydrological model
Jason Wever	HIS-SSM (Damage model)
Julian Hak	3Di Flood model
Anne Thewissen	WFLOW SBM & lumped HBV model
Thirza van Noppen	D-Hydro
Celina Frijns	Blokkendoos Ruimte voor de Rivier
Sebastian Hartgring	WFLOW SBM + ProMaIDes
Emma Poppelier	WFLOW TOPOFLEX
Rosalie Middendorp	SOBEK1D

Most important findings

Angela Klein - angela.c.klein@gmail.com	What was the hydrologic response of the Geul Catchment to the rainfall event in July 2021?	.During the flood event a significant amount of the rainwater was stored in the soil and thereby the flood peak was reduced. Variations in soil and geology are important in the catchment. Antecedent moisture conditions were important for runoff amount
Anne Thewissen Anne.thewissena@gmail.com	How unique was the flood event of July 2021 in the Ahr, Vesdre and Geul?	Precipitation for all catchments differed significantly (also within the catchment), leading to a different forcing of the hydrological response. The varying geology

TUDelft | Delta Futures Lab

		enhanced this difference, which finally resulted in a wide range of discharges.
Jesse Frunt - jessefrunt@hotmail.com	Calibration, sensitivity analysis and application of a hydrologic model	*Reservoirs seem to be dimensioned and used correctly. With larger return periods, there seems potential to optimize the operation e.g. choose a later inflow moment in order to reduce the discharge peak.*
Athanasios Tsiokanos - atsiokanos96@gmail.com	Investigation of the Impacts of Climate Variability and Land Use Changes on the Hydrology of the Geul River Catchment	*There is a strong relation between precipitation increases and discharge increases over the last 30 years, especially in summer. No significant relations between land use changes and discharge could be found over the same period, yet this could partly be due to the coarse resolution of the land use data set.*
Sven Suijkens - svensuijkens@gmail.com	Flood risk reduction capacity of resilience measures in regional systems in The Netherlands	*Dry-proofing houses most at risk is effective. It can reduce the flood risk by 25 - 45 percent with different dry-proofing rates and is effective at low percentages of application (e.g. dry-proofing 20% of the houses most at risk cost-efficiently reduces risk 25-32%) Wet-proofing possible as build-back-better measure.*
Gabriela Godlewski - Gabgodlewski@gmail.com	Improvement of the Flood Early Warning System and for Valkenburg along the Geul River	*By including 2D effects in the SOBEK model under FEWS flood peaks can be adequately reproduced. The Flood Early Warning System (FEWS) application can help to reduce damages significantly by assisting evacuation decision making.*
Multidisciplinary Project - joosttrommelen@hotmail.com	Assessing and redesigning Valkenburg's flood risk management system	*Quick assessment of measures in Valkenburg directy after the floods Conclusion was that different combinations of measures possible to increase safety level in the Geul at different prices with most solutions ranging from 0.2 million to 50 million euros. Measures range from heightening of quay walls to increase discharge capacity, installing a flood tunnel and installing flat or movable bridges.*

TUDelft | Delta Futures Lab

Section I: Geul Characteristics and Climate Change

Angela Klein - Sweco: What was the hydrologic response of the Geul Catchment to the rainfall event in July 2021?

Angela's work focussed on determining the hydrologic response of the Geul catchment to the precipitation event of the summer of 2021. The Geul is an atypical catchment for the Netherlands as there is an average slope of 3% and elevation ranges from 50 – 400 meters.

In her research, she used data from rainfall stations (13), discharge stations (10) and groundwater wells (19) and uses these measurements in a WFlow SBM model. In this model, the topography is the most dominant factor and vertical flows may be better represented than vertical flows. In addition, deeper surface flows (>2 meters) are not represented well. In order to make a better model of the precipitation event, soil thickness and lateral connectivity were modified compared to the standard model setup.

During the 2021 the precipitation event showed great heterogeneity. This caused return periods to vary significantly in the catchment. Discharge return periods range from 50 years to 500 years, precipitation ranges from 2 to 1000 years. This is depicted in Figure 1 for 48 hours accumulations.

From analysis of the discharge data during the flood event, three peaks in the can be identified; the 13th at 17:00, and the 14th on 08:00 and 13:00. The first peak originated mostly from the lower part of the catchment whilst the latter peaks originated mostly from the upper part. During the event, the catchment showed different runoff behaviour than usually. The prior saturation of the soil has likely influenced the discharge-runoff behaviour. Measurements from the event can be problematic, however, it seems that 60% of the discharge in Gulpen originated from Belgium

Despite the small spatial scale of the catchment, there is a wide variety of hydrologic response. These differences are especially noticeable between the Dutch and Belgium parts of the catchment and in smaller tributaries.

In the 4 weeks prior to the event there was, on average, 50% more precipitation than usual. An average soil saturation could possibly have reduced peak discharge by 30% and could have stored an additional 4.2 million cubic meters of water.

Figure 1: Geul Catchment precipitation and discharge return periods for 48 hour accumulation

Subcatchment	Event RC [%]	Longterm RC [%]
Kelmis	45	39
Sippenaeken	41	39
Eyserbeek	23	15
Gulp	21	31
Meerssen	32	32

Table 1: Runoff coefficients during the 2021 flood event and longterm

Relatively the Geul contributed more than usual to the discharge downstream. Usually the contribution of the Geul is 60-72% (depending on the season). During the 14th this the discharge contribution of the Geul was 76%. This increase seems correlated to the soil saturation. Angela also showed that urbanisation adds to the flashiness of flood peaks, but that every catchment shows different sensitivity to land-use change.
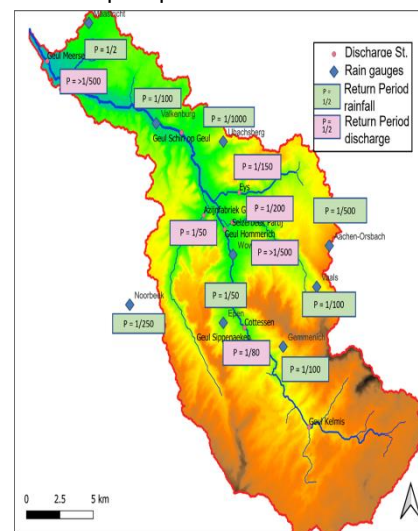
TUDelft | Delta Futures Lab

Angela concludes that the role of (hydro-)geology cannot be underestimated as the tributaries show different behaviour than the main branch of the Geul, that a high contribution to the flood peak originated from the Belgian part of the catchment and that land-use plays a secondary role compared to geology.

In addition she states that the catchment has a high storage capacity despite the loess soil type and that the impact of antecedent conditions to the hydrologic response is significant.
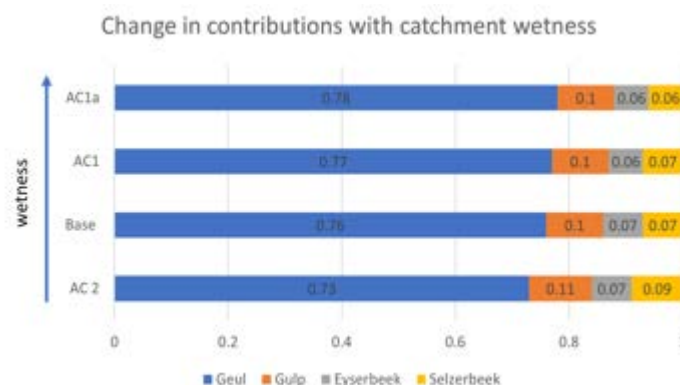

Figure 2: Change in contributions from different tributaries for different antecedent moisture conditions

Anne Thewissen – Uniqueness of flood event of July 2021 in Western Europe

The goal of researching flood events is to understand the hydrological and hydraulic behaviour under extreme conditions. Only then can adequate measures be designed and implemented. But not all catchments respond the same and not all storm events trigger the same behaviour. Whether behaviour of the water is general or not has a great influence on the efficiency and feasibility of measures. Anne compares flow behaviour in both space and time to provide a possible base of generalization. In space, the three most critical catchments of Germany (Ahr), Belgium (Vesdre) and the Netherlands (Geul) are compared. The forcing, response and flow mechanisms are analysed for both the flood event and normal conditions. As such, Anne seeks to identify how unique this flood event was for each catchment and at the same time see if the local differences are limited enough to generalize conclusions from smaller case studies. Transboundary research adds value as this is not often done due to its complications with language and data access.

The conditions of the forcing, namely the cold core low with humid air inflow, was a unique situation. The return periods of both the resulting forcing and response were high, between 100 and 1000 years. However, due to limited record periods the uncertainty of such high return periods increases considerably. The inclusion of reconstructed historical floods would help to lengthen the reference period. Mostly, it would prevent the forgetting of large flood events and thus the overestimation of the return period. For the Ahr, a return period of the peak discharge of 1000 to 10 000 years was predicted even though similar discharges have been reconstructed for two flood events in the past two centuries. Not only return periods, but also the insight in the timing of floods would benefit from including historical events as it can be shown for both the Vesdre and the Ahr that summer floods are not unique.

Event runoff coefficients provide important insight in the hydrological behaviour. Low values indicates high infiltration and groundwater flow, which was the case for the Geul with values between 0.25 and 0.6. This could be explained by the permeable chalk soils. High runoff coefficients point to overland flow and little storage, as was the case for the Ahr and the Vesdre (values between 0.6 and 0.9). This behaviour was probably enforced by the thin soils and steep valleys, both reducing storage capacity. Additionally, both catchments received considerably more rain than the Geul, hence the much larger discharges and higher damage. According to radar data (resp. RADOLAN, REGNIE, KNMI Reanalysis) the total precipitation volume for the Ahr, Vesdre and Geul were respectively 127, 90 and 47 $[m^3*10^6]$. In comparison, the estimated peak discharges for the outlets are around 1000, 600, 100 $[m^3/s]$. Not just the magnitude of the discharge time series differs considerably, also the shape varies. More gradient in the landscape leads to a narrow hydrograph (the Ahr has a much more narrow hydrograph than the Vesdre and the Geul). A narrow hydrograph points to flash flood behaviour, but due to unclear quantitative conditions, it is difficult to define the floods as such.

The exact flow paths are to be analysed with two models (1 lumped and simple, 1 complex and distributed), but these results are not yet conclusive. For now, it seems that the relief and geology play an important role in spatially varying behaviours.

Data of such extreme events is often limited due to damages or measurement setups meant for normal flows. This data limitation also includes the uncertainty of measured data. Estimations have been by multiple reports

5

TUDelft | Delta Futures Lab

with multiple methods, but the results vary strongly and only provide an order of magnitude. Any conclusions must be treated with care. More focus on the observation of extreme events is recommended.

For now, it is clear that the precipitation for all catchments differed significantly (also within the catchment), leading to a different forcing of the hydrological response. The varying geology enhanced this difference, which finally resulted in a wide range of discharges. Nevertheless, for each catchment this flood event was an extreme case. Both precipitation amounts (especially for longer periods), discharges and water levels were unique for most locations compared to measurements. The flood event of 2021 proves that these smaller tributaries of the large rivers require more attention in flood risk management by using a local approach that is specifically aimed to their hydrological and hydraulic behaviour. We have been reminded of the dangers of small and fast-responding catchments, now is the time to learn from these unique responses and prepare for future events.

Jesse Frunt - **Calibration, sensitivity analysis and application of a hydrologic model (WSP commissioned by Water Authority Limburg)**

During his internship, Jesse Frunt worked with an ArcGis tool called ArcMap. This tool is developed by WSP. The tool models the surface runoff in 5-minute increments and can do this for multiple rainfall durations and intensities. This makes it possible to make a hydrograph of the precipitation-discharge behaviour. The model uses a D8 flow direction delineation method to determine the flow in one cell based on the flow directions of the 8 surrounding cells. This method uses the slope to determine the flow direction. After this, it calculates the flow accumulation. This is the area contributing to the flow in that cell. The model bases itself thus on slopes and therefore makes assumptions about processes such as percolation and infiltration and works with simultaneous regulation. In addition, precipitation events are homogenously mapped, both spatially and temporally. The model assumes a saturation soil and no evaporation and transpiration losses. The maximum infiltration speed is assumed to be equal to 1.2 mm/hour. When precipitation intensity exceeds this, it is assumed that the initial infiltration will be 6 mm/5 minutes with a decline of 20% every 5 minutes thereafter. The flow rate is based on the Manning formula; $v = \frac{k}{n} R^{2/3} S^{1/3}$. In this formula roughness coefficients are determined for different types of area. The model is used in Jesse's work in the Melcherbeek valley.

Figure 3: Contributing areas of the Mechelderbeek

The output of this model is used to determine an ideal deployment moment for a rainwater buffer in Vijlen on the Vijlenstraat. The buffer is designed for a return time of 25 years with precipitation lasting 2 hours. The volume of the buffer is approximately 5000 m^3. There is also a reservoir upstream in Groenenweg, which has a volume of 8400 m^3.

Maximum discharge in the Mechelderbeek occurs when all parts of the catchment area contribute to the discharge. As a result, a short (<1 hour) heavy shower does not lead to the highest discharge, but rather a longer precipitation event (>1 hour), such as the precipitation event for which the water buffer is designed. In Figure 2 an example of the discharge of different precipitation events with a recurrence time of 25 years is shown.

The water buffers are normally deployed when the flow rate of the Mechelderbeek is 0.5 m³/s. This appears to be a sensible moment for showers with a return time; it is estimated that the peak discharge can be reduced from 26 $\frac{m^3}{s}$ to 20 m^3/s. For discharges with a longer return time, the water board must evaluate the inflow moment; Here the discharge peak can be most flattened by choosing the inflow point at 5 m^3/s. The effect is shown in Figure 4.
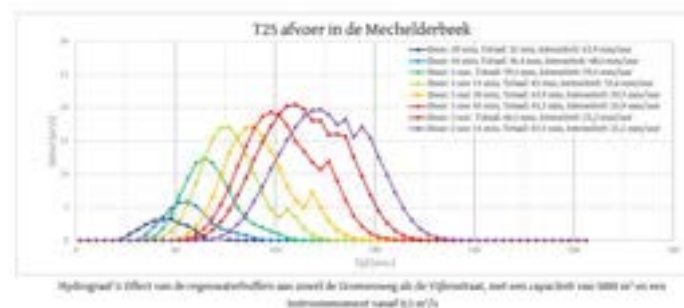
TUDelft | Delta Futures Lab

Figure 3: 25 year return period events and their respective discharge

Figure 4: The discharge as a result of reservoir deployment again with T25 events

**Athanasios Tsiokanos - Investigation of the Impacts of Climate
Variability and Land Use Changes on the Hydrology of the Geul River Catchment (Sweco)**
Athanasios investigated the trends noticeable in historic data in order to find trends in precipitation and discharge related to climate change. He does this annualy and also per season and does this for multiple locations in the Geul river catchment.

Athanasios uses data ranging from 1951-2018 (precipitation), 1965-2021 (evaporation), 1970, 1974 and 1992 (depending on the location) until 2022 (discharge) and 1990-2018 (land-cover). He uses these datasets to find variations in hydrological behaviour (runoff pattern, discharge) and tries to relate those to changes, either in land-use or in climate. In the following section, findings will be presented per category. In the end, conclusions drawn from the research are summarized.

Land-Use
Changes in the land-use are evaluated using CORINE annual land cover maps for the period 1990-2018 from Google Earth Engine (100 meter resolution). Changes in discharge regimes are investigated using a multi-temporal approach in which trends are evaluated in every possible combination
of start and end years. The land use change did not significantly change from 1990 until 2021. The most significant change is the 1% increase in built-up area and the 1.1% decrease in pasture area. Spatially there can be significant land-use changes. In Meerssen, the built-up area increased 20% from 11.4% of the sub catchment to 13.5%. The trend is similar in Selzerbeek.

	Area km² - 1990				Area km² - 2018			
	Built-up	Pasture	Agriculture	Forest	Built-up	Pasture	Agriculture	Forest
Sippenaken	32.6 (26.5%)	45.4 (36.9%)	23.4 (19.1%)	21.5 (17.5%)	33.2 (27.1%)	45.6 (37%)	22.9 (18.6%)	21.2 (17.3%)
Hommerich	0.40 (1.3%)	19.1 (62%)	3.80 (12.4%)	7.54 (24.3%)	0.74 (2.4%)	18.4 (59.7%)	4.20 (13.6%)	7.50 (24.3%)
Meerssen	9.2 (11.4%)	10.3 (12.7%)	54.5 (66.8%)	7.30 (9.0%)	11 (13.5%)	10.0 (12.4%)	52.7 (64.6%)	7.60 (9.5%)
Eyserbeek	4.12 (15.1%)	1.78 (6.6%)	20.9 (77.1%)	0.15 (0.7%)	4.26 (15.9%)	1.35 (5.1%)	21.2 (78.5%)	0.10 (0.4%)
Selzerbeek	2.40 (8.4%)	13.6 (47.3%)	8.2 (28.5%)	4.50 (15.7%)	3.50 (12.2%)	11.5 (40.2%)	9.30 (32.4%)	4.34 (15.2%)
Gulp	5.15 (11.1%)	8.0 (17.4%)	28.7 (62.3%)	3.90 (8.5%)	5.10 (11.2%)	7.25 (15.8%)	29.15 (63.5%)	4.25 (9.3%)

Table 2: Land-Use changes in different subcatchments from 1990 to 2018

Discharge trends
Mixed trends are observed for Meersen. Most of these trends are positive, however, they are not statistically significant. Positive trends are also more frequent for Hommerich, but none of these are significant. Discharge in Gulp seems to be decreasing. Maximum annual discharges are significantly (around 20%) decreasing in Selzerbeek and an insignificant decreasing tendency can be observed in Eys.

(Extreme-) precipitation trends 1951-2021
Temporal changes in (extreme) precipitation regimes for the period 1951-2021 and potential evaporation for the period 1965-2021, are identified by calculating trends for each 30-year moving period within the available time frames. The total precipitation (R_{tot}) shows slightly more upward trends (17.1% increasing and 10.4%

TUDelft | Delta Futures Lab

decreasing), however this. difference is not considerable. Overall, the difference between increasing and decreasing trends is not clearly disproportionate to the increasing side, however strong trends in the most extreme indices are moving towards an upward direction to a greater extent compared to the downward direction. These trends show heterogeneity within different seasons.

Runoff Patterns

Strong positive correlations in are observed between extreme precipitation indices and maximum discharge in the Geul river catchment. The annual maximum discharges thus change at the same rate as extreme precipitation in directions, magnitudes and time frames indicating the variability in high flows is mainly a result of variability in extreme precipitation.

Water balance seperation

Athanasios work also includes the use of a water balance separation framework to estimate the attribution of alternations in mean stream flows to land use and climate changes.

The low value of the length of the vector R (arrow M1-M2 in Figure 5) indicates that the magnitude of the combined changes is relatively small. The proportion of changes in mean discharge flows attributed to LUC and CC is estimated to be 34 and 66%, respectively.

Evaporation

A strong and stable increase in evaporation can be seen between 1965 and 2020 (confidence interval 99%). Approximately this is about 100 mm increase per year. Trends in summer and spring are significant with an increase of 0.87 and 0.7 mm per year respectively. Winter and autumn are increasing at a lower significance level (95 versus 99%) at o.07 and 0.2 mm per year respectively.

Figure 5: Water balance separation

Change Points

Athanasios was able to identify changepoints before and after which the mean of an indicator is roughly the same. He was able to do this for discharge and evaporation. All changepoints occurred roughly at 1990.

Conclusions

 A statistically significant increase in very wet days is reported in the area that mainly derives from the winter period. The extreme summer precipitation shows a relatively strong increase since the 1980s. The trend analysis in the potential evaporation time series suggests a very strong and stable increase. The main land use changes dominated before the 1970s while no significant changes are found between 1990-2018. Extreme discharges show an increasing insignificant tendency while mean flows are generally decreasing.
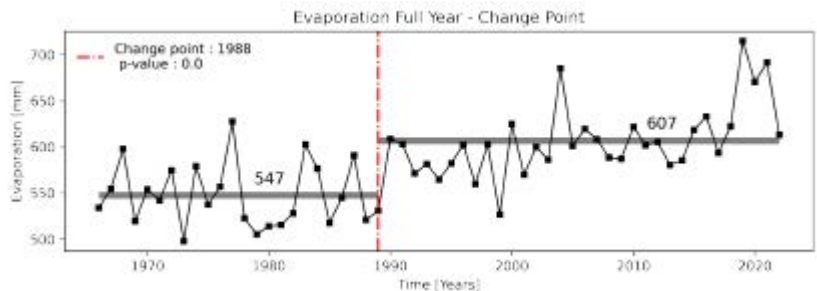

Figure 6: Change point visualization of the evaporation during a full year

Results suggest that the variability of extreme and mean flows is driven mainly by climate variability while at the same time the effects of land use changes in runoff patterns are not visible for the period 1970-2021. This study emphasizes that climate change should be incorporated into flood designs and climate adaptation strategies should be provided.

Section II: Risk Reduction Strategies

TUDelft | Delta Futures Lab

Sven Suijkens - Flood risk reduction capacity of resilience measures in regional systems in The Netherlands (Sweco)

Flood risk management is often focused on flood prevention. A multi-layered safety approach is often too expensive and therefore not cost-effective. Resilience and self-reliance are sometimes underexposed. Resilience is seen here as the quality to prevent, adapt and recover.

Sven is looking at ways to reduce the flood risk. In his work, this is divided into two categories; wet-proofing and dry-proofing. The first concerns the reduction of vulnerability to flooding (use of waterproof materials, adapted interior) and the latter concerns the prevention of inundation of a building. (sandbags, panels, closing of cracks).
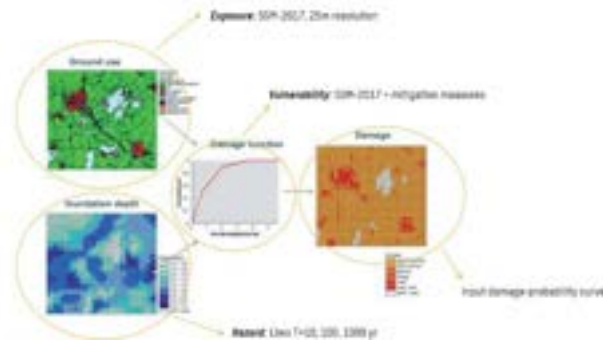
Figure 7: Inputs into damage assessment and the creation of a damage assessment map

Flood risk is defined as hazard x exposure x vulnerability. Combining the three, one can make a damage function and one can map this spatially as well. Sven looked at the effect on risk reduction of dry- and flood-proofing of 20, 40 and 60% of the houses. This is done either randomly or at the houses most at risk. He does this for residential and commercial areas.

In Figure 8, the results of this calculation are shown. It catches the eye that with the dry- and wet-proofing of houses mostly at risk, there is a steep initial risk reduction in the first scenario of 20% floodproofing. The 40%, 60% and even 100% scenarios show a far more gradual risk reduction. It also stands out that the random floodproofing is less effective at a coverage of 60% than floodproofing the 20% houses most at risk : or Residential content category 89% of the risk occurs within the top 40% of locations. This corresponds with 591 houses of the in total 1313 at risk. In general, dry-proofing the houses at the most risk is 3 times as effective as dry-proofing houses at random. The research on effectiveness of random and non-random dry- and wet-proofing originates from the fact that the Water Authority is not willing to communicate to the public which are the houses most at risk. This has legal reasons for the Water Authority.
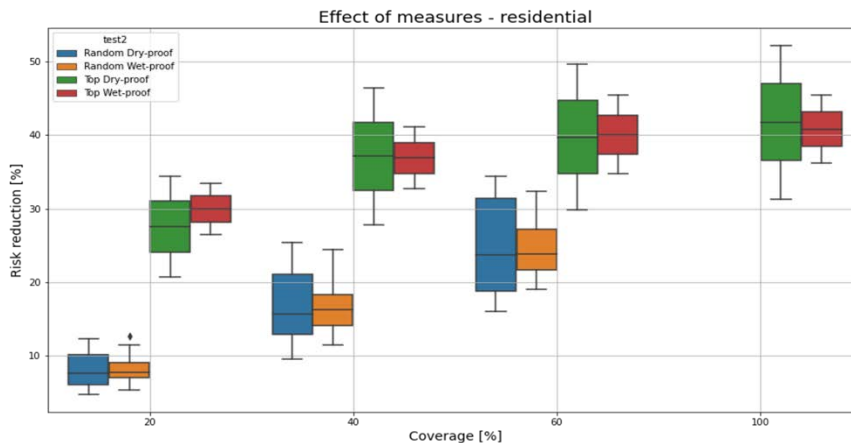

Figure 8: Effects of flood-proofing (wet and dry) at random or at the houses most at risk

When conducting a cost-benefits analysis, it stands out that the dry-proofing is indeed far less effective when applied randomly and that the wet-proofing is not that easily attractive from a CBA perspective.

There are, however two factors that are important to mention in floodproofing; Obviously inundation depth makes a lot of difference for the CBA analysis; One can imagine a floor is ruined at 0.1 meters of water, while other significant damages occur higher on (when the electrical grid of the house is damaged or when the second floor floods). This causes the current damages function to underestimates damages at very low inundation. Therefore, dry-proofing might even be more interesting than initially estimated at low

Table 3: CBA analysis of flood-proofing measures

CBR <1.0 after 65%

Residential cost-benefit ratios per measure

Scenario	Coverage [%]	Dry-proof low	Dry-proof High	Wet-proof low	Wet-proof high
Top	20	1.84	3.07	1.08	1.37
Random	20	0.61	1.44	0.33	0.64
Top	40	1.48	2.47	0.78	0.97
Random	40	0.63	1.44	0.33	0.58
Top	60	1.06	1.77	0.54	0.68
Random	60	0.66	1.39	0.35	0.55
Full	100	0.76	1.26	0.36	0.45

TUDelft | Delta Futures Lab

inundation depths. In addition, the CBA relies on the cost of installing these measures at any time. There is a window of opportunity to wet-proof areas when rebuilding (e.g. use tiles instead of wood as a floor).

Gabriela Godlewski - Improvement of the Flood Early Warning System and for Valkenburg along the Geul River (HKV)

In communities such as Valkenburg, flood early warning systems (FEWS) are emerging as potential non-structural solutions to flooding. FEWS networks are adaptable to different areas depending on the type of disaster they are being designed to warn against. The FEWS for the Geul, though offline at the time of the event, is designed to forecast potential discharges and water levels of the Geul River using meteorological input data.

Figure 9: Geul FEWS workflow

Models under the FEWS shell did not always performed desirably. For the rainy period, the HBV and SOBEK models demonstrated a consistent overestimation in the underflow and total water in the system with each rainfall. For the dry period, the models showed an underestimation in the total water in the system, likely due to lack of water source and also due to evaporation. Gabriela included a 2D model and reanalysed the event. This showed that discharge up to 140 m^3/s flowed through the Geul and its tributaries and an reasonably accurate reproduction of water levels and flood patterns. Without the 2D grid, the SOBEL-Rural 1D predicted a water level of 76.5+ m NAP at Valkenburg Hertenkamp, over 6.5 meters above the expected value. The 70+ m NAP was correctly predicted by the 2D model.

Four precipitation events were chosen to study the effect of soil moisture and the effect of temperature and evaporation on the results. The effect of soil moisture was tested by comparing the discharge and water level results between a simulation using high-frequency precipitation data and a simulation of a precipitation event after a dry season. The effect of temperature and evaporation was tested through the comparison of the results for a precipitation event during the winter, when temperature and evaporation are low, and the summer, when temperature and evaporation are high.
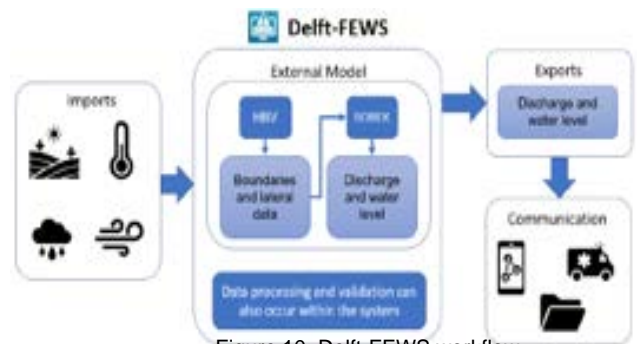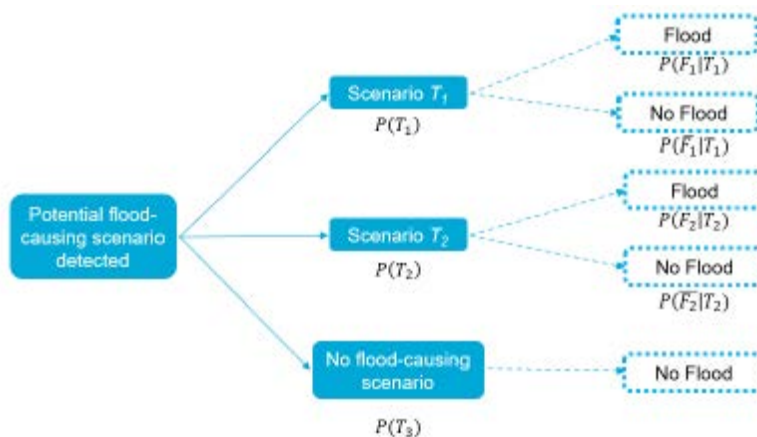

Figure 10: Delft-FEWS workflow

The extents were then inputted into the Damage and Casualties Model (SSM2017) to create a cost-benefit analysis that was used for warning communication decision-making and to determine whether investing into a working and trusted Delft-FEWS system would have a noticeable impact on the damage.

Action is not necessarily free, but steps such as moving valuables to higher elevations have minimal disruption on day-to-day life. This cost is not affected whether or not the flood actually occurs. Preparing for the greater flood T2 costs €230,000 based on the assumptions made, but according to the results of the cost calculations, the reduction in damage costs is equivalent to approximately €26.67 million.

Figure 11: Early Warning decision making

This result suggests that sending a warning may be worthwhile even if the event does not happen because the cost of the money saved in damage reduction is ten times greater than the economic costs of preparation for this event.

What was not reflected in the decision tree or cost-benefit analysis is the consequences of preparation for the wrong event. For example, if a warning is given out for event T1 but event T2 occurs, then then €0 was spent on preparation but €88 million in damages occurred. In the event of over-preparation, where the population prepares for T2 but T1 occurs, then the cost of evacuation as well as the disruption of daily life that comes as a result is not justified. Because the evacuation costs for T1 are 1/10 of the reduction in damage costs for the same event, it can be concluded mathematically that up to nine false alarms are justifiable, but when one takes into consideration the emotional impact of the evacuations and false alarms on the citizens, it can be argued that only one false alarm is the maximum amount.

Using real time simulation, the flood warning could have been given 12 hours prior to the flooding. This is insufficient time for an evacuation. Forecasting could provide an additional 2 days and is therefore necessary. The FEWS could reduce the expected damage by more than 50% but for floods with return periods of 1, 5 and 10 years it is not cost efficient. With floods with a return period of equal to 25 years, no cost efficiency is calculated, however, With increasing flood intensity (return period) cost efficiency increases.

Multidisciplinary Research Project - Assessing and redesigning Valkenburg's flood risk management system (Daniel Kallan, Geert Schouten, Joost Trommelen, Stijn Vermeulen)

This research was conducted shortly after the floods and is added to this memo for completeness. Since than more in depth work is conducted by Deltares and others into solutions for the flood management system.

Valkenburg currently has a lower safety level than other areas in the region; protection against events with a return time of 25 years compared to the usual 100 years. This lower standard is based on a cost-benefit analysis of possible interventions in the area. The MDP group indicates that this CBA (Cost-Benefit Analysis) is a *back of an envelope* calculation. By exploring possible interventions and interviews in the city, they looked at which (innovative) measures can be taken and in amounts and entrepreneurs in Valkenburg are open to changes in the aesthetics in the city of a tax increase.

The MDP group refers to an analysis of the Stuurgroep Water, which indicated the Geul as potentially risky. The steering group defines more than 40 million damage at inundation at the safety level. At De Geul it was estimated that the damage would be between 25 and 50 million euros and that there was also a risk of 1-5 fatalities. This indicates that there is a need to increase the security level.

Residents of Valkenburg (n=17) indicated during interviews that they wanted a higher level of safety. Half of the respondents said they would pay a triple tax increase for this, 20% would pay double that and the remaining 30% would not pay a tax increase for a risk reduction. Of the options that were explored, residents indicated that they mainly prefer raising the quay walls. Aesthetics was of less importance to residents. However, respondents were mainly older people and the group contained few entrepreneurs, who prefer more aesthetic options. The group also indicates that they have already thought about measures in their own home.

4 options have been explored:
1. Install Flat Bridges
2. Sealing holes/cuts in the quay walls
3. Install a water tunnel
4. Apply Meersen's 4-step approach

The flat bridge is a concept where the usual arches at the bottom of bridges have been removed. The design is such that it can bear the traffic load. According to the research, the bridges have the potential to increase the discharge capacity from approximately 65 m^3/s to approximately 80 m^3/s. This translates to a return period of 60 years. Removable bridges could even provide a discharge capacity of 107 m^3/s, which should occur once every

1500 years. Installing the flat bridge (depending on length and width of course) should cost about €475,000, a retractable bridge would cost about €2,800,000.

Raising the quay walls can be done (semi-)permanently or flexibly. In increasing the drainage capacity, it may also be relevant to remove the notches. Raising the quay walls by one meter should increase the discharge capacity to 103 m^3/s. If one also removes the notches, this would increase to 108 m^3/s. This translates to return periods of 869 and 1709 years, respectively. This can be increased even further by combining this action with installing, for example, flat bridges.
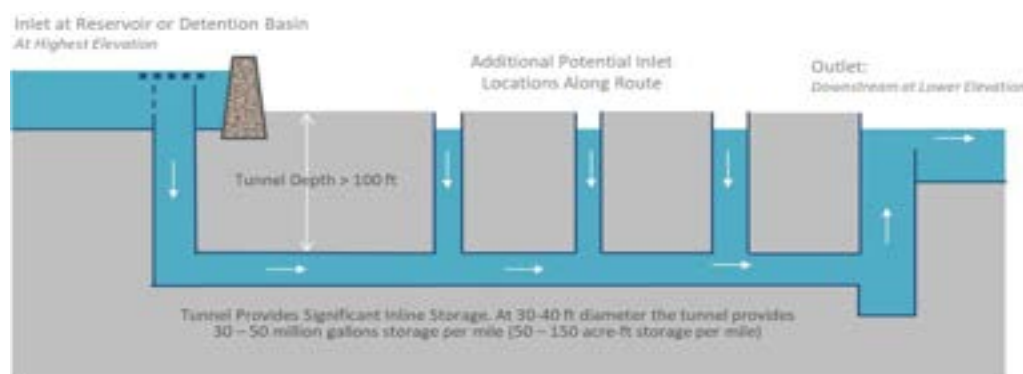
Figure 12: Flood tunnel schematic view

An innovative concept that could also be applied is a flood tunnel. The tunnel would have an inlet upstream of the city and let this water out again downstream. In this way a bypass is created, as it were. The concept can be applied with different tunnel sizes (diameter 2.5, 3.5 and 4 meters) at different discharge capacities (13.9, 29.6 and 39.8 m^3/s), costs (9-19, 12-27, 14-30 million euros) . It results in a safety level of 100, 635 and 2580 years respectively. It is shown in Figure 12.

Meersen's 4-step approach consists of rural area planning, urban planning, actions by homeowners and drainage capacity of the water system.

A comparison between the methods can be seen in Figure 13. Here you can find an overview of different (combinations of) measures. Here one would have to make a political choice about the most desirable alternative. It is clear that there are plenty of options on the table.

TUDelft | Delta Futures Lab

(a) Investment costs and safety level
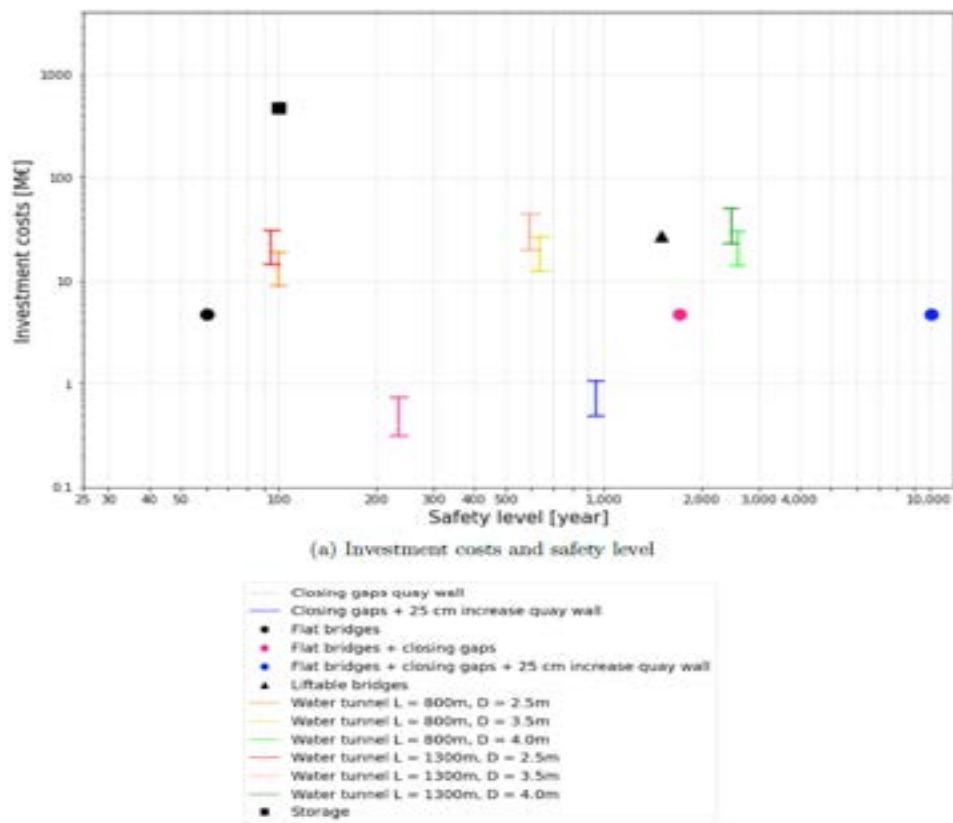
Figure 13: Solutions (combinations), their respective safety levels and their costs

3 Appendix 2: Extreme discharge estimates for the river Geul (TU Delft)

Ir. Guus Rongen

3.1 Introduction

This memo describes the extreme discharge estimates for the Geul that were made within a larger study focusing on estimating extreme discharges for the Meuse river. The goal is to see if using expert judgment, in combination with simple models and measured data, can lead to credible estimates for extreme discharges. This, as an alternative to an approach that uses primarily hydrological models.

For 10 of the larger tributaries, experts estimated the discharges that are exceeded on average once per 10 and once per 1000 years for the Geul. In this study we'll call them the 10 year ARI or 1000 year ARI discharge, or T10 and T1000, for brevity (ARI being an abbreviation for annual return interval). The 10 y ARI discharge can be calculated from data with sufficient certainty as well, and was therefore used to weight the experts. These weights were then applied to the 1000 y ARI discharge, our variable of interest. We translated these estimates to discharges on the river Meuse using a correlation model.

Within this study, the experts made estimates for the relatively small sub-catchment of the Geul as part of the total catchment. This document presents these results, and the relation to the other tributary estimates. The next section briefly described the used method. Section 3 shows the results, which are then discussed in Section 4.

3.2 Method

Cooke's method for structured expert judgment

In this research we use Cooke's method for structured expert judgment (Cooke and Goossens, 2008). Cooke's model assigns a weight to each participating expert. The expert makes an uncertainty estimate for each question by estimating a number of percentiles. Mostly these are the 5th, 50th and 95th percentile, which are combined into a probability density function. Two scores are calculated from these estimates. The calibration score, which is a measure of the statistical accuracy, and the information score, which shows the informativeness of the experts (narrow estimates give more information on the target variable than wide estimates). The product of the two scores is the weight that is used for the expert (after normalization) to calculate the so-called decision maker (DM).

Hydrological data for making estimates

To support their estimates, experts received an overview of the following hydrological data:

- Digital elevation map (EU-DEM)

- Land use (CORINE land use)

- Soil composition (DSMW)

- Rainfall intensity-duration-frequency curves (E-OBS)

- Tributary steepness (from the DEM)

- Precipitation and hydrograph shape for a number of large events (from E-OBS and discharge measurements)

Data were presented in a reader with maps and tables, and as GIS or tabular information. This made it easier for experts to make simple calculations with the data, in case they want to.

Before making estimates for the Meuse, an exercise was done for the Weser. Based on its evaluation, the experts could see the results of their estimates. For the Weser, the same hydrological data were provided as for the Meuse.

3.3   Results

Extreme discharge estimates

The experts' estimates for the extreme discharges are shown in Figure 1. Each expert estimated the 5th, 50th, and 95th percentile. A Metalog distribution (Keelin, 2016) was fitted through this, resulting in the continuous smooth curves. In the bottom row, the decision makers (DMs) are shown. These are weighted combinations of the individual estimates. The global weights DM (GL) is dominated by Exp04 and Exp05. In the equal weights (EQ) DM all experts are represented equally.
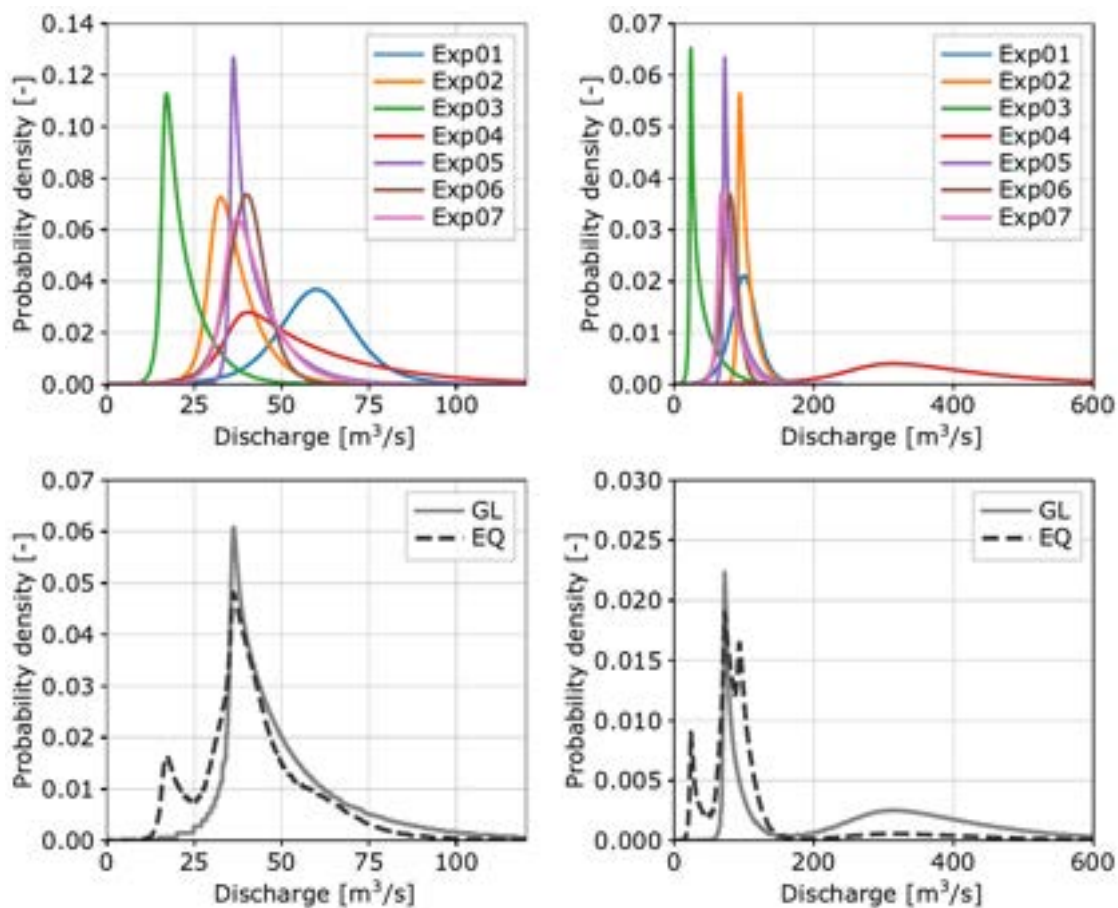
Figure 1: Extreme discharge estimates for the Geul. The two top graphs are the experts estimates for 10 y ARI (left) and 1000 y ARI (right). The bottom row shows the combined estimates for 10 y ARI (left) and 1000 y ARI (right).

Based on the available gauging data at Meerssen, the 10 year ARI discharge is 44 m³/s. Note that this is based on historical measurements. Climate change or land use changes could cause a trend in this data, potentially leading to a different 10 year ARI discharge if we would consider the current climate. Most experts approximate this 44 m³/s pretty well.

For the once per 1000 year discharge, most experts give a best guess (50th percentile) of 75 to 100 m³/s. Expert 4, which scored best on the calibration, expects a much larger discharge, with a best guess of 350 m³/s.

Rationale for estimating the Geul compared to other tributaries

Many experts used a simple calculation or rule of thumb to estimate the tributary discharges. For most, this followed a rationale in which they estimated a representative rainfall duration, an estimate of the 10 or 1000 year ARI rainfall event, and how this translated to the river discharge. This was then tailored to the specific tributary characteristics (size, steepness).

To see how experts estimated the Geul discharge in relation to the other tributaries, the 10 and 1000 year ARI discharge are divided by the area. These relative discharges are estimated to be average compared to the other tributaries, as Figure 2 shows. The experts estimated that the tributaries in the middle of the Ardennes (Vesdre, Ambleve, Ourthe) have, on average, a higher discharge per square meter, while the more flat tributaries (French Meuse, Sambre, Niers) had a lower discharge per square meter.
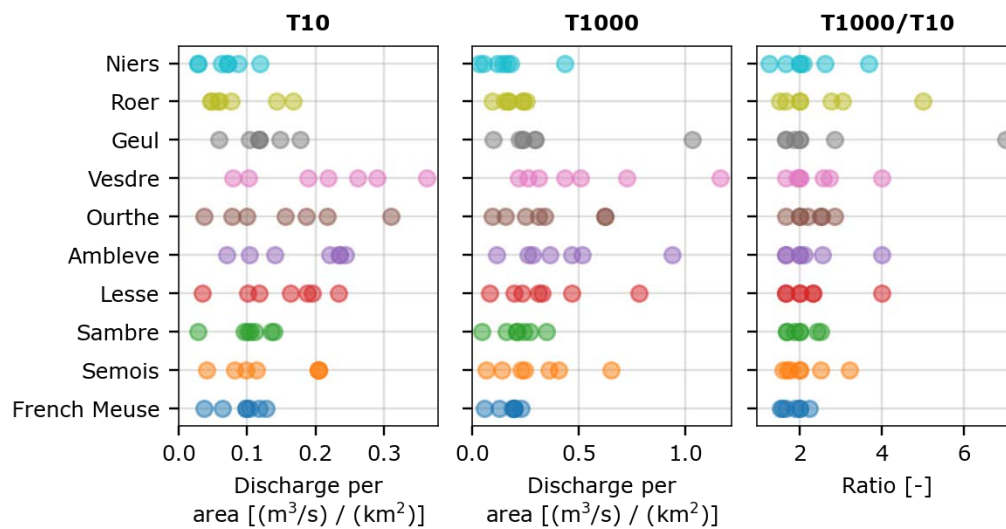
Figure 2: 50th percentile estimate for the tributary discharge, divided by the sub-catchment area. On the left for the once per 10 year discharge, in the middle for the once per 1000 year discharge (note the different horizontal scale), and on the right the ratio between the two.

Another measure for to qualify the tributary discharges, is by comparing the 10 year ARI and 1000 year ARI estimates, which is shows in the right in Figure 2. For the Geul, this led to, on average, the largest ratio between the 10 and 1000 year ARI discharge.

Correlation to high Meuse discharges

In the process of combining data with expert judgments, we selected events with a high discharge at Borgharen and determined the corresponding discharge at (amongst others) the Geul. Figure 3 shows on the left the discharges for both locations during these events, and the ranks (largest to smallest: 1/N,2/N,...,N/N) on the right.
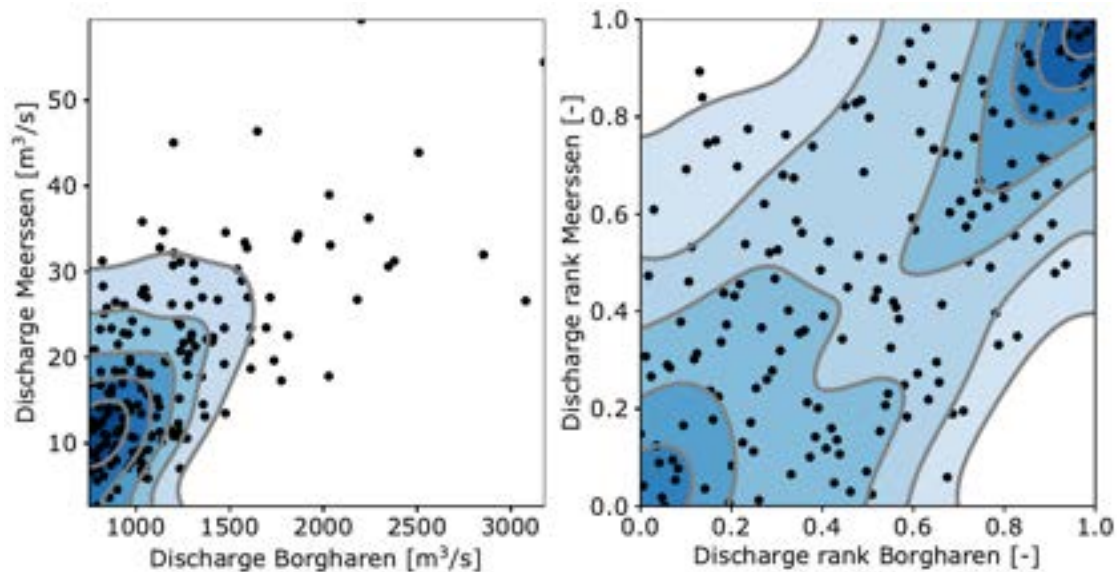
Figure 3: Scatterplot with the discharge at Meerssen for events with a high discharge at Borgharen. On the left, the measured discharges, on the right, the ranks of these discharges.

The plots shows that high discharges often coincide. This makes sense, as the Geul tributary is located close to the tributaries of the Vesdre, Ourthe, and Ambleve, for which a large rainfall event can already cause a high discharge on the Meuse. The rank plot on the right shows some upper tail dependence (i.e., the upper right has a higher probability density than the lower left). This indicates that a Gumbel copula would be a suitable model for modeling the coincidence during extreme events (refer to (Nelsen, 2007) for details on copulas).

3.4 **Discussion**

The resulting 1000 year ARI discharge estimates for the Geul has a large bandwidth. This is mostly due to a single expert with a large uncertainty in its estimates. This expert did however perform very well in the calibration, supporting the validity of the estimated discharge. Cooke's method has shown that combining multiple experts' estimates gives better results, than using a single expert or equal weights (Cooke and Goossens, 2008).

This study's focus is estimating extreme discharges on the Meuse, not specifically on the Geul. The Geul is only a relatively small tributary in the complete catchment, so the absolute results did not receive the experts' full attention when making estimates. The comparison to other tributaries does however put the results of the Geul in a broader context.

The experts were provided with hydrological data for all the catchments, but not with the measurements themselves, as this would undermine the use of the 10 year ARI discharge to test the statistical accuracy of the experts. The experts tributary estimates were used to calculate the discharge at Borgharen. Even though the model we used for this is relatively simple, they did not receive feedback on this. Both knowing the historical discharge measurements and receiving feedback on the results after processing their answers, could lead to experts adjusting their estimates to fit their expectation of the discharge at Borgharen.

The bandwidths of the estimates provided in this study are relatively wide. This can be unsatisfying for decision making, as it is easier to base policy on a single number than on an uncertain set of possibilities. It does however show the uncertainty that is inherently connected to estimating events that we have likely never experienced in recent history (at least, if we use this method of expert

judgment). Using an approach with a larger focus on hydrological models does often narrow down the range of possibilities, but we have to be aware that we do not ignore uncertainty while making modelling choices. In the end, uncertainty estimates are still quantitative results, that can be translated to expectancy for, for example, economic cost benefit analysis.

3.5 References

Cooke, Roger M., and Louis L. H. J. Goossens. 2008. "TU Delft expert judgment data base." *Reliability Engineering and System Safety* 93 (5): 657–74. https://doi.org/10.1016/j.ress.2007.03.005.

Keelin, Thomas W. 2016. "The Metalog Distributions." *Decision Analysis* 13 (4): 243–77.

Nelsen, Roger B. 2007. *An Introduction to Copulas*. Springer Science & Business Media.

4   **Appendix 3: Land cover assessment Geul catchment (Deltares)**

Dr. ir. Kymo Slager

Land cover potentially play an essential role in the hydrological response of a river catchment, as it directly influences the rate of soil infiltration, surface water runoff and evaporation. In this rapid assessment, it is analyzed what is the spatial distribution of land cover throughout the Geul river catchment. Van Winden (2022) and Klein (2022) did a comparable analysis as well; van Winden (2022) provided a good overview of land cover, but did not provide a data source, as Klein (2022) used CORINE land cover 2018 (Copernicus, 2018) as the source. CORINE land cover is often used in hydrological analyses for European catchments, however for this specific catchment, seem to be inconsistent with more detailed land cover, topographic maps and recent aerial photographs publicly available (see figure 1).
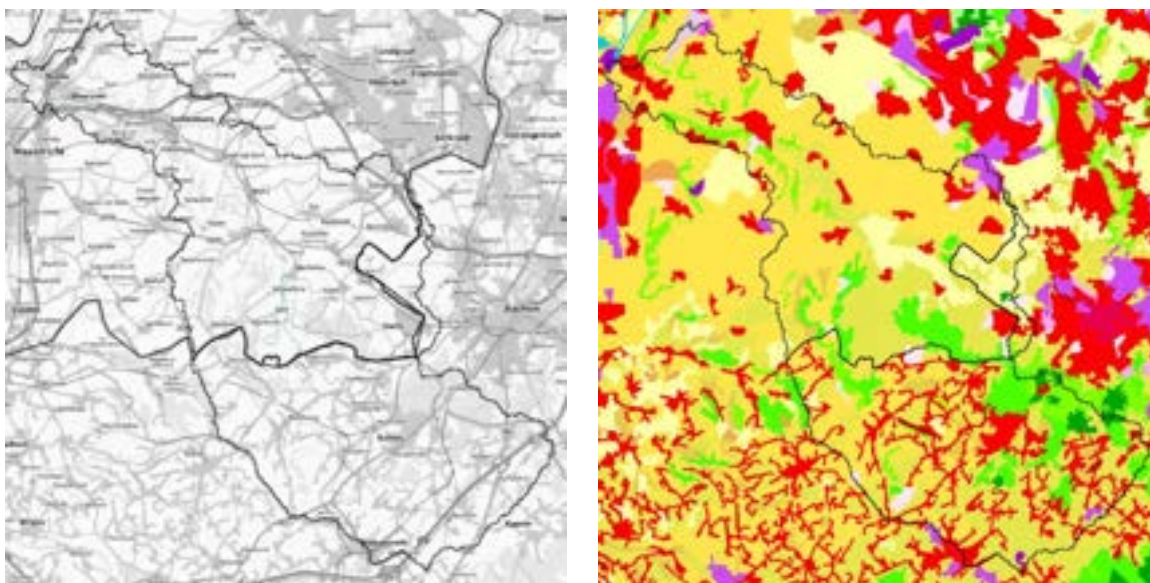
Figure 1. Topographic map of Geul catchment (left) and Corine Land cover (right)

The dendritic urban pattern shown in the Belgian part is atypical and seems to be completely differently interpreted than at the Dutch and German side. Klein (2022), determined that ~41.5% is covered by heterogeneous agricultural areas, followed by pastures (27.5%), urban areas (17%) and forests (13%).

In order to get more insight in the detailed land cover in the catchment, it was decided in this study to use openstreetmap[1] data from July 2022 as another reference (see figure 2). Land cover classes available in the dataset are aggregated to 7 broader landcover classes (see annex for table). Road and railway infrastructure is included by a 6-m buffer around the centerline of a road segment. Residential areas are further detailed with roads and buildings. The rest of the urban area (orange in figure 2) is public space and is estimated to be 50% impervious surface.

---

[1] Openstreetmap.org is considered to provide a reliable, detailed, actual and consistent landcover map and is based on open governmental data and further detailed by a community of users.
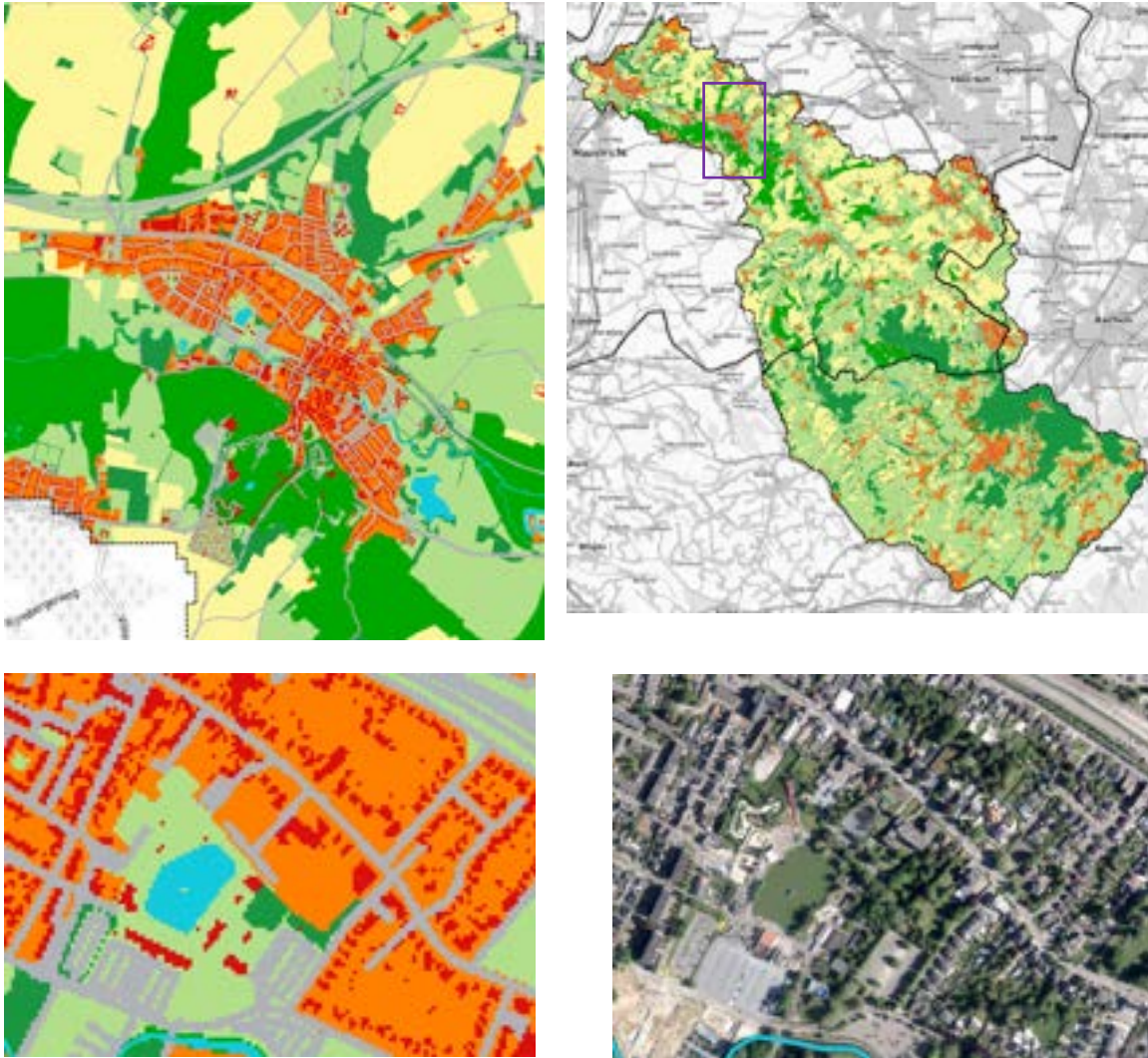
Figure 2. Reclassified land cover map from openstreet map of Valkenburg (top-left), for total river Geul catchment (top-right) and for part of centre of Valkenburg (bottom-left); this is compared visually with Google Satellite for the same area (bottom-right)

Figure 3 shows the percentages of main landcover classes for the total catchment, and separately for the Netherlands and Belgium. This chart shows a different picture than made from CORINE land cover. Impervious urban areas (buildings, infra and semi-urban) are at most up to 10-15% of the catchment area. Grassland, mainly pastures, is around 46% of the area, and arable land around 19%. Forests are classified to cover up to 20% of the total catchment area.

A striking difference between the Belgian and Dutch part of the catchment is that in the Netherlands, much more area is covered and used as arable production land (*mainly maize and potatoes*) – up to 28% compared with up to 8% in Belgium. This comes at the cost of grassland area; in the Belgian part up to 55% is classified grassland, while on the Dutch side this only amounts up to 38%. Urban fractions are not very different between the two countries.

These results on the urban area delineation is lower than in Klein (2022) and Van Winden (2022). Both conclude that the urban area with impervious surface for the whole catchment is higher than the highest estimate from this study, for the total catchment: both up to 17%, while Klein also marks a considerable difference between both countries: 27% in Belgium vs. ~13% in the Netherlands.
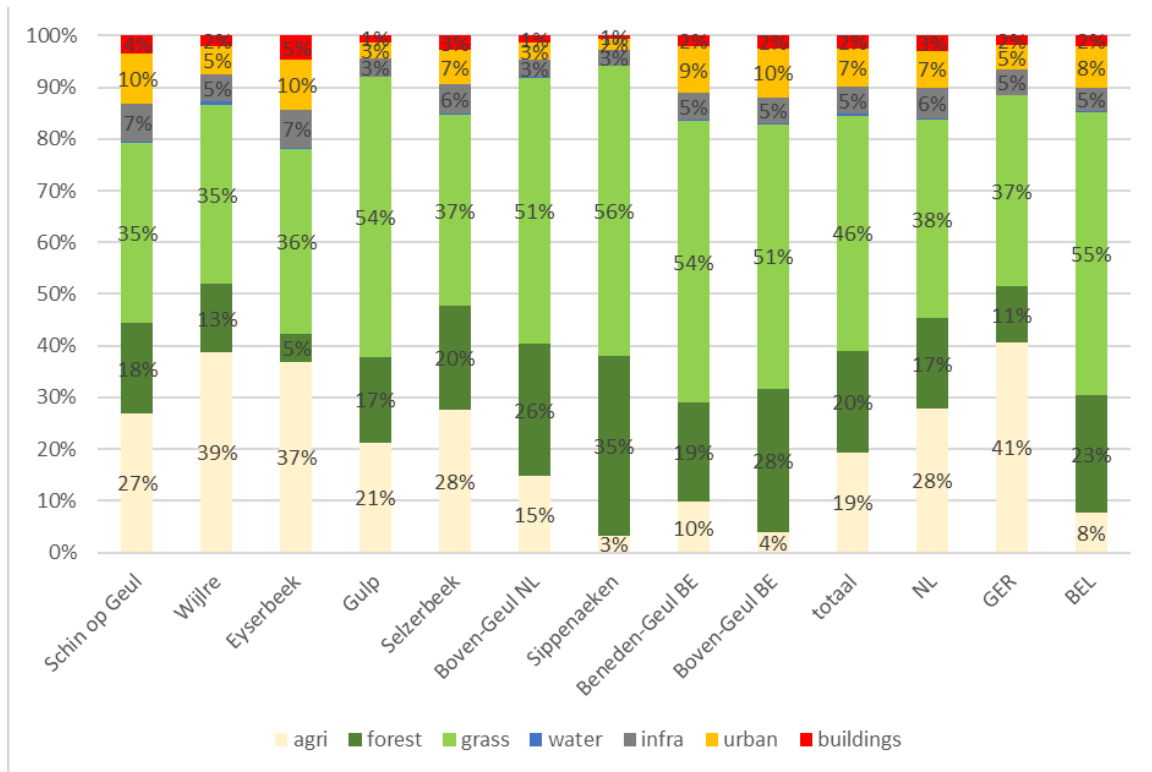
Figure 3. Land cover percentages for different parts of the Geul catchment

5   Appendix 4: Hydrological model setup and runs (Deltares)

Dr.ir. Laurène Bouaziz

This chapter describes the setup of the hydrological model used to assess Geul river basin characteristics, as well as analyses of the different model simulations supporting the rapid assessment.

5.1   Model set-up

A distributed wflow_sbm model (van Verseveld et al. 2022) is set-up at a 1000 m x 1000 m resolution. The model includes vertical processes to represent snow, interception, transpiration and soil processes (Figure 1). The water flow is routed downstream along the river network for river flow, overland flow and subsurface flow, based on the kinematic wave model. The model uses land use and soil properties maps to estimate input parameter values. An initial calibration of the model was performed by Klein (2022).

Several additional adjustments have been made to the calibrated model, including adjustment of:
- the threshold to delineate river cells: upstream area threshold changed from 25 km^2 to 2 km^2
- the land use map: from CORINE to a reclassified OpenStreetMap (see appendix 3)
- A multiplication factor of 0.7 was applied to the saturated hydraulic conductivity for lateral subsurface flow (parameter KsatHorFrac). A decrease of this parameter leads to a slightly flashier response of the river basin with increased peak flows and decreased base flow.

The hydrological model is forced with radar data for the period 2019-2021. For the two days of the event, this radar data is replaced by a reanalysis of the radar data in combination with local observations, which was performed by KNMI (Deltares, 2022)
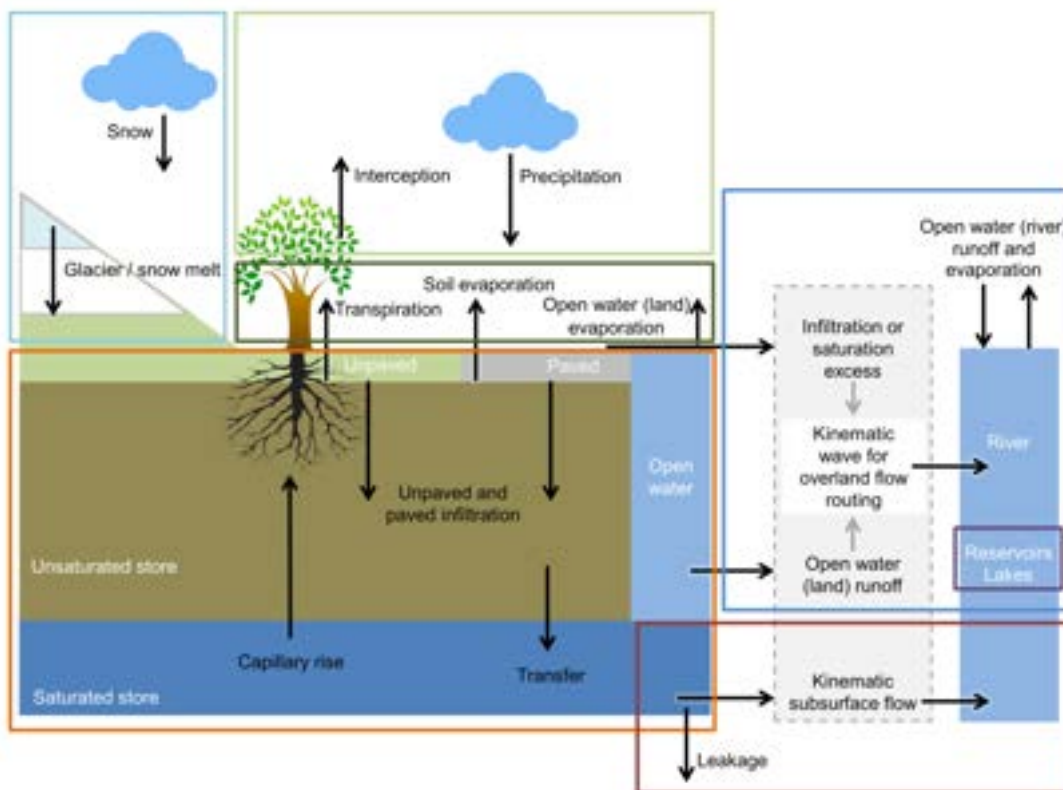
Figure 1 schematic representation of the wflow_sbm model

As the wflow_sbm model does not account for floodplain processes (storage and hydraulic flow), we coupled the wflow_sbm model with a SOBEK hydraulic model. To couple the wflow model with the hydraulic model, relevant 'connection pits' are created along the river network to obtain the streamflow generated only for the subcatchment (Figure 2).
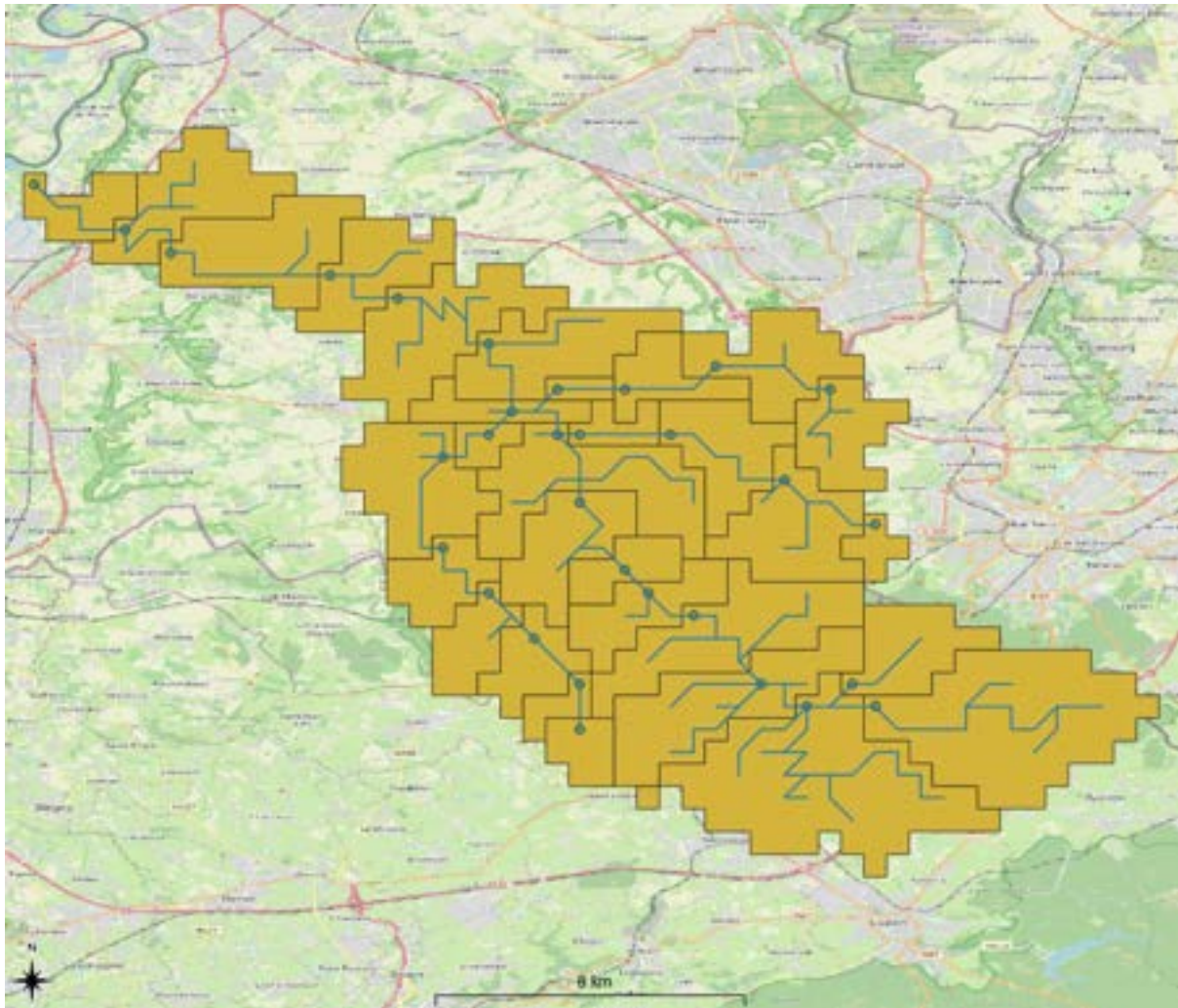

Figure 2 Location of pits in the wflow model (dots). The streamflow obtained is generated only in the represented subcatchments which enables an easy coupling with SOBEK.

5.2 Model performance

The model's ability to reproduce discharges throughout the basin, is mainly evaluated for the summer 2021 event itself using observed streamflow data when available (retrieved from the operational system of Waterschap Limburg). Unfortunately, not many measurement stations functioned during the July 2021 floods, and as such could not be used for a detailed verification.
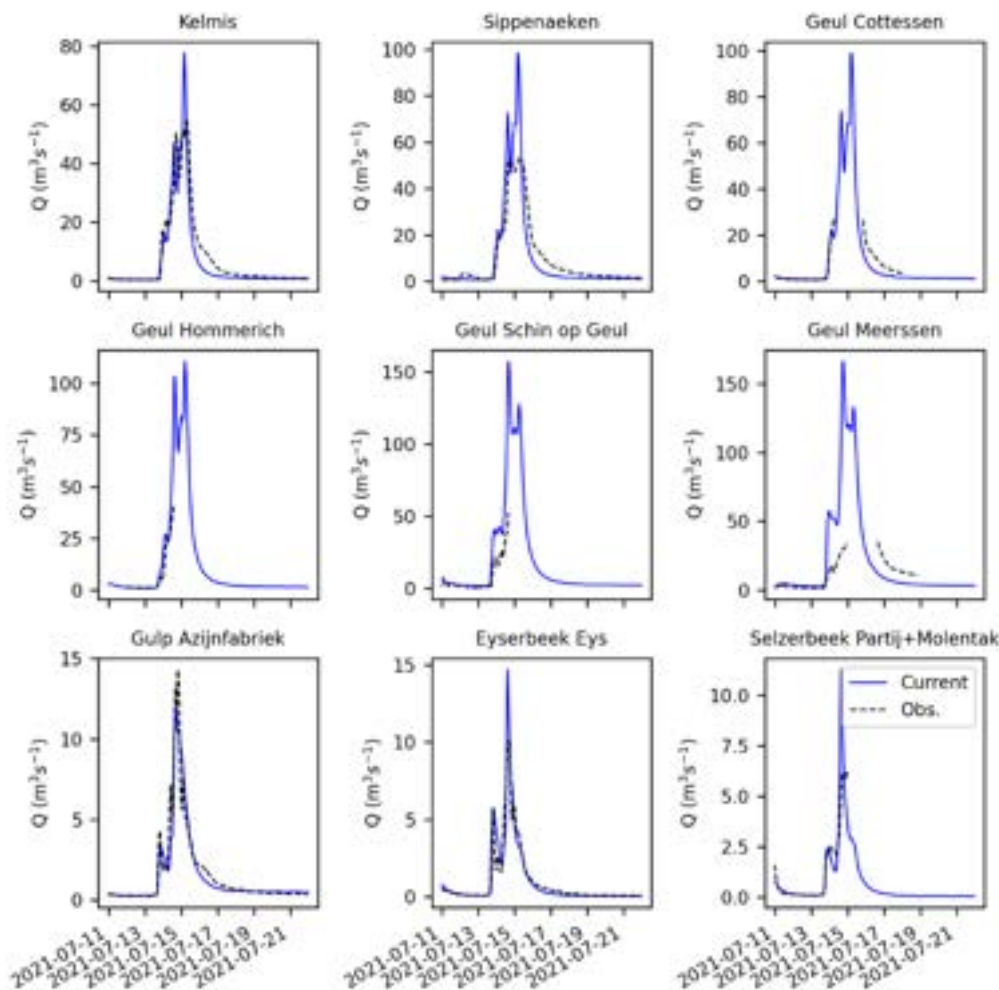
Figure 3 Observed and modeled (label = Current) streamflow during the event for the different station within the Geul river basin.

The comparison of observed and modeled streamflow (Figure 3) for different discharge stations throughout the basin shows a likely overestimation of peak flows by the wflow model. This overestimation is reduced after running the SOBEK hydraulic model, as a result of delay and dampening of the peak due to inundation of the floodplains, especially in the broader Geul river valley. Note that in the observations, the increase in peak flow between Kelmis and Sippenaeken is almost zero, which is not likely considering that approximately one third of the contributing area is added between these two stations.

It can also be seen from Figure 3 that the timing of the rising limb of the peak is relatively well simulated by the model until Schin op Geul. For the station of Schin op Geul and Meerssen, there is a clear delay of the rising limb of the peak in comparison to the modeled streamflow. This is likely caused by underestimated storage in the floodplain.

As can be seen in Figure 4, which shows the same simulated and observed streamflow at the same scale, most of the flow originates from the upstream area of the Geul (Kelmis until Hommerich), while the fraction of the three tributaries (Gulp, Elserbeek and Seyzerbeek) to the total peak is very limited.
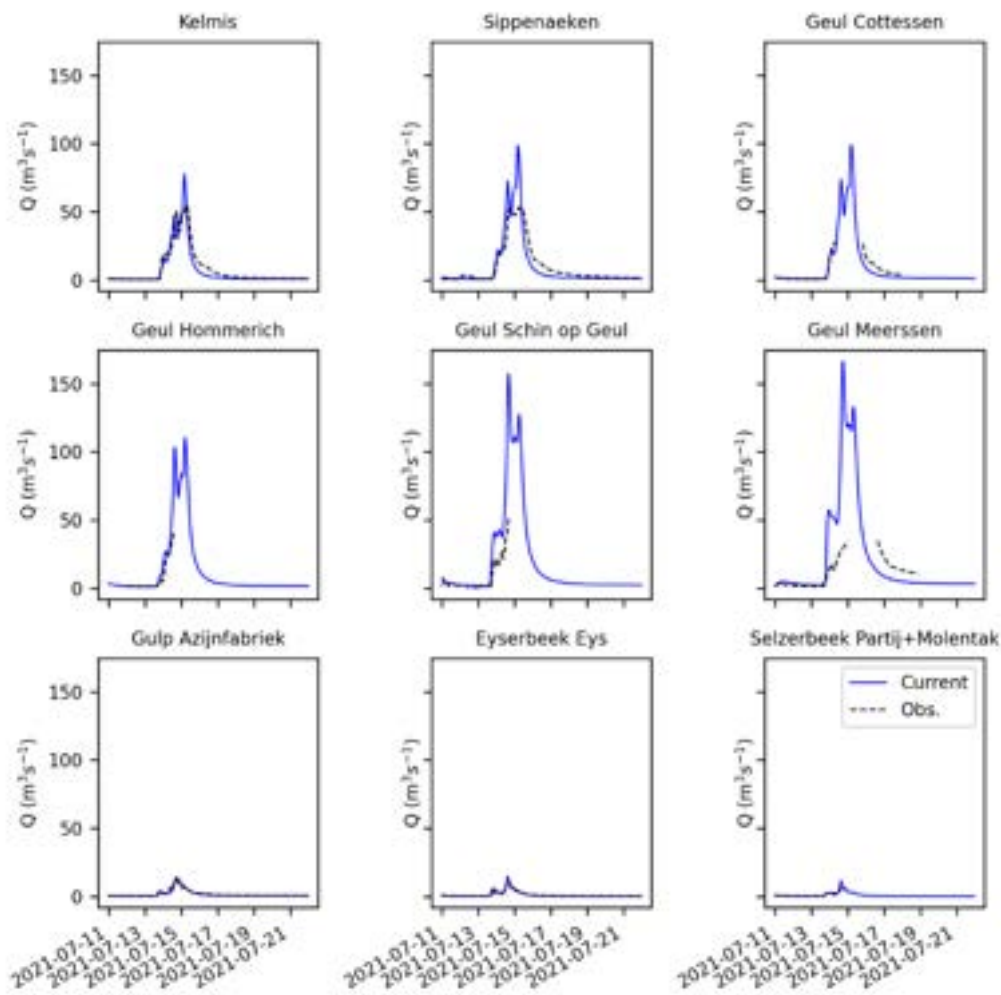

Figure 4 Observed and modeled streamflow during the event for the different station within the Geul (same y-scale).

The Belgian part of the Geul catchment (Kelmis + Sippenaeken) has a relatively high (modeled) contribution to the overall flow of 47% (for the specified period) in contrast to the three tributaries (Gulp, Eyserbeek and Selzerbeek) which only have a contribution of 19%, further exemplified in Figure 5 and Figure 6.
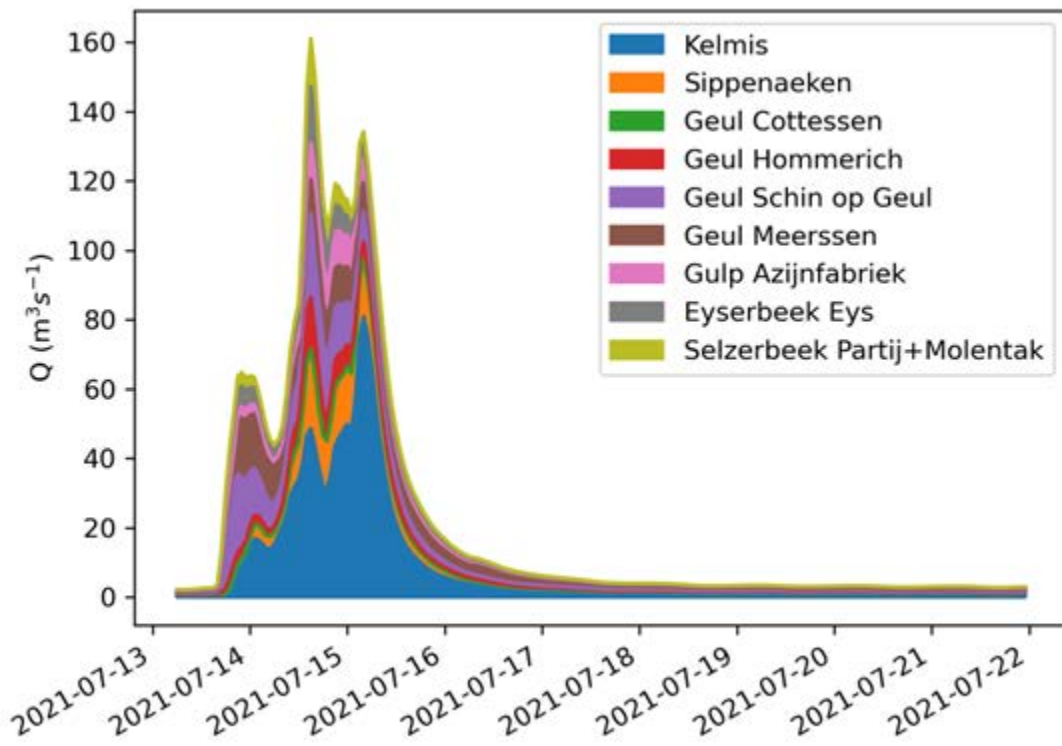
Figure 5 Modelled contributions of streamflow of the different subcatchments of the Geul
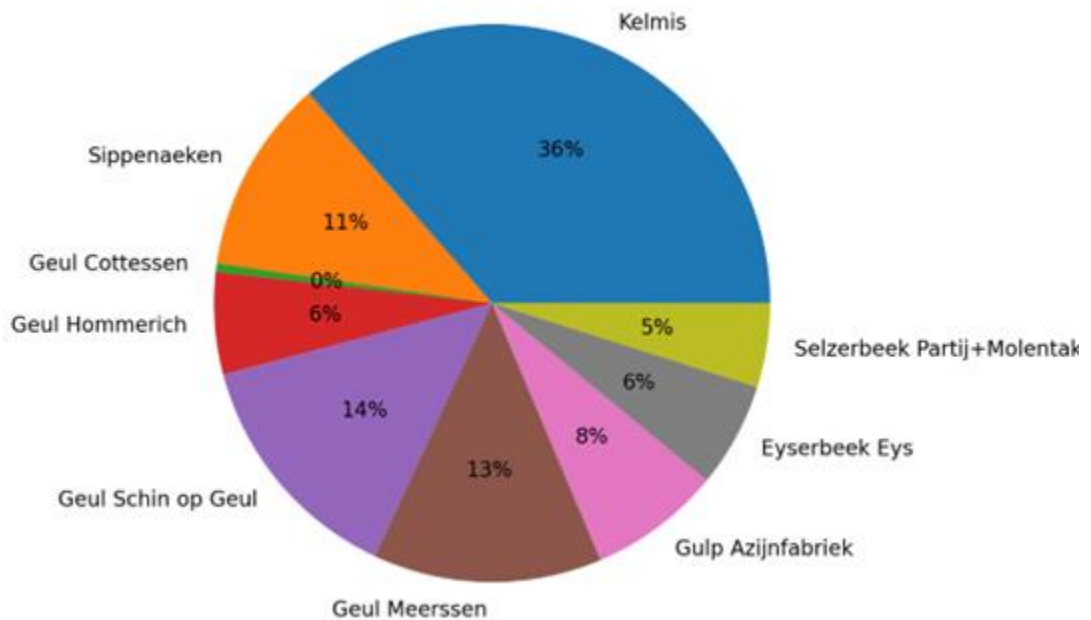
Figure 6 Modelled contributions of each of the subcatchments of the Geul for the event (13-07-2021 until 21-07-2021)

Rainfall-runoff coefficient

The three tributaries received relatively less precipitation (~130mm for July 13th 6AM until July 21st) than the upstream areas of the Geul catchment (Kelmis ~175 mm for July 13th 6AM until July 21st), as can be seen in Figure 7. However, the cumulative runoff coefficient of the three tributaries was also considerably lower than along the Geul river (~0.20 versus 0.45), as shown in Figure 8.
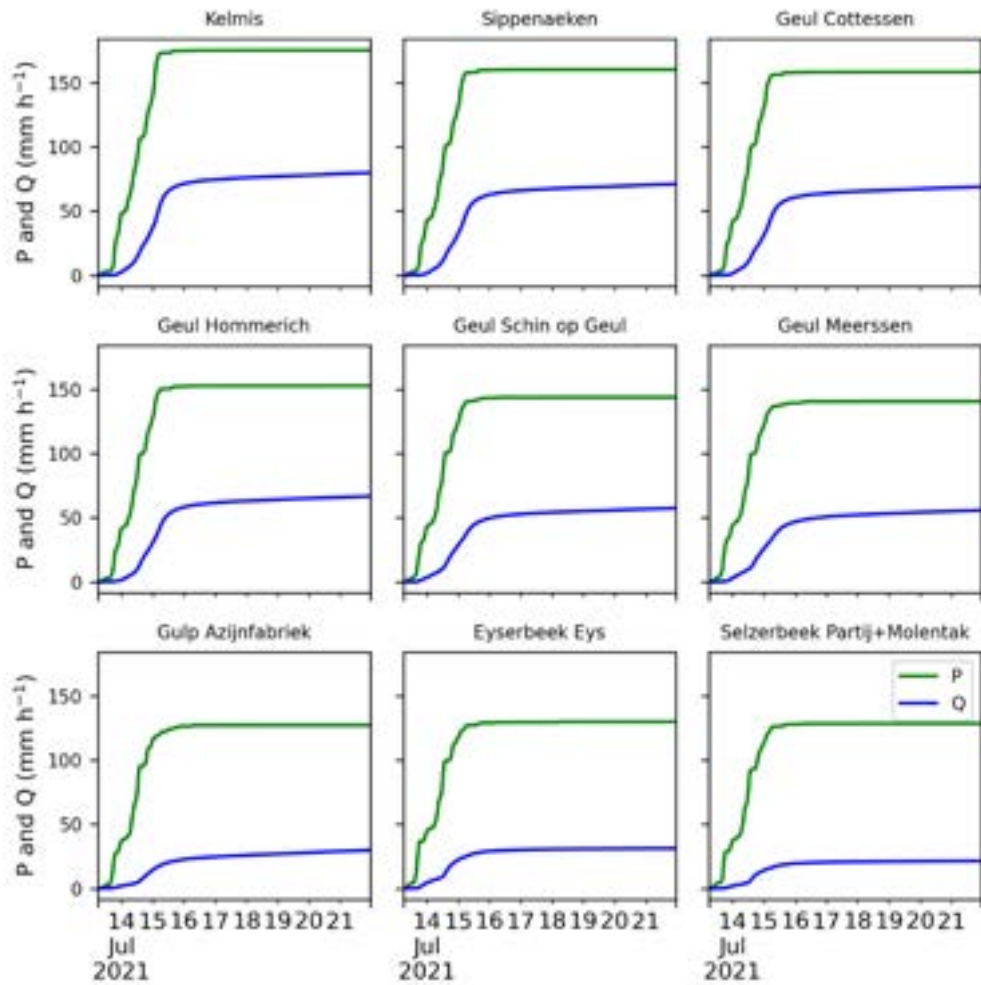
Figure 7 Cumulative precipitation (P) and streamflow (Q) in (mm / hour) for each of the catchments of the Geul during the event
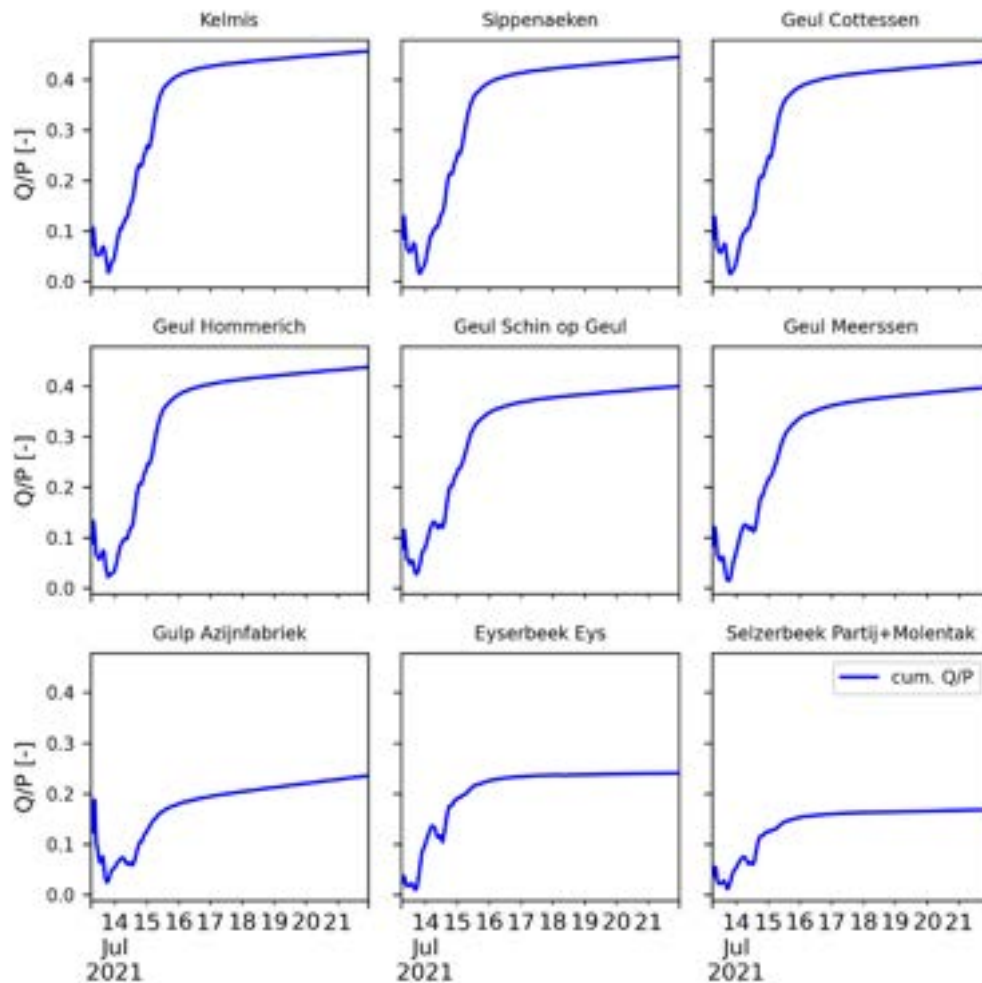
Figure 8 Cumulate runoff coefficient [-] for each of the catchments of the Geul during the event

5.3 Model scenarios

The model was subsequently used to test several scenarios:
- Conversion of current land use to urban area for the entire catchment,
- Conversion of current land use to forested area for the entire catchment,
- Conversion of current land use to forested area, keeping current urban area,
- Conversion of current land use to cropland area, keeping current urban area,
- Adding 14 reservoirs of 50000 m³ in the upstream areas (Figure 9). The configuration of the reservoirs in wflow is as follows:
  - Area reservoirs 5000 m2
  - Target minimum fraction: 0.0
  - Target full fraction: 0.1 (between 0.0 and 0.1, the demand will be squeezed – reservoir designed to be empty)
  - Demand: 50000/(3600*24): designed to empty in approximately 1 day
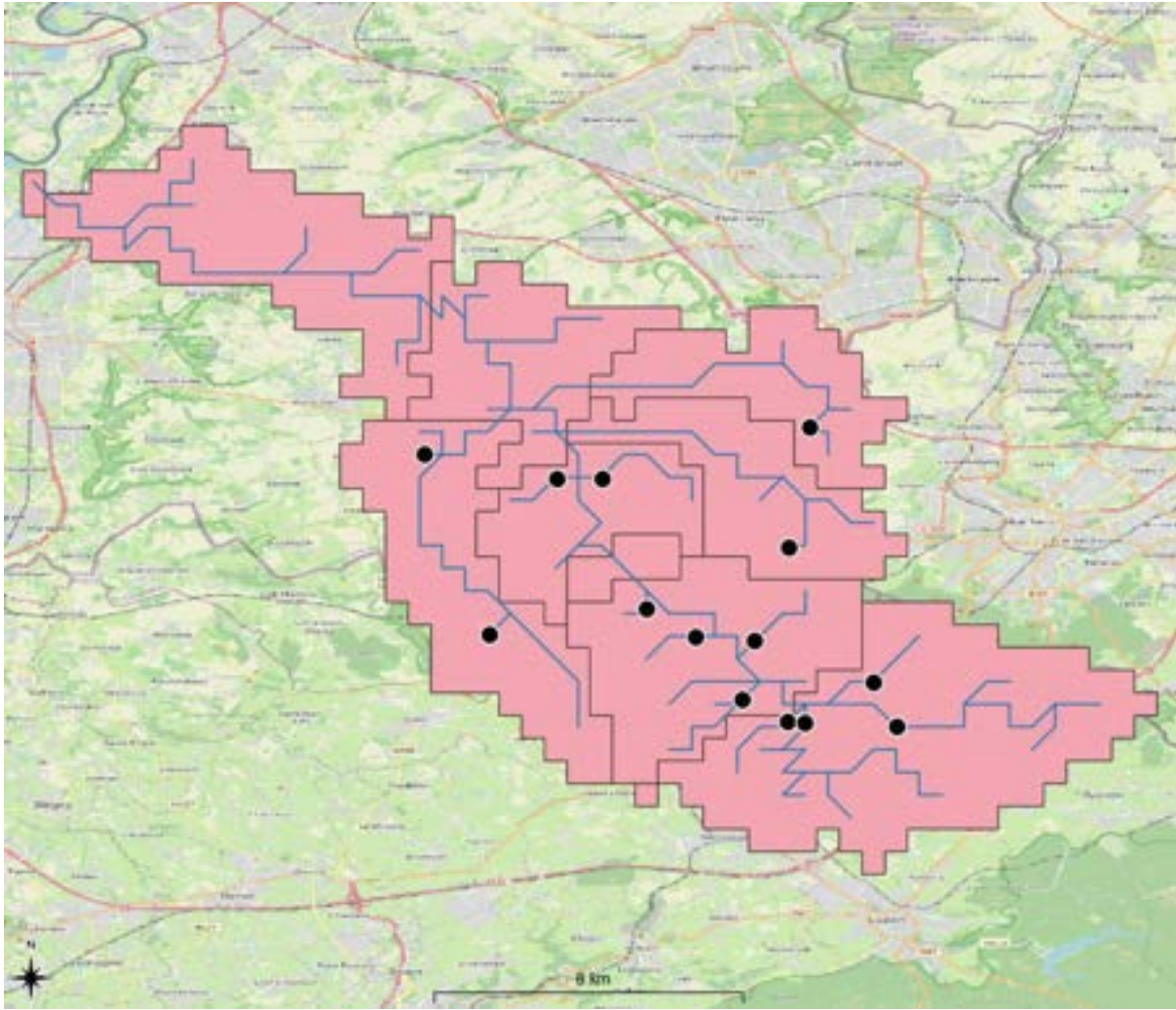 - Max release before spilling: idem as demand.

Figure 9 Location of the reservoirs in upstream tributaries (black dots)

When land use is changed in the wflow_sbm model, the parameters listed in Table 1 are also changed.

Table 1 wflow sbm parameters which depend on land use

	Kext extinction coeff for canopy gap (-)	N land Manning	Rooting depth (mm)	Paved fraction (-)	Storage leaves (mm)	Storage wood (mm)
Pasture (231)	0.6	0.15	107	0.0	0.127	0.01
Crops (241)	0.6	0.20	390	0.0	0.127	0
Mixed forest (313)	0.8	0.50	406	0.0	0.039	0.5
Urban (111)	0.6	0.011	256	0.9	0.04	0

The expected impact of land use conversion in the model on the model's hydrological response is described below:

- Potential land use conversion from current to mixed forest (while keeping current urban areas)
  - Manning N from 0.15 to 0.5 (factor 3.3) implies a more delayed/damped flow and therefore more time for infiltration
  - Increased interception
  - Increased transpiration

  The largest effect is expected from Manning N increase (see sensitivity analysis in Figure 12) When converting the total area including the urban areas to forest, an additional decrease in streamflow is expected as a result of an increased infiltration capacity due to the absence of paved areas.

- Potential land use conversion from current (mostly pasture) to crops (keep urban areas)
  - Manning N from 0.15 to 0.20 (slight increase)
  - higher rooting depth – more transpiration – however relatively small transpiration during such an event

  Not so much change expected.

- Potential land use conversion from current to urban
  - Manning N from 0.15 to 0.011 – large decrease will lead to more flashy peaks
  - Infiltration capacity unpaved is 5mm/d versus 600 mm/d in unpaved (so almost no infiltration)
  - Paved fraction from 0 to 0.9 – no infiltration – overland flow dominated response

  Much flashier response expected.

These results are indeed observed in the modeled streamflow for each of the land use scenarios (Figure 10 and Figure 11).
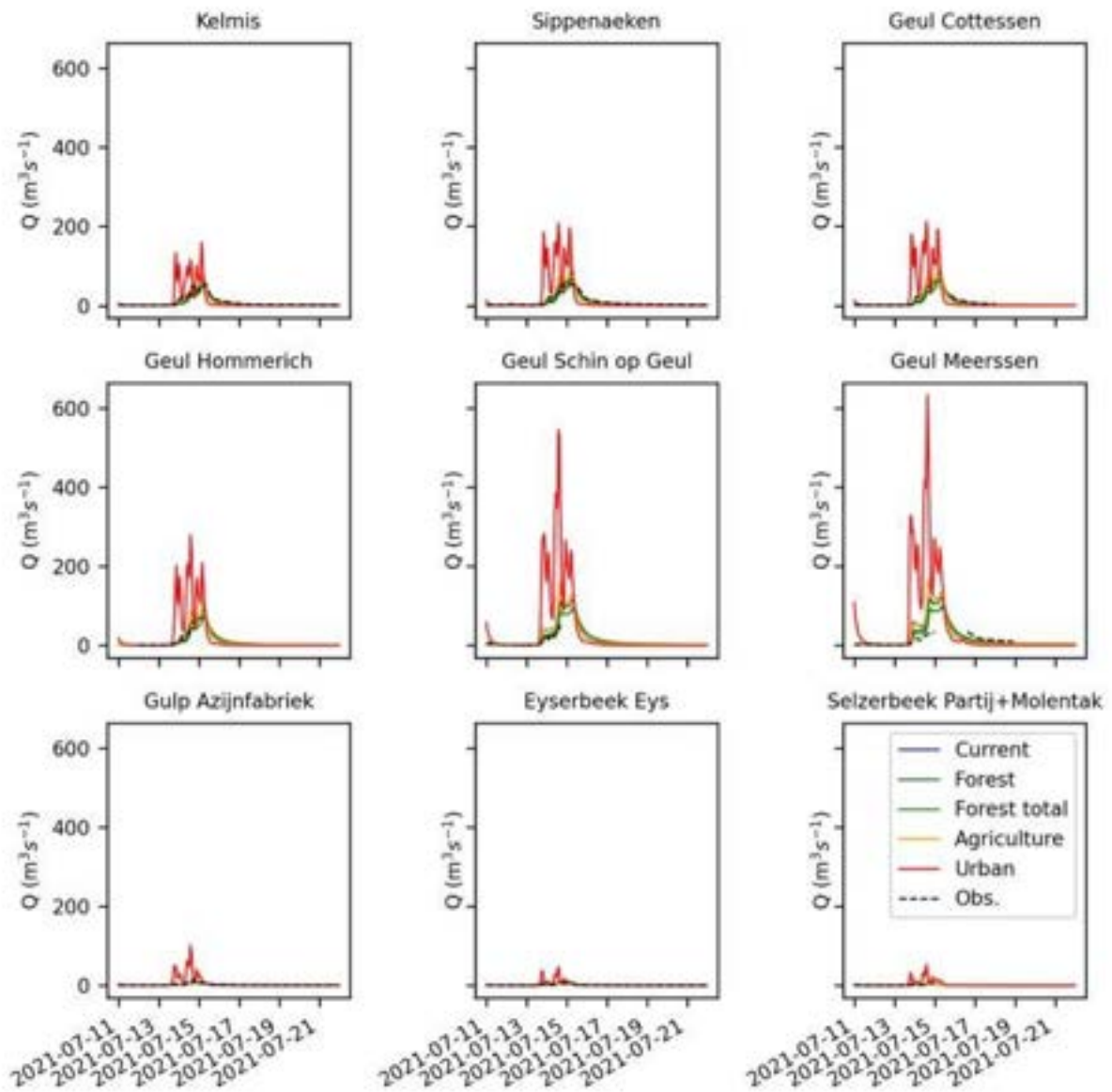
Figure 10 Modeled streamflow for the land use scenarios. The urban scenario generates extremely high streamflow. A figure without the urban scenario is shown in Figure 11
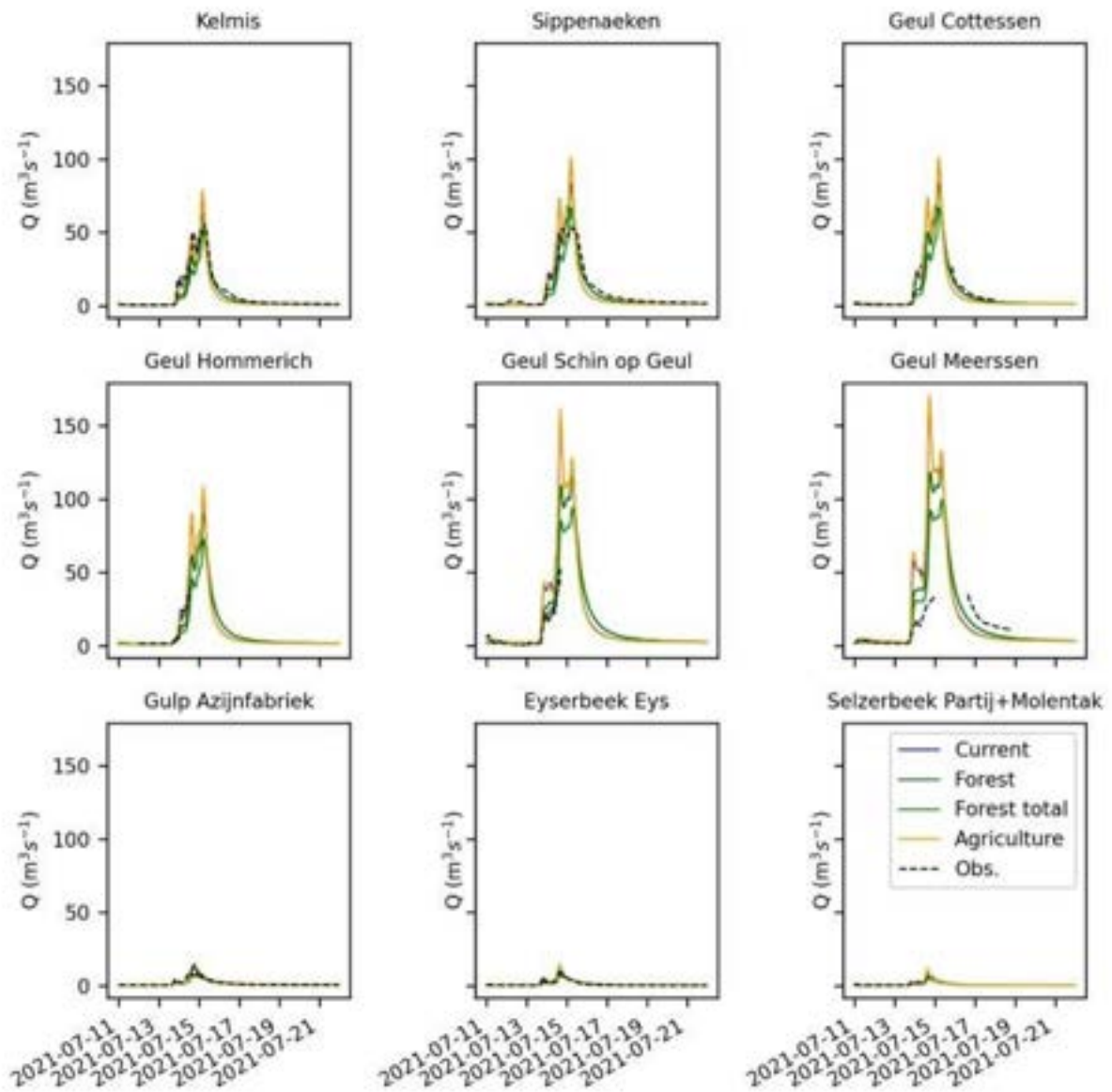
Figure 11 Modeled streamflow for all land use scenarios, except the urban scenario which generates extremely high streamflow
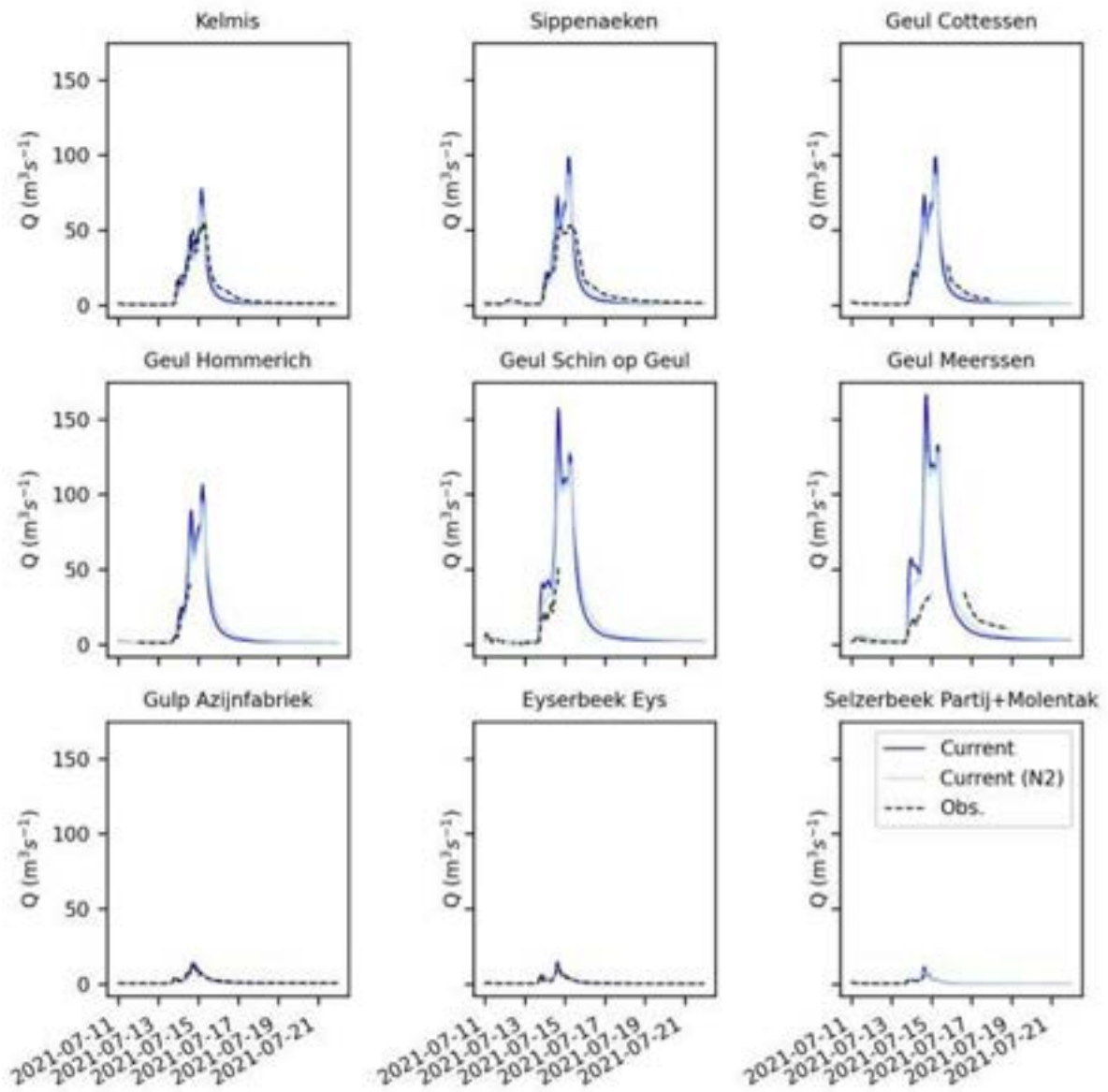
Figure 12 Sensitivity of model to Manning N roughness (light blue line shows the effect of increasing Manning N with a factor 2).

In addition, peak flows are also reduced in the scenario with 14 reservoirs in the upstream tributaries as shown in Figure 13. The modeled reservoir volumes for each of the 14 reservoirs are shown in Figure 14. It should be noted that the reservoirs are not all fully filled during this event. This is due to modelling choices and assumptions in selecting locations for reservoirs; areas discharging into the reservoir are sometimes too small. In further assessments this can be further optimized in the combined model, but does not change the overall interpretation of the results and has only a minor impact on the main conclusions.
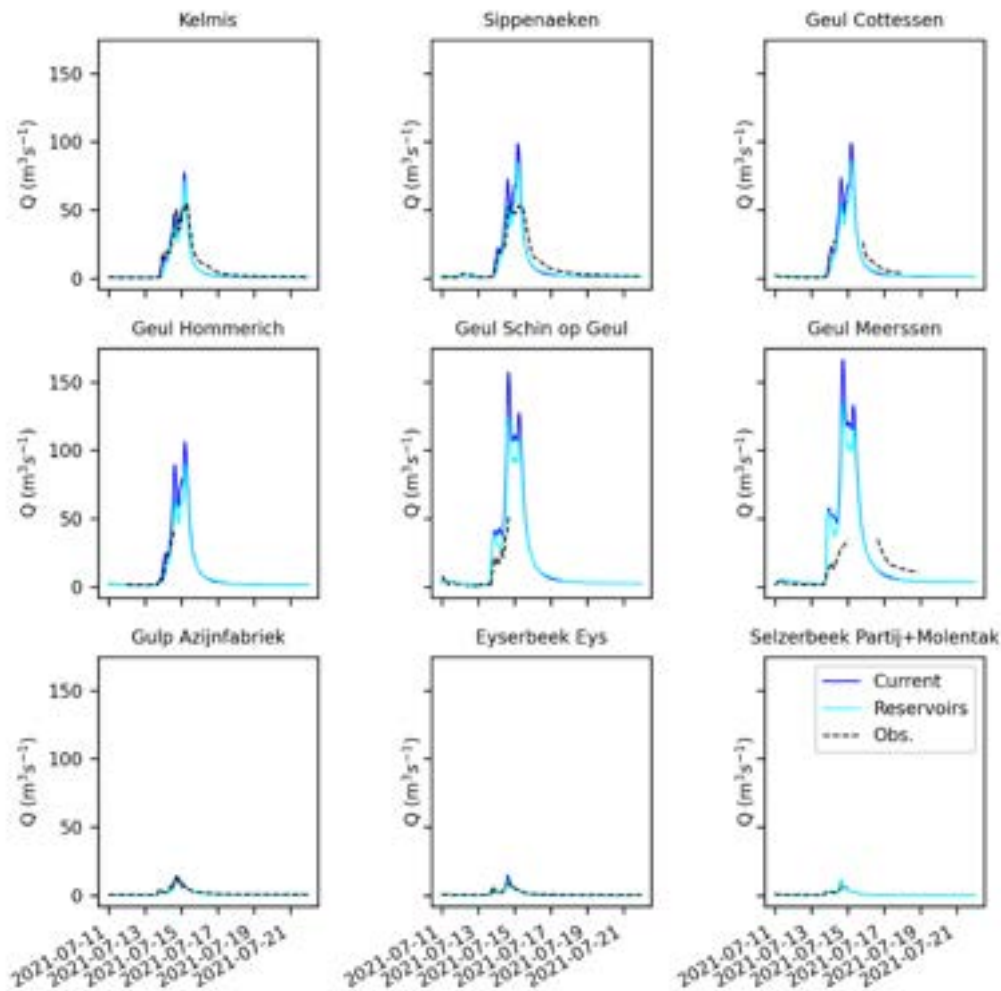

Figure 13 Modeled streamflow for the current scenario and the reservoirs in upstream tributaries scenario.
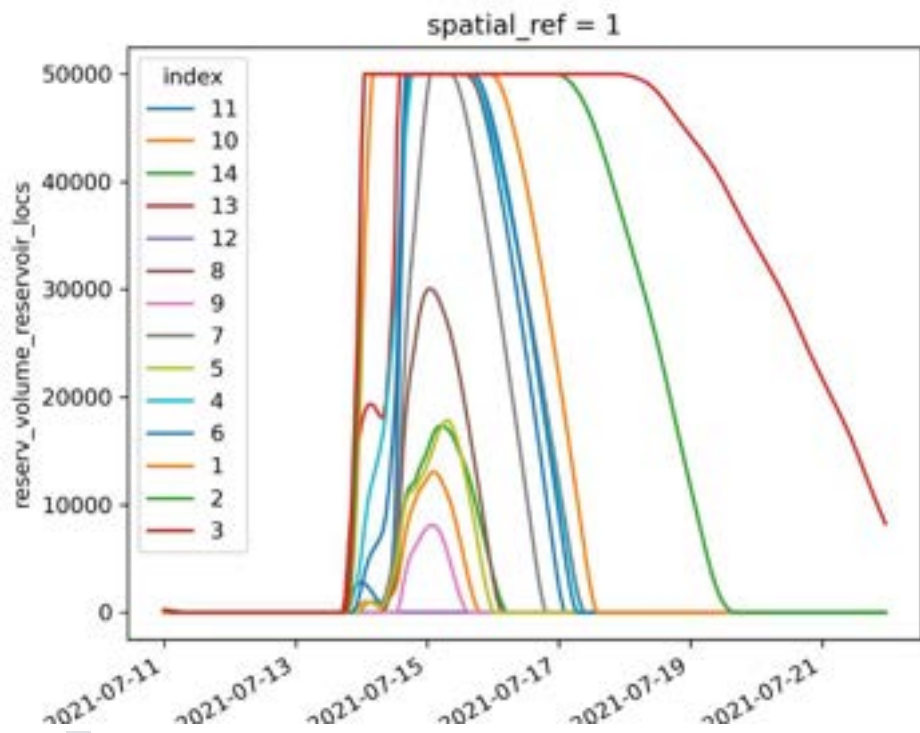
Figure 14 Reservoir volumes (m³) of the 14 reservoirs in the tributaries

For each of the scenarios, the maximum modeled peak flows during the event are shown in Table 2 and the change compared to current condition is shown in Table 3.

Table 2 Maximum modeled peak discharge for the event for each of the scenarios for each station in the Geul

	Current	Forest	Forest total	Agriculture	Urban total	Reservoirs
Kelmis	77	62	51	79	158	71
Sippenaeken	98	82	66	100	207	85
Cottessen	98	83	66	100	211	85
Hommerich	106	90	72	108	278	89
Schin op Geul	157	114	94	161	545	124
Meerssen	166	121	99	170	631	135
Gulp	11	7	6	13	101	10
Selzerbeek	14	9	7	14	46	11
Eyserbeek	11	7	5	11	52	11

Table 3 Ratio of maximum modeled peak discharge for the scenario over maximum modeled peak discharge for current conditions for each station in the Geul

	Current	Forest	Forest total	Agriculture	Urban total	Reservoirs
Kelmis	1.00	0.81	0.66	1.03	2.05	0.92
Sippenaeken	1.00	0.84	0.67	1.02	2.11	0.87
Cottessen	1.00	0.85	0.67	1.02	2.15	0.87
Hommerich	1.00	0.85	0.68	1.02	2.62	0.84
Schin op Geul	1.00	0.73	0.60	1.03	3.47	0.79
Meerssen	1.00	0.73	0.60	1.02	3.80	0.81
Gulp	1.00	0.64	0.55	1.18	9.18	0.91
Selzerbeek	1.00	0.64	0.50	1.00	3.29	0.79
Eyserbeek	1.00	0.64	0.45	1.00	4.73	1.00

5.4   Limitations / Recommendations

- The hydrological model likely overestimates the peaks; this will be corrected by the hydraulic coupled model (see appendix 5)
- Recommendation: evaluate the model for a longer time series
- Recommendation: do more sensitivity analyses on the different modelling setup choices (e.g. resolution, upstream thresholds, soil characteristics)
- Recommendation: further substantiate the chosen input parameter values; ideally by collecting empirical local evidence on the soil characteristics, and research on factors contributing the most to soil retention and infiltration capacity (at plot and basin scale)

5.5 <u>References</u>

Klein, A., 2022. Hydrological response of the Geul Catchment to the Rainfall in July 2021, Master Thesis Delft University of Technology, pp. 103

van Verseveld, W. J., Weerts, A. H., Visser, M., Buitink, J., Imhoff, R. O., Boisgontier, H., Bouaziz, L., Eilander, D., Hegnauer, M., ten Velden, C., and Russell, B.: Wflow_sbm v0.6.1, a spatially distributed hydrologic model: from global data to local applications, Geosci. Model Dev. Discuss. [preprint], https://doi.org/10.5194/gmd-2022-182, in review, 2022.

6   Appendix 5: Explanatory hydro-dynamic modelling notes (Deltares)

Author: Dipl.-Ing. Anke Becker

6.1   Starting point

The hydrodynamic modeling within this study used an existing model of the Dutch part of the Geul, including the Dutch part of tributaries Gulp, Selzerbeek and Eyserbeek described by Vermulst (2014), as starting point (Figure 6.1). It already contained the necessary boundary conditions for the July 2021 floo (Deltares, 2022).

Figure 6.1   Extent of the Sobek2 model of the Geul, including the existing Dutch and (within the red polygon) the new Belgian part. The dark blue lines represent the 1D component of the hydrodynamic model, the brown areas are the DEMs of the 2D component.

This model consists of a 1D hydrodynamic model in SOBEK2, coupled to a rainfall runoff component (RR). It extends from the Dutch-Belgian border near Cottessen (Geul) and Slenaken (Gulp), the Dutch-German border at Vaals (Selzerbeek) and Bocholtz (Eyserbeek) till Meerssen, where the Geul flows into the Meuse.

6.2   Modifications to and extension of the SOBEK model

To be able to analyze potential measures for flood hazard reduction in the entire catchment of the Geul, the branches of Geul and Gulp in the hydraulic model were extended into Belgium up to just upstream of Kelmis (Geul) and Hombourg (location Crucifix) (Gulp). To allow coupling to the rainfall runoff model recently developed in wflow_sbm, the original rainfall runoff component (RR) was deleted from the Sobek model. Instead, lateral flows were added at the most downstream locations of subcatchments from the wflow_sbm model. The paragraphs below describe the extension, coupling and modifications in more detail.

Extension of Geul and Gulp in Belgium

The extension of the Geul and Gulp in the hydro-dynamic model were done in a simple way, because they were needed for a quick assessment which did not leave time for extensive data collection nor extensive calibration and validation. The model extension, as much as possible, follows the same principles as applied to the original model of the Dutch Geul, i.e. the 1D branches represent the river main channels, while the flood plains are modeled in 2D with a grid resolution of 25 m x 25 m.

The location of the branches was based on OpenStreetMaps data. The 2D elevation grids were based on a high resolution (1 m x 1 m) DEM of Wallonia/Belgium (Relief de la Wallonie - Modèle Numérique de Terrain (MNT) 2013-2014). No cross section data was available for the river channels. Therefore, rectangular channels were carved into the high resolution DEM, and cross-sections were derived from this DEM along lines of 40 m width perpendicular to the channels (see Figure 6.2).

A constant Manning roughness coefficient was applied to the main channel and flood plains[2]. The roughness of the flood plains in the Dutch part, as present in the original model, is spatially variable, based on land use. This is kept as is in the extended model.

Bridges were not (yet) included into the Belgian part of the model for the quick assessment.

---

[2] Initially, a value of 0.05 $s/m^{1/3}$ was applied to both main channel and flood plains. Later, the main channel roughness was increased to 0.07 $s/m^{1/3}$ (in the entire model, not only the Belgian part), because this helped to better reproduce observed water levels around the city of Valkenburg (NL), and in order to compensate for not (yet) including the various bridges present in the Belgian part into the model. Tests with a flood plain roughness of 0.07 $s/m^{1/3}$ in the Belgian part of the model were run as well, but the influence of the change in roughness was minor compared to the impact of potential flood mitigation measures and the overall uncertainty in model results.

Figure 6.2   Location of transects for deriving river cross-sections along Belgian part of Gulp and Geul.

Coupling to hydrological model

The extended Sobek model contains four upstream boundaries (Kelmis/Geul, Hombourg crucifix/Gulp, Vaals/Selzerbeek and Bocholtz/Eyserbeek) and one downstream boundary (Meerssen/mouth into Meuse). The water level boundary condition downstream at Meerssen is left unchanged, it contains the observed water level in the Meuse river for July 2021. At the other three (upstream) boundary conditions the model is fed with discharge time series generated by wflow_sbm (see appendix 4) for the most upstream subcatchments of the Gulp, Geul, Eyserbeek and Selzerbeek as shown in Figure 6.3. Discharges from the remaining wflow_sbm subcatchments are applied to a series of laterals along the river branches.

The laterals in Sobek are placed onto the river branches at suitable locations as close as possible to the locations of the corresponding subcatchment discharge from wflow_sbm. The new laterals are given names that contain the corresponding subcatchment number from wflow_sbm in order to facilitate the coupling. All laterals that existed in the original SOBEK model were removed. After this modification, the SOBEK model is fully forced with discharges from wflow_sbm (and the water level in the Meuse).
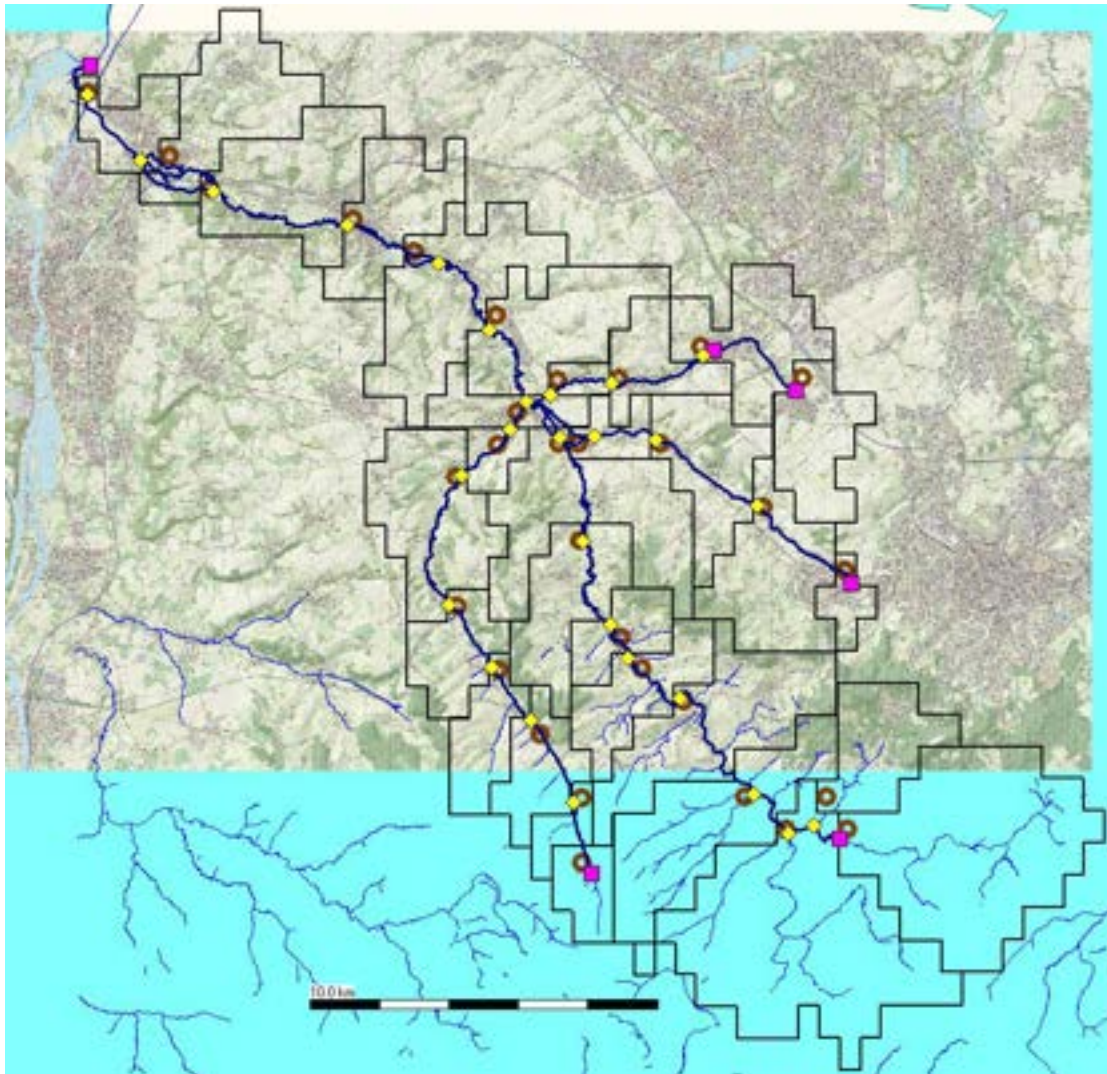
Figure 6.3   Coupling between hydraulic model in Sobek and hydrological model in Wflow. Pink squares mark the upstream and downstream boundaries of the hydrodynamic model in Sobek, yellow diamonds are locations with lateral inflow. The black polygons represent the subcatchments from the Wflow model, and the brown "rings" show the locations for which Wflow produces subcatchment discharges.

Verification of model results

Due to time constraints in this quick assessment, a plausibility check of model results was carried out instead of a proper calibration and validation of the extended model. The calculated discharges at several gauging stations were compared to observed values. However, measurements at most stations stopped due to damage to the stations during the peak of this extreme event. Furthermore, a closer look at the observations shows that they are maybe not too trustworthy (since measuring discharges during flood is very difficult): e.g. there is hardly any increase in observed discharge between Kelmis and Sippenaeken, although a significant subcatchment area is located in between. The difference in shape of the observed discharge time series between these stations indicates that there is some storage e.g. in the flood plains taking place along this river reach though.

Furthermore, the extent of flooding of the flood plains in Belgium was compared to flood maps produced by Wallonia for the EU flood directive for a 1/100 years flood[3]. A direct comparison of water depths was not possible, because we do not know which discharge this map corresponds to. But along the Geul flood extents in the model are very similar to the ones on the maps. Along the Gulp, with its very steep valley, the model shows hardly any flooding, compared to some (but little) flooding in the official flood maps. This is caused by an underestimation of the discharge in the Gulp by wflow_sbm. In earlier test simulations that use a higher discharge, some flooding was seen approximately in the areas that also appear on the official flood maps.

No further checks were carried out in the Dutch part of the model, since that part of the model already existed and had been calibrated before (Vermulst, 2014).
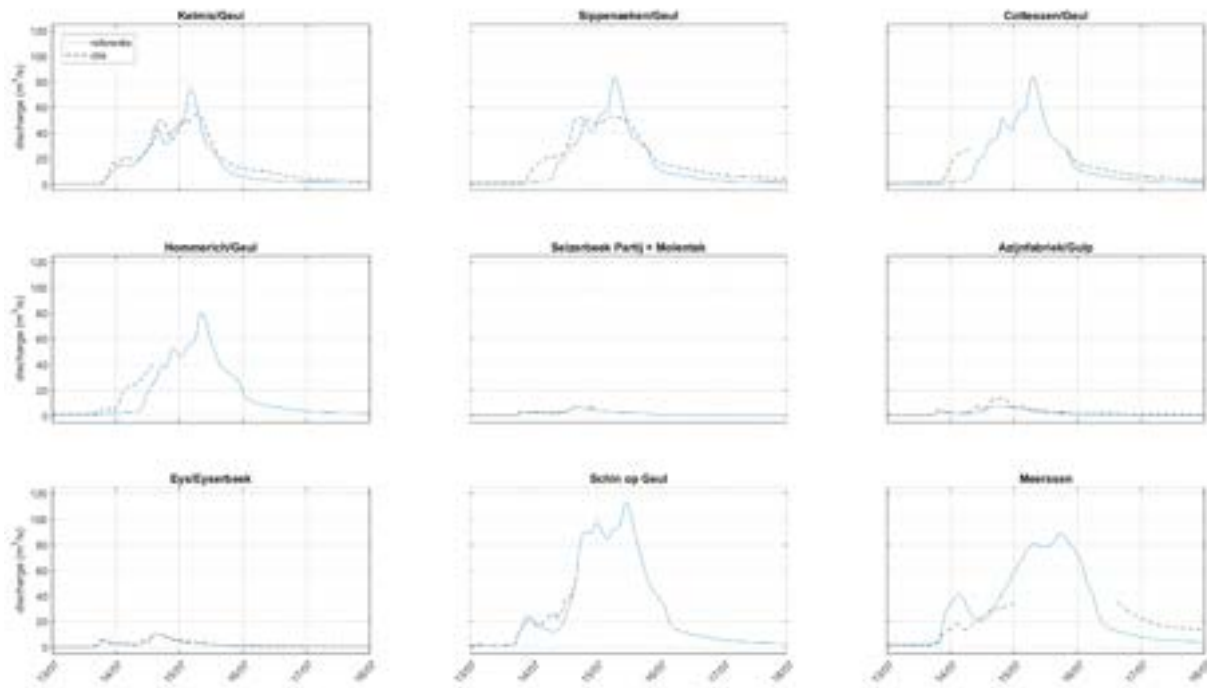

Figure 6.4. Modelled discharges of wflow_sbm + SOBEK model vs. observed discharges at nine discharge stations in the basin

---

[3] Carte de l'aléa d'inondation - Inondations en Wallonie | Inondations en Wallonie

6.3   Schematization of flood mitigation measures

At the start of this quick assessment, different possibilities for flood mitigation measures were discussed:

- land use changes (reforestation),
- storage by means of small scale rainfall retention basins in the hills of the catchment,
- storage in the flood plains along the rivers by means of dams or retention basins,
- re-meandering of the rivers to slow down and attenuate the flood,
- increasing the resistance of the river channels (e.g. by placing/not tidying up dead (branches of) trees) to achieve the same effect.

The first two are measures in the catchment and were therefore modeled in the hydrological model in Wflow. They were implemented into the Sobek-model by means of modified boundary conditions (upper boundaries and laterals, cf. section 0). As an extreme re-forestation scenario, the model run with re-forestation in the catchment was also tested in combination with re-forestation of the river flood plains themselves. The latter was implemented by means of a change in flood plain roughness to a value of n = 0.15 m/s$^{1/3}$. This corresponds to the resistance of an average flood plain forest according to Arcement and Schneider (1989).

Storage in the flood plains was implemented by building a dam across the flood plain by raising the corresponding cells in the 2D elevation grids and closing off the river (1D part) itself by means of a weir (Figure 6.4). The weir remains open during normal flow conditions and is closed during passage of the flood. The influence of the weir operation is discussed in the next section.

At the start of this quick assessment, different locations were deemed suitable (at the Dutch-Belgian border close to Slenaken on the Gulp, upstream of the bridge at Kelmis on the Geul, in the former mining area at Plombières/Geul, between Schin op Geul and Wijlre). Before implementing a dam into the model, these locations were checked based on the model results for the current situation. Since the Gulp only contributes little to the total discharge at Valkenburg and its valley is very narrow, a dam close to Slenaken would not sufficiently decrease the discharge at Valkenburg[4]. The areas at Kelmis and Plombières already function as large retention basins in the model (and in reality) of the current situation and therefore do not offer room for further retention (unless very extreme measures such as the digging of large caves or the excavation of a large part of surrounding mountains are taken). Therefore, a dam was implemented only between Schin op Geul and Wijlre (Figure 3.1). The crest level of the dam was set to 82 M+NAP, compared to an elevation of about 77 m+NAP at the deepest point of the river valley at this location. The crest of the weir is made 12 m wide and initially given a level of 77 m+NAP. When the weir closes, its crest is moved to a level of 82 m+NAP. Note that water can still overtop both the weir and the dam, also in "closed" state.

The re-meandering was implemented in the model by increasing the length of the Geul in both the Dutch and Belgian parts (but upstream of Valkenburg) by approximately 20% in total, see Table 6.1. The increased resistance of the river channels was achieved by changing the Manning roughness coefficient in the rivers to n = 0.15 m/s$^{1/3}$ (which is rather extreme).

---

[4] This was tested in an early version of the extended model but not repeated in the final version because of its limited effect.
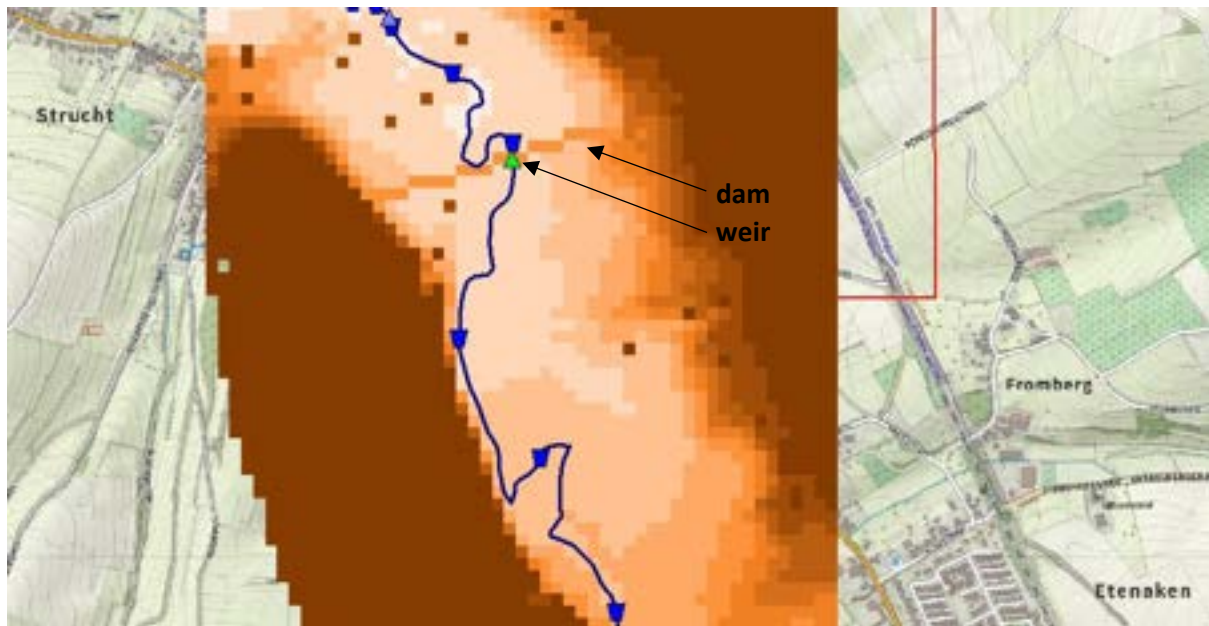
Figure 6.4   Dam and controllable weir implemented in the model between Schin op Geul and Etenaken/Wijlre as measure to block the flow during peak passage and therewith create additional storm water retention.

Table 6.1 Length of the river Geul branch in the model.

Model version	Length of branches in the model [km]		
	Geul in BE	Geul in NL	Geul total (up to upstream of Valkenburg)
Geul longer	16.1	26.6	42.7
original	12.8	22.7	35.5
Percentage of lengthening in model version with longer Geul	25.8%	17.2%	20.3%

6.4   Model results

Land use in the catchment

Changing the entire catchment (apart from the river valleys) into urban area results in significantly larger peak discharges at Valkenburg and along the entire river (Figure 6.5). The catchment loses its storage capacity entirely, which also results in an earlier arrival of the flood wave in the river and a much flashier behaviour. In the other extreme scenario, in which the entire catchment underwent re-forestation (apart from the river valleys), the peak discharge at Valkenburg is reduced by about 50 m³/s compared to the current situation. About half of this decrease can be attributed to the Belgian part of the catchment.

These two scenarios represent the limits of what can (theoretically) be achieved by changing land use. The more realistic scenario, in which only currently agricultural land is re-forested, results in a reduction of the discharge peak of only about 15 m³/s at Valkenburg, at the Dutch-Belgian border on the Geul the reduction is similar. So it seems as if the re-forestation in the Dutch part does not have any effect, but that's not true: the Dutch part mainly contributes to the first (and in our model smaller) flood peak, while the Belgian part mostly contributes to the second (but also partly to the first) flood peak.

If the river valleys are re-forested as well, this adds little extra peak reduction (about 5 m³/s) and a delay of the peak of about 2 h in the Belgian part of the catchment. At Valkenburg, both the peak damping and delay are significantly larger (about 45 m³/s and 6 h). The following paragraph gives some more reflections on the influence of increased flood plain resistance in the hydraulic model. The reason why the resistance in the Dutch part of the river valley has so much more influence on these parameters than the Belgian parts are that

1) the flood extent is larger in the Dutch part due to the wider river valleys, and
2) the average resistance in the current situation is lower in the Dutch part of the model than in the Belgian part. Extra simulations have shown that the spatially varying resistance in the Dutch flood plains is equivalent to using a constant roughness coefficient of about 0.025-0.03 m/s$^{1/3}$ (*Figure 6.7*), while a value of 0.05 m/s$^{1/3}$ is used in the Belgian part.

Note that despite the lower discharge, this strongly increased roughness in the river valleys also leads locally to significantly higher water levels than in the current situation! Depending on the location, water levels can even be several decimeters higher than in the current situation, despite the lower discharge!

Figure 6.6 shows the same results in terms of water volume passing through the river (a sort of indicative "cumulative discharge"). It gives an impression of how much water is stored in the catchment and the flood plains in the different scenarios. An interesting finding is that an increased resistance of the flood plain in the hydraulic model mainly leads to a delayed flood propagation and peak damping but does cause only little extra storage. That is due to the underlaying model concept: the hydraulic model does not take into account any hydrological process such as storage on leaves or (increased) infiltration into the soil. This is no problem for this analysis, because these processes are already taken into account in the hydrological model which covers the entire catchment, i.e. they are accounted for in the hydrodynamic model via the modified boundary conditions. The hydraulic model then adds the effects of delay and wave damping due to increased resistance, and only some change in storage due to the change in (peak) water levels.

Changing the current land use to cropland (except the urban areas) has only little effect on the river discharges, since the current land use is mostly pasture, and the associated hydrological parameters are similar to those of cropland.
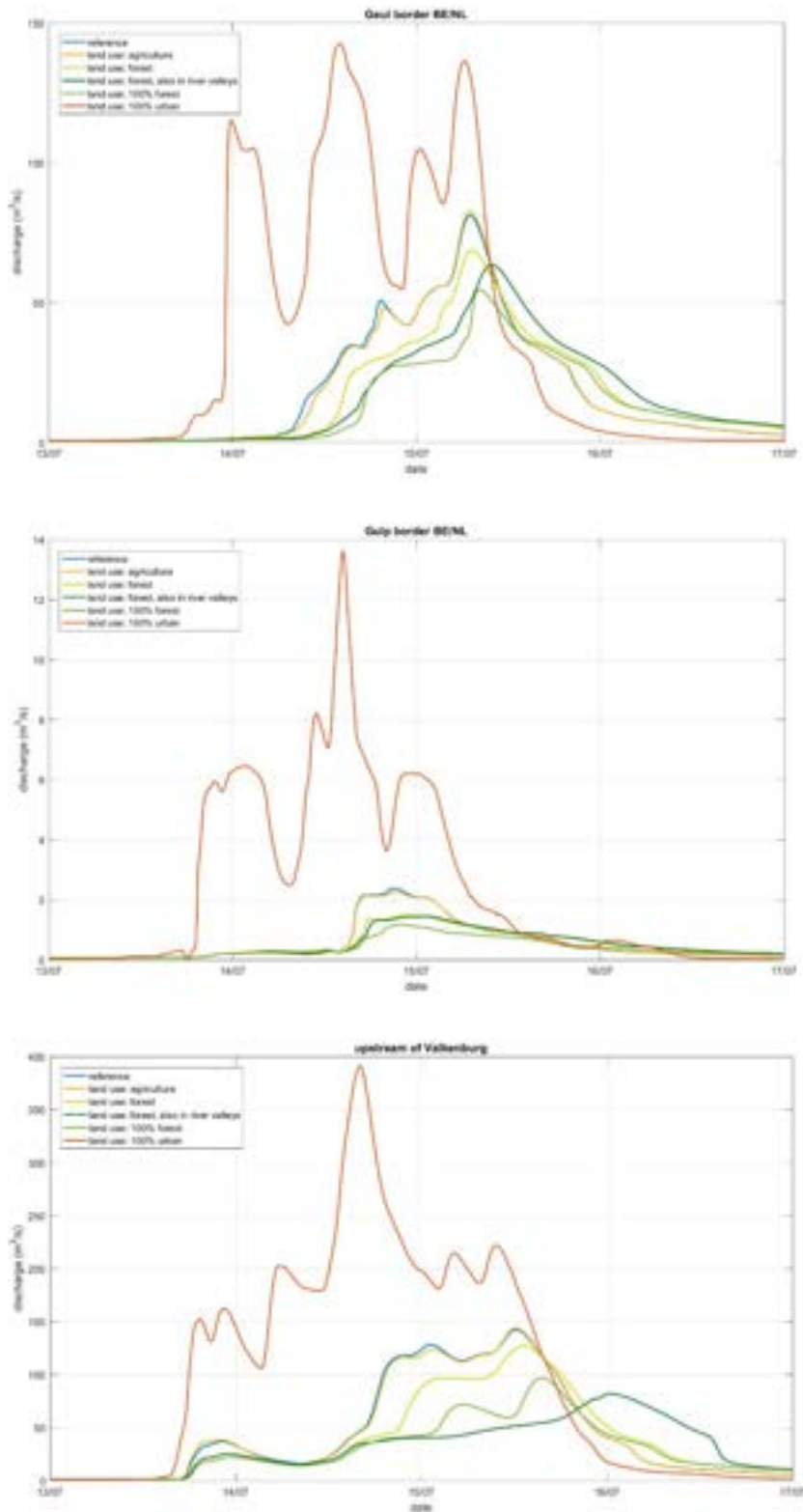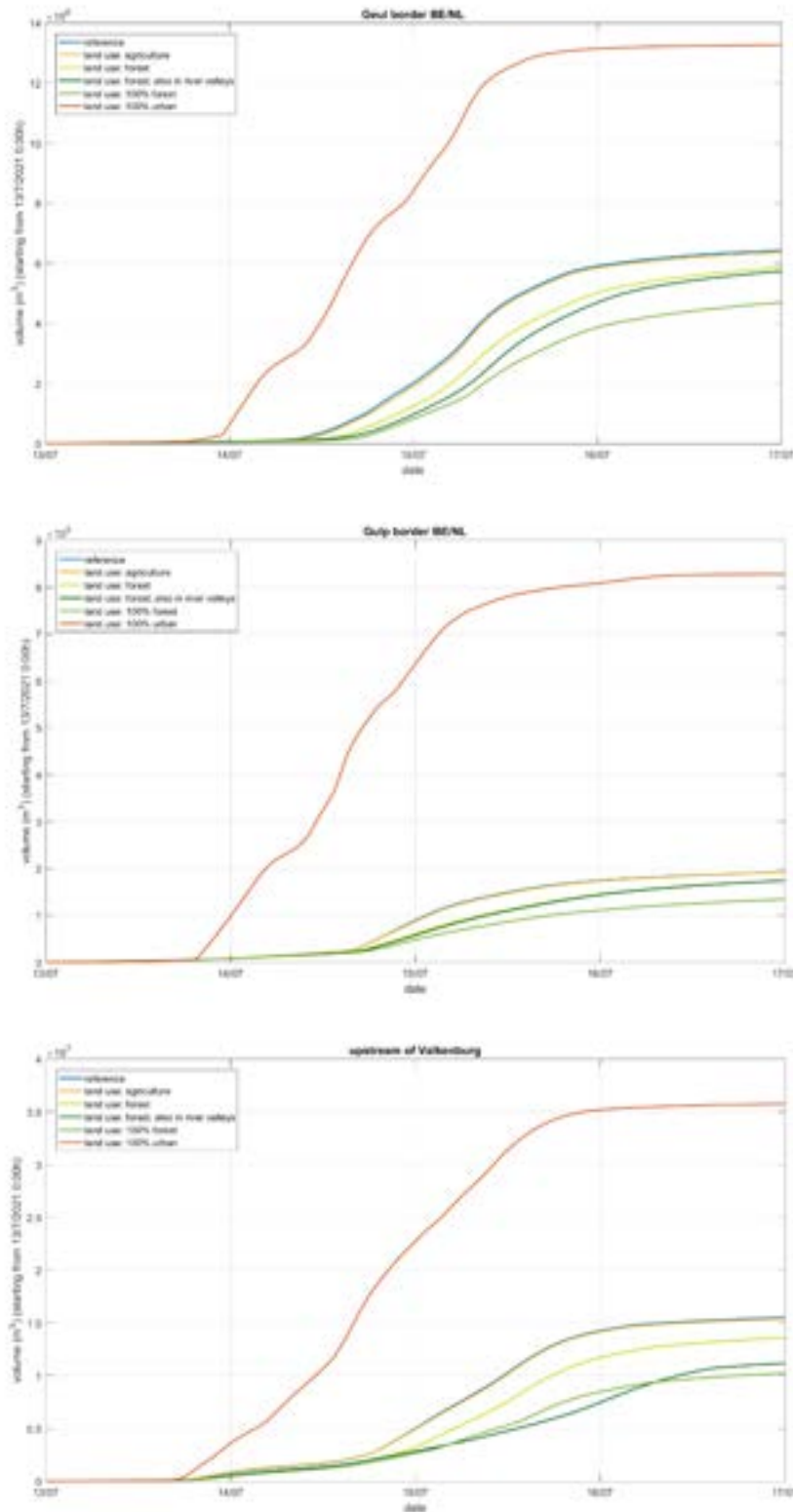
Figure 6.5   Modelled discharge upstream of Valkenburg (gauging station Hertenkamp) and at the Dutch-Belgian border in Geul and Gulp for different land use scenarios. Blue = current state (reference), yellow = current land use (apart from urban areas) replaced with cropland, light green = current land use (apart from urban areas) replaced with forest, dark green = idem, but also river valleys with forest, medium green = 100% of catchment area replaced with forest, but not the river valeys, red = 100% of catchment area replaced with urban area.

Figure 6.6   *Modelled volume of water ("cumulative discharge") upstream of Valkenburg (gauging station Hertenkamp) and at the Dutch-Belgian border in Geul and Gulp for different land use scenarios. Blue = current state (reference), yellow = current land use (apart from urban areas) replaced with cropland, light green = current land use (apart from urban areas) replaced with forest, dark green = idem, but also river valleys with forest, medium green = 100% of catchment area replaced with forest, but not the river valeys, red = 100% of catchment area replaced with urban area.*
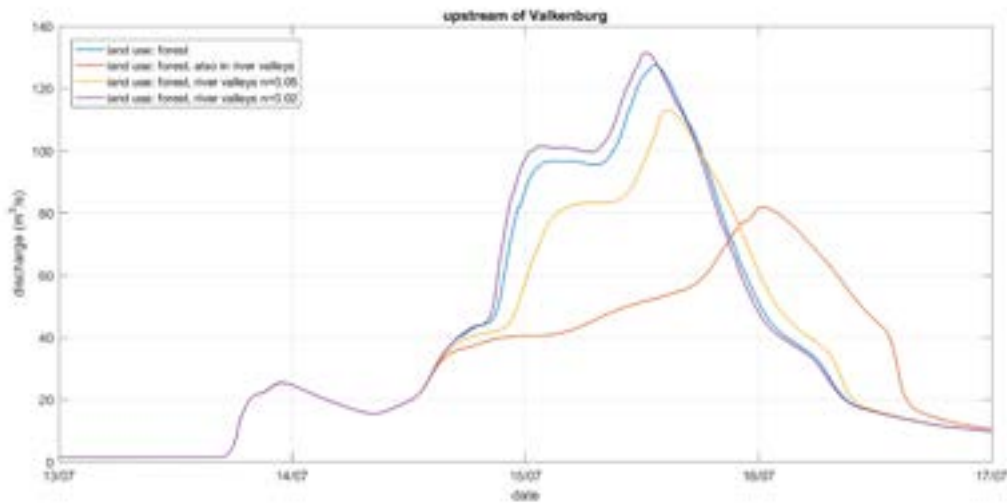
Figure 6.7   Modelled discharge upstream of Valkenburg (gauging station Hertenkamp) for different roughness coefficients in the Dutch 2D grids. Blue = current state, red = reforestation of all river valleys, yellow = current state but roughness in NL replaced with n = 0.05 s/m$^{1/3}$, purple = current state but roughness in NL replaced with n = 0.02 s/m$^{1/3}$.

Small-scale rainfall retention basins in the catchment

Figure 6.8 shows that the small-scale reservoirs in the catchment have some effect on the discharge in the rivers. However, they mainly lower the discharge during the rising limb of the flood, because that is the period during which they are filled. For a more significant influence on the actual flood peak of this extreme event, they would have to be made bigger or controllable and activated only at a later moment.
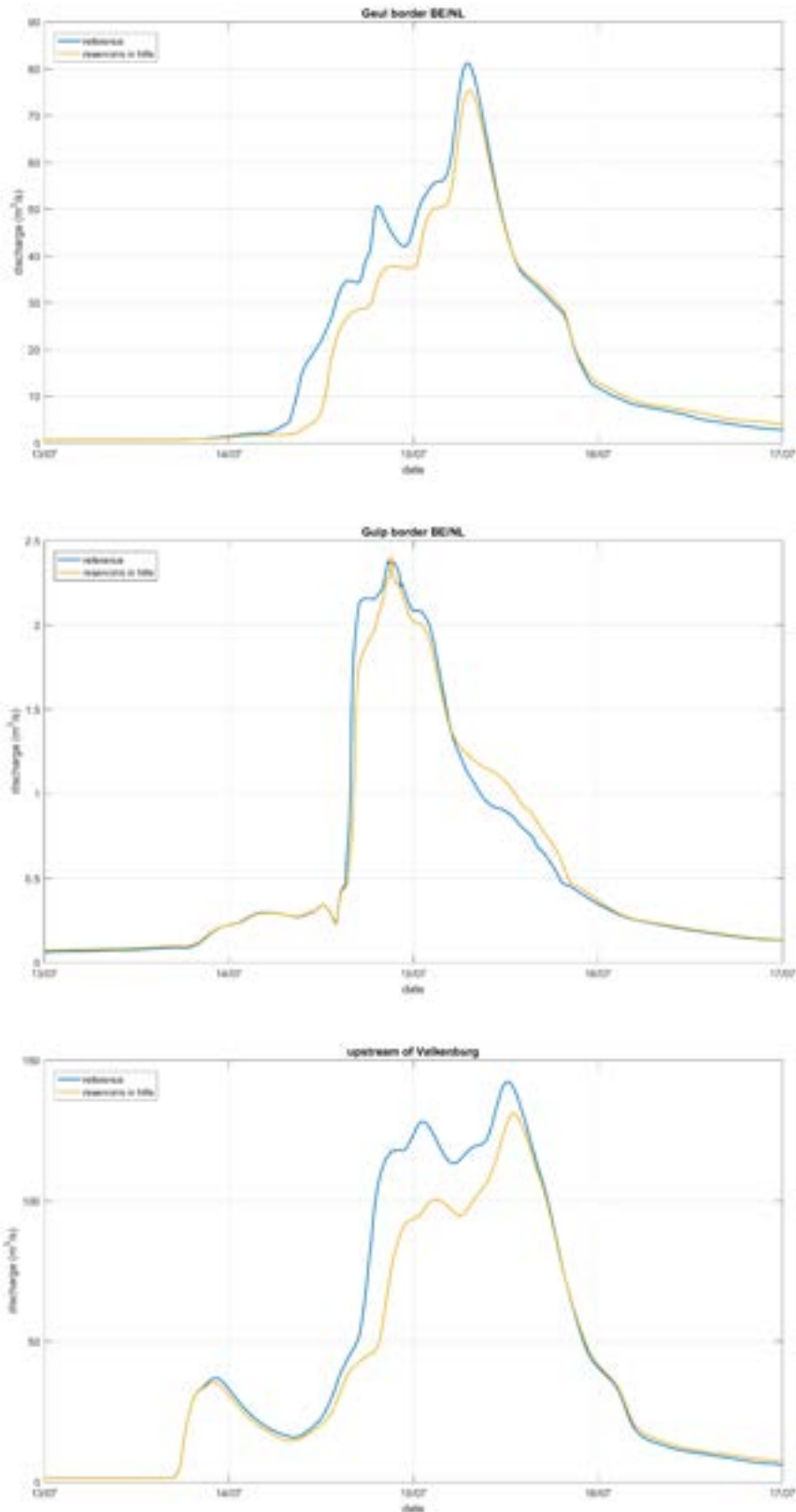
Figure 6.8   Modelled discharge upstream of Valkenburg (gauging station Hertenkamp) and at the Dutch-Belgian border in Geul and Gulp for the current situation (blue line) and the scenario with small-scale retention basins in the catchment (yellow line).

Dam at Schin op Geul

In contrast to the small-scale retention basins in the catchment, the dam at Schin op Geul is a rather extreme measure. With a dam crest level of up to 5 m above the current terrain, it can store a significant volume of water, that is about 2 Million m³, so similar to the volume that can be stored in the catchment. This can be seen in the difference between the volume in the reference situation (blue line) and all the other lines in *Figure 6.10* on 16th July, which is just after complete filling but before release of water after the flood.

The reservoir behind the dam stores the same volume of water in all three scenarios. However, Figure 6.9 shows that this only decreases peak flow at Valkenburg if the storage is activated at the correct moment in time (i.e. the weir is closed at the correct moment in time). So this measure only works well if

- the dam is controlled, and
- the dam operator knows the shape and dimension of the expected flood wave very well and sufficiently in advance.

That means that a well-working flood forecasting system is needed in combination with such a dam.

Do note that the dam not only decreases discharges and water levels downstream (*Figure 6.12*) but also increases water levels and flood extent upstream of the dam (*Figure 6.11*). Just upstream of the dam water depths of up to 5 m are reached, and the extent of the flooding gets significantly larger than in the situation without dam. The water level rise extends to approximately Stokhem, some 1,5 km upstream of the dam. Downstream of the dam, flood extent stays similar as before in the model. That is due to a combination of the relatively flat terrain with a modelled grid size of 25 m, which is relatively coarse.
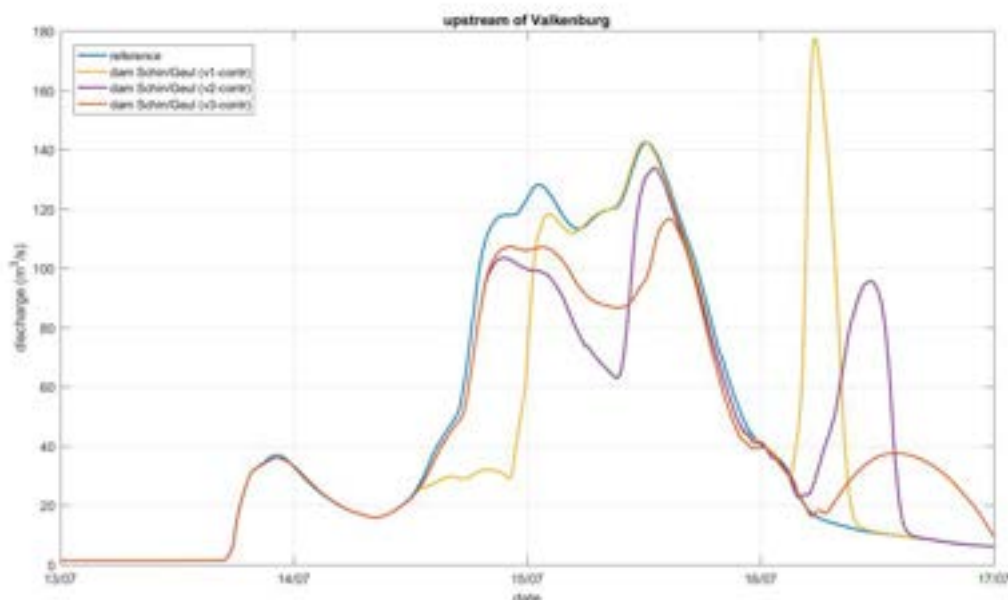

Figure 6.9   Modelled discharge upstream of Valkenburg (gauging station Hertenkamp) for the current state (blue line) and after implementing a dam between Schin op Geul and Wijlre with different operation (red, yellow and violet lines).
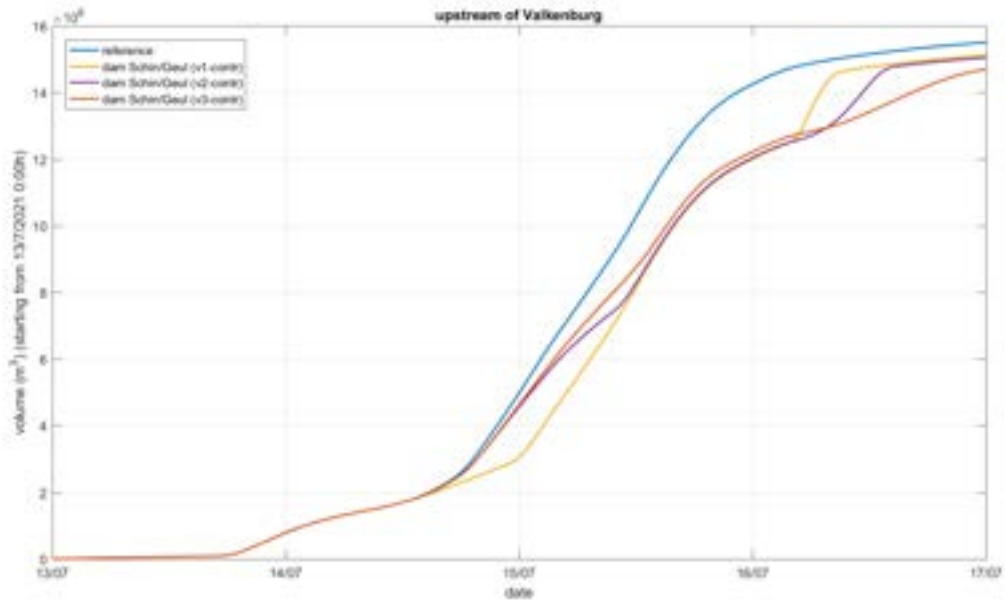
Figure 6.10   Modelled volume of water ("cumulative discharge") upstream of Valkenburg (gauging station
               Hertenkamp) for the current state (blue line) and after implementing a dam between Schin op Geul and
               Wijlre with different operation (red, yellow and violet lines).
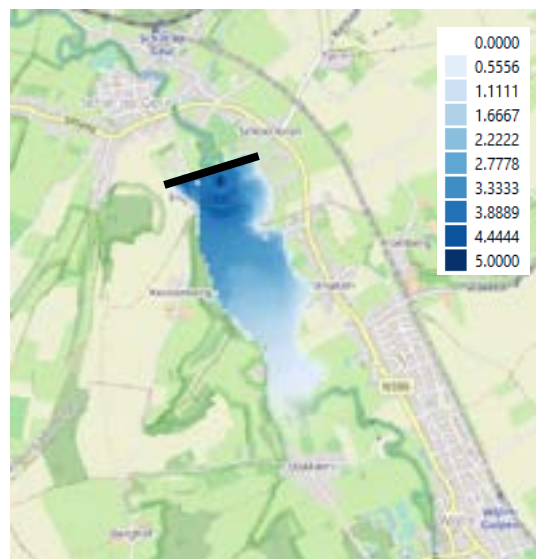

Figure 6.11   Water level difference (m) upstream of the dam (v3, i.e. the red line from the previous figures), the black
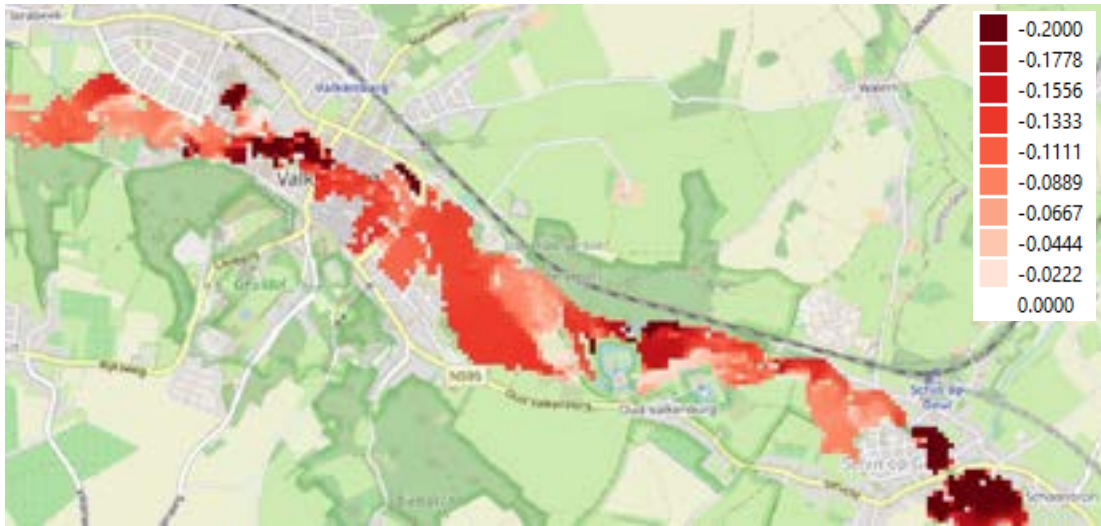   bold line indicates the location of the dam.

Figure 6.12   Water level difference (m) downstream of the dam (v3, i.e. the red line from the previous figures).

Re-meandering

Adding length to the rivers by re-meandering only has a slight effect on the timing of the flood peak and less on the peak discharge (*Figure 6.13*). Furthermore, the rivers are already pretty close to natural along large stretches, so it will be difficult to introduce much more meandering.
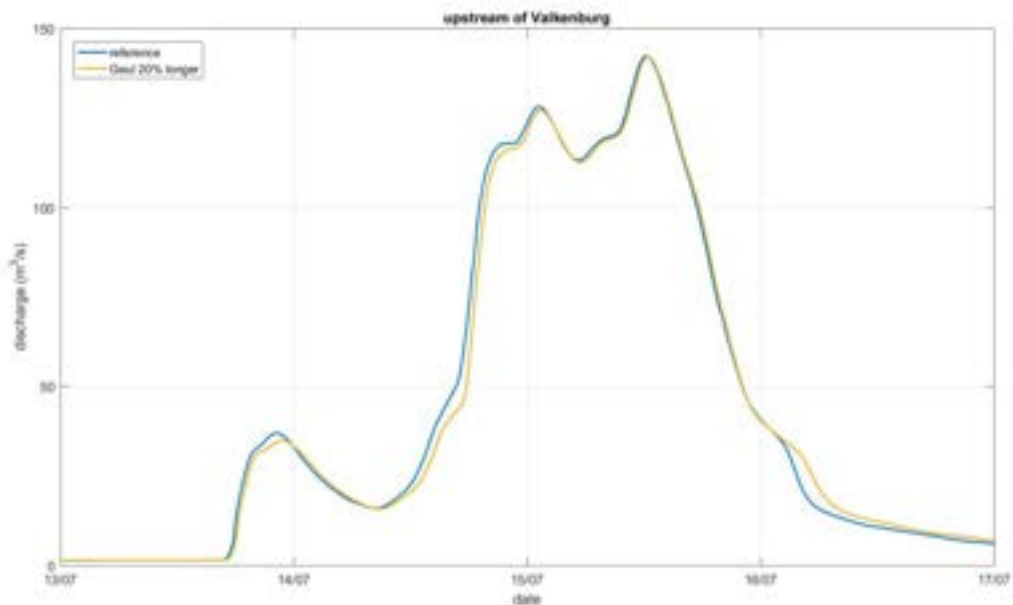

Figure 6.13   Modelled discharge upstream of Valkenburg (gauging station Hertenkamp) for the current state (blue line) and after re-meandering the Geul (20% extra length, yellow line).

Increased resistance in river channels

Increasing the resistance in the river branches leads to some delay and different timing in the storage of water along the rivers branches. The total volume of water that reaches Valkenburg remains the same (*Figure 6.15*). Note that increasing the resistance also leads to higher water levels on and upstream of the sections with increased resistance.

Also note that the increased resistance in the river bed is rather extreme and thus not realistic (n = 0.15 s/m$^{1/3}$ along all river branches).
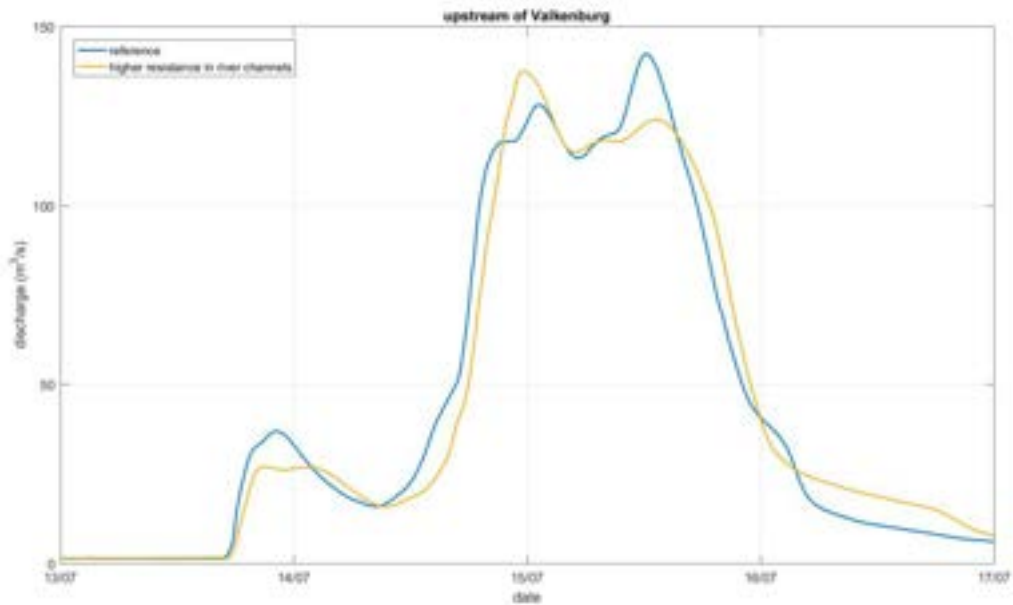
Figure 6.14   Modelled discharge upstream of Valkenburg (gauging station Hertenkamp) for the current state (blue line) and with higher resistance on all the river beds (yellow line).
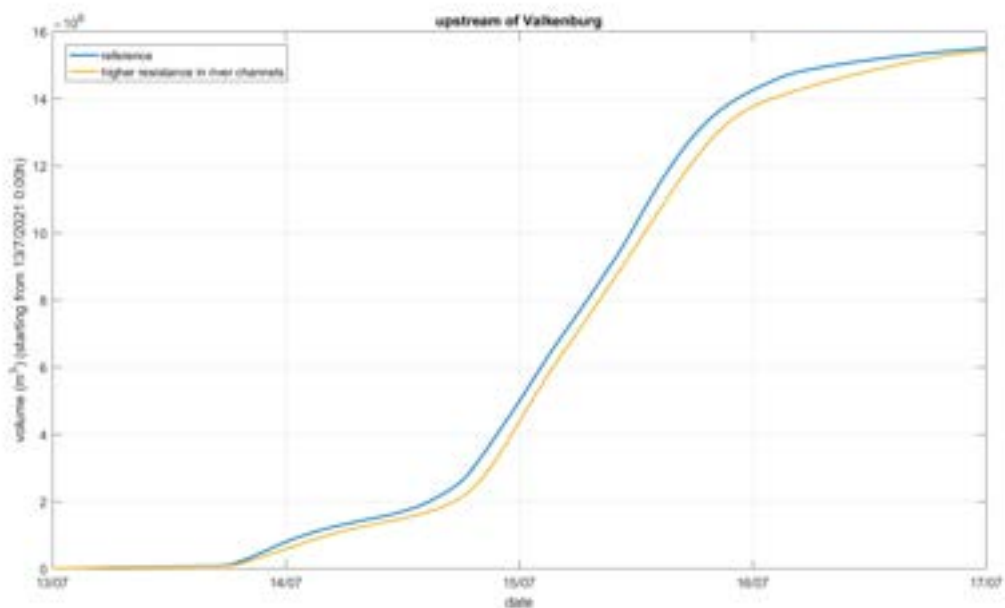

Figure 6.15   Modelled volume of water ("cumulative discharge") upstream of Valkenburg (gauging station Hertenkamp) for the current state (blue line) and with higher resistance on all the river beds (yellow line).

References

Arcement, G.J., and V.R. Schneider (1989): Guide for Selecting Manning's Roughness Coefficients for Natural Channels and Flood Plains. United States Geological Survey Water-Supply Paper 2339.

Vermulst, J.A.P.H. (2014): Watersysteemtoets Geul, Geleenbeek en Roer. Report Royal Haskoning DHV, 6 november 2014.

7   Appendix 6: Overview of flood protection measures in Cologne district (RWTH Aachen)

Technical appendix report by IWW at RWTH Aachen University (Klopries, 2022)

Lehrstuhl und
Institut für
Wasserbau und
Wasserwirtschaft

RWTHAACHEN
UNIVERSITY

Rapid assessment study on the Geul river basin: floods and adverse cosequences
Technical appendix report by IWW at RWTH Aachen University

September 2022

Dr.-Ing. Elena-Maria Klopries

Mariana Vélez Pérez, B.Sc. RWTH

Rapid assessment study on the Geul river basin: floods and adverse co-sequences
Technical appendix report by IWW at RWTH Aachen University

Dr.-Ing. Elena-Maria Klopries
Mariana Vélez Pérez, B.Sc. RWTH

Lehrstuhl und Institut für Wasserbau und Wasserwirtschaft
RWTH Aachen University
Mies-van-der-Rohe-Str. 17
D-52056 Aachen

Content

Figures

1 Introduction

1.1 Background

The July 2021 flood hit western parts of Germany severely. After an above-average rainy June, further heavy to very heavy precipitation occurred in the course of storm low "Bernd" in mid-July. The daily precipitation totals were in some cases well above 100 mm over several days. The high soil moisture combined with the heavy precipitation led to flooding at several small and large water bodies in western Germany, in some cases significantly exceeding the predicted effects of extreme flooding.

Reasons for the sometimes catastrophic consequences of the flood are manifold and in some cases not yet conclusively understood and addressed. In expert circles, it is assumed that several factors were responsible for the extent and that these partly overlapped and accumulated. These include but are not limited to:

- The meteorological severity of the rain event
- High soil moisture before the event
- High slopes in catchment areas
- High degree of sealing within catchment areas
- Little to no warning time before flood peaks reached cities
- Failure of the gauges and thus missing situation picture
- Failure of critical infrastructures such as streets, railways, bridges, electricity, communication, fresh water, wastewater treatment, …
- Lack of awareness that such an extreme event is possible in administration, disaster response, and the general public
- Lack of awareness in general public how to behave in an extreme event like this
- And several more

Since July 2021, IWW has been involved in several small and large research projects on the processing, classification and management of the flood event. Two ad-hoc projects funded by the German Research Foundation (DFG), the two BMBF-funded projects KAHR and HoWas2021, the European-funded Interreg project EMFloodResi-lience, the project "Hochwasserresiliente Stadtentwicklung Stolberg und Eschweiler" (flood resilient urban development Stolberg and Eschweiler) led by the Waterboard Eifel-Rur and several water-related expertises on the flood are only a few selected ongoing and completed projects on the 2021 flood.

1.2 Objectives

These existing projects focus mainly on German catchment areas but can yield great value for similar areas in the Netherlands and Belgium as well since there has been substantial damage there as well in July 2021. The object of this technical report is to give an overview of potential mitigation measures and how they have been evaluated regarding their efficacy for small catchment areas in Germany (Part One) and an overview of two technical flood mitigation measures in the catchment of the river Eifel-Rur in Germany (Part Two).

1   Rapid assessment on the Geul river basin – technical appendix report IWW

2 Part One – List of potential flood protection measures

Between September 2021 and March 2022, the District Government Cologne funded a project called "Flood resilient urban development for Stolberg and Eschweiler" as a result to the flood event in July 2021. In this project, a set of experts from municipalities, administration, disaster response, universities and public organisations worked together on the development of a list of possible measures to reduce flood risk in the specific area of the two cities Stolberg and Eschweiler. This list has been developed in four workshops during which an initial evaluation on the measures' expected effectiveness, realizability and time line was performed by the experts.

The measures are divided in two main objectives: the potential flood protection measures in the catchment areas (Table 1) and the flood protection in urban areas (Table 2). They are divided again in sub-categories.

Table 1: Potential flood protection measures in the catchment areas

I Unsealing of soil	
a)	Unsealing and creating infiltration-capable areas with water-permeable coatings respectively
b)	Avoidance of building in risk areas (adaptation, new delimitation, translation of building areas)
II Surface management in hazards areas	
a)	Consideration of historical street names to identify sinks and waterways during inundations
b)	Protection, rehabilitation, and regeneration of forests in areas of origin during heavy rainfall
c)	Use of forests as retention areas
d)	Protection and preservation of meadows and pastures
e)	Adaptation of agricultural and forest management practices
f)	Use of agricultural areas as retention areas
g)	Terracing (arable terraces)
h)	Conversion of arable land into grassland or deciduous/mixed forest
i)	Demolition of agricultural and forestry roads or design of drainable unpaved roads
j)	Adaptation of water crossings (avoidance of bridges/pipes)
k)	Permanent greening of drainage channels with erosion risk
l)	Blue and green infrastructure (residential areas)
m)	Ditch and trough systems for surface water drainage
n)	Bank stabilization as erosion barriers in rivers
o)	Creation of swales on agricultural areas
p)	Creation of buffer areas through appropriate riparian vegetation
q)	Creation of structures to retain debris/trees/wood
III Renaturation	
a)	Increasing the retention capacity of existing channels and floodplains
b)	Renaturation of riparian forests and floodplains, natural succession
c)	Providing space along the river - "Space for the river"
d)	Rewetting of wetlands (e.g., renaturation of marshlands/moors)
IV Flood and rainwater retention basins	
a)	Creation of rainwater retention basins and swales
b)	Creation of floodplains (e.g., controlled polders).
c)	Consideration of localized measures (e.g., also in smaller tributaries)

Table 2: Potential flood protection measures for urban areas

	I Redirecting flood streams
a)	Targeted drainage or storage of floodwater via selected routes and areas (roads, flood control channels, parks, playgrounds and sports fields, railway lines)
b)	Collection, drainage, and retention of rainwater via adapted urban drainage systems
c)	Ditch and trough systems for surface water drainage
d)	Creation of culverts with an appropriate hydraulic design
e)	Draining run-off away from buildings into infiltration areas on properties (e.g. rain garden)
f)	Redirecting water to areas with low damage potential e.g. by linear protection structures
g)	Consideration of historical street names to identify sinks and waterways during inundations
	II Dikes and flood protection walls
a)	Construction of permanent walls and ground sills to protect areas with high damage potential
b)	Implementing management rules on operational safety at flood protection structures (e.g. blockage removal before an event)
	III Mobile flood protection
a)	Planned mobile flood protection
b)	Unplanned / emergency mobile flood protection
	IV "Space for the river"
a)	Avoidance of settlements in floodplains or, if necessary, abandonment of settlements
	V Flood-adapted land use and construction
a)	Consideration of different flood risks in urban land use planning
b)	Flood-adapted building, especially for critical infrastructure
c)	Avoidance of building in hazard zones
d)	Re-evaluation of building locations and their use, reassignment of building use
e)	Creation and maintenance of retention areas in settlement areas
f)	Underground storage (e.g. sponge city)
	VI Object-related protective measures
a)	Financial promotion of object-related protective measures
b)	Promotion of elemental damage / natural hazard insurance for buildings
c)	Obligation to consultation for flood-adapted construction for new buildings in risk areas
d)	Consideration of flood-adapted construction, especially for critical infrastructure
e)	Sealing of house walls (e.g. black tubs, white tubs)
f)	Sealing of pipe feedthroughs
g)	Consultations from independent flood protections experts
h)	Design of flood-proof wastewater treatment plants
i)	Safe storage of potentially harmful substances to prevent contamination
j)	Flood-adapted construction of bridges, bridge railings and bridge foundations
k)	Establishing operating regulations during flood events for commercial and industrial facilities
	VII Education and information
a)	Explaining and comprehensively visualizing specific risks to the population at their own houses
b)	Raising public awareness of flooding and constant reiterations
c)	Conveying information on correct procedures and behavior in the event of flooding
d)	Promotion of establishing and maintaining relationships with relevant persons of contact (especially within governmental and civil protection context) → "Knowing heads in the crisis"
e)	Adapt flood hazard maps regarding to specific requirements of civil protection services
f)	Transparent communication of measures, public and citizen participation
g)	Promotion of individual, in-depth consideration of personal flood risk (e.g. flood identification cards, flood protection cards)
h)	Raising awareness in previously flooded areas (e.g. installation of high-water marks)
i)	Promotion of constant coordination, exchange, and feedback discussions between stakeholders (e.g. water boards, district governments, water authorities, municipalities)

In total, 196 individual measures were identified. Most measures belonged to the three categories "flood and rainwater retention basins", "redirecting flood streams", and "space for the river" (Figure 1). Out of the 196 measures, 24 were deemed "unrealistic" with regard to their realizability, 72 were categorized as "good" and 100 as "favored approach". The 172 measures that have been categorized as "good" and "favored" were further condensed into 63 projects. Each project can contain one or more measures that are to be considered as interrelated. An example for the condensation into projects is measures that describe different variations of a flood retention basin at the same river section, where only one will be realized in the end. Amongst the 63 projects, 16 % were estimated to be "Quick win" projects that can be realized within 1 to 3 years. An example are structures that can retain debris upstream of cities. Another 8 % of the projects actually describe measures that have already been on-going but haven't been finished yet. 11 % of the projects are estimated to be implementable without any considerable pre-studies regarding their realizability but open questions regarding their feasibility and cost-effectiveness. The remaining projects were classified as "open projects" that would first require detailed technical re-views and study of their effectiveness. Thus, these open projects are considered to be realizable within more than 3 years and possibly even more than 10 years.
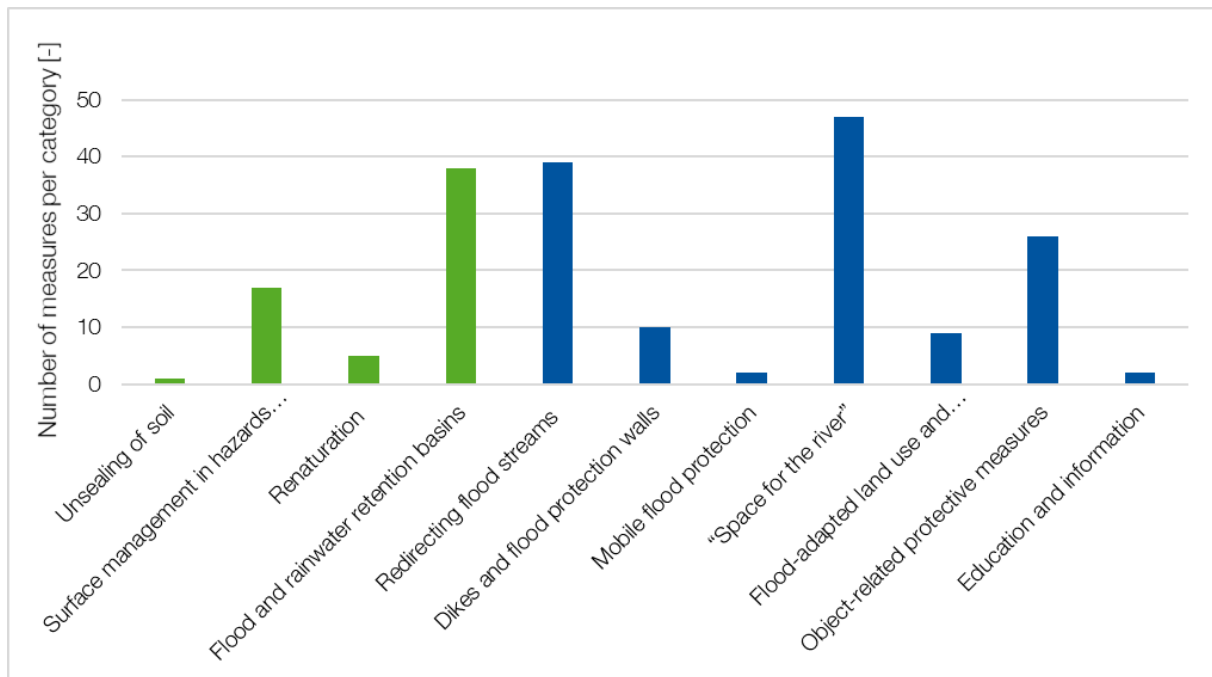

Figure 1: Result of expert workshop regarding possible flood protection measures for the cities Stolberg and Eschweiler

3   Part Two – Flood / rainwater retention basins in Eifel-Rur catchment area, Germany

3.1 Terminology and difference between both systems

Retention basins are excavated areas or even natural depression areas that capture runoff water temporally and release it time-delayed back into the environment via surface flow primarily, or via evapotranspiration and infiltration. The main difference between flood retaining and rainwater retention basins is their location in the water system.

Flood retention basins are basins, which temporarily store flood water in watercourses. The main purpose is the regulation of the discharge of a watercourse during floods. Generally, the structure blocks off the cross-section of a watercourse over the entire valley profile. Flood retention basins are thus largely equivalent to dams in terms of effect within the river. However, they differ from these in terms of their task, their mode of operation and often also their dimensions. Depending on the degree of filling, a flood retention basin is called a dry basin or green basin (empty basin) or a permanent reservoir (filled basin). Flood retention basins in the "mainstem" are flowed through directly by the watercourse, whereas flood retention basins in the "tributary" are not directly flowed through by the watercourse, but the basin is located laterally next to the river.

Figure 2: Flood control reservoirs, (a) flood retention basin Düren, (b) flood retention basin Broicherbach

Rainwater retention basins are artificially created basins that serve to store large precipitation water volumes. However, in contrast to the flood retention basin, they are not located in or on a river course. It is often found in cities and along highways where drainage of large areas without intermediate storage would overload the downstream drainage collection system. The reservoir temporarily stores rainwater runoff from a drainage catchment from small to moderate flood events and reduces their outflow to allow the downstream flow rates to be kept within the design capacity of the drainage system. Rainwater retention basins usually have a useful volume of 150-250 cubic meters per connected hectare of paved area, but more or less depending on local conditions.

Figure 3: Rainwater retention basin Ulm

3.2 Distribution of flood and rainwater retention basins in the Eifel-Rur catchment area in Germany

In the catchment area of the Eifel-Rur in Germany, there are several dozens of retention basins. Their locations and sizes vary widely depending on their explicit purpose and design. Official information on retention basins can be found online in ELWAS-WEB (https://www.elwasweb.nrw.de/). ELWAS-WEB is an electronic water management system for the water management administration in NRW. The system provides data in the fields of wastewater, groundwater, surface water, drinking water and the Water Framework Directive.

In the Eifel-Rur catchment area in Germany, there are a total of 33 flood retention basins situated at tributaries of the Rur in the Eifel (Figure 4). Their maximum capacity varies between approximately 2.000 m³ to around 100.000 m³. Their affected aboveground basin catchment area also varies significantly between 1,2 mio. m² to 41 mio. m² (Table 3).
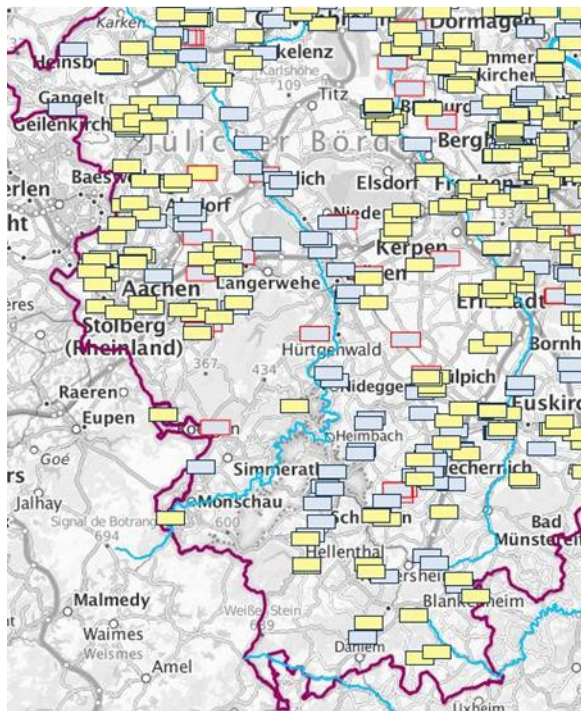

Figure 4: Flood retention basins in the Eifel-Rur catchment area

Table 3: Flood retention basins operated by the Waterboard Eifel-Rur

Flood retention basin	Municipality	Water body index	Water body name	Capacity [m³]
Katzem	Erkelenz	28256	Baaler Bach	
Lövenich	Erkelenz	28256	Baaler Bach	
Beeck	Geilenkirchen	28288	Beeckfließ	22.490
Drove	Kreuzau	2823792242	Boicher Bach	10.155
HRB Herzogenrath	Herzogenrath	28284	Broicher Bach	97.000
Konzendorf	Langerwehe	282386	Derichsweiler Bach	28.500
HRB Rabental	Aachen	2828322	Dorbach	5.000
Hetzerath	Hückelhoven	282562	Doverener Bach	20.100
Doverhahner Bach	Hückelhoven	2825622	Doverhahner Bach	6.521
Thum	Kreuzau	28237922	Drover Bach	18.200
HRB Euchen	Alsdorf	282844	Euchener Bach	90.000
Jüngersdorf	Langerwehe	28238684	Geicher Bach	8.250
Gereonsweiler Fließ	Linnich	282882	Gereonsweiler Fließ	76.470
Schleiden	Aldenhoven	2825342	Hoengener Fließ	21.800
HRB Ritscheider Hof	Aachen	2824322	Holzbach	1.785
Evertzbruch	Hückelhoven	282574	Hückelhovener Bach	7.870
Uetterath	Heinsberg	282894	Kötteler Schar	
Berzbuir	Düren	28238	Lendersdorfer Mühlen-teich	23.460
Golkrath	Erkelenz	28258	Millicher Bach	
Schaufenberg	Hückelhoven	28258	Millicher Bach	20.100
Kleingladbach	Hückelhoven	28258	Millicher Bach	20.000
Faulendriesch	Hückelhoven	28272	Mühlenbach Ratheim	
Altmyhl	Hückelhoven	28272	Mühlenbach Ratheim	23.000
Randbach	Düren	2823852	Randbach	3.812
Nierstraß	Geilenkirchen	281822	Rodebach	
HRB Siepenbusch	Übach-Palenberg	281822	Rodebach	
Kleinwehrhagen	Gangelt	2818222	Saeffeler Bach	
Echtz	Düren	2823868	Schlichbach 1	46.000
Merode	Langerwehe	2823868	Schlichbach 1	9.700
In der Schroiff	Übach-Palenberg	282872	Uebach	
HRB Rahe	Aachen	282832	Wildbach	80.900
Herb	Geilenkirchen	2828	Wurm	
HRB Neuköllnerstraße	Aachen	2828	Wurm	7.000

The ELWAS system classifies rainwater retention basins on the basis of two main characteristics, the sewer type and the municipal and industrial basins. In total, there are 47 rainwater retention basins in the area of Waterboard Eifel-Rur (Figure 5) and 87 % of them are installed at a combined sewer type (Table 4)

Figure 5: Rainwater retention basins in the Eifel-Rur catchment area

Table 4: Rainwater retention basins operated by the Waterboard Eifel-Rur

Rainwater retention basin	Municipality	Sewage treatment plant	Sewer type
Kleebach/Krebsstr.	Aachen	Eilendorf	Combined sewer
RRB 604 Horbacher Str.	Aachen	Aachen-Horbach	Combined sewer
Hüttenstraße	Aachen	Aachen-Soers	Combined sewer
Karl-Friedrichstr.	Aachen	Aachen-Horbach	Combined sewer
Messweg, Kalterherberg	Monschau	Kalterherberg	Combined sewer
Walther-Dobbelmann-Straße	Stolberg (Rhld.)	Steinfurt	Combined sewer
Höhenstraße K6	Stolberg (Rhld.)	Steinfurt	Combined sewer
In der Schart	Stolberg (Rhld.)	Steinfurt	Combined sewer
Breiniger Berg	Stolberg (Rhld.)	Steinfurt	Combined sewer
Amaliastraße	Stolberg (Rhld.)	Steinfurt	Combined sewer
Krähwinkel	Monschau	Konzen	Separate sewer
Gartenstraße	Eschweiler	Eschweiler-Weisweiler-ZKA	Combined sewer
Wollenweberstraße	Eschweiler	Eschweiler-Weisweiler-ZKA	Combined sewer
Röhe Nord	Eschweiler	Eschweiler-Weisweiler-ZKA	Combined sewer
An der Wasserwiese	Eschweiler	Eschweiler-Weisweiler-ZKA	Combined sewer
Otto-Hahn-Straße	Baesweiler	Setterich	Combined sewer
Adenauerring	Baesweiler	Setterich	Combined sewer
Franzosenkreuz	Stolberg (Rhld.)	Steinfurt	Combined sewer
Gressenich	Stolberg (Rhld.)	Eschweiler-Weisweiler-ZKA	Combined sewer
Hauptstraße	Herzogenrath	Herzogenrath-Worm	Combined sewer
Ackerstraße	Herzogenrath	Steinbusch	Combined sewer
Kleebach/Krebsstr.	Aachen	Eilendorf	Combined sewer
RRB 604 Horbacher Str.	Aachen	Aachen-Horbach	Combined sewer

Rapid assessment on the Geul river basin – technical appendix report IWW   8

Anna-Klöcker-Str.	Herzogenrath	Herzogenrath-Worm	Combined sewer
Hüttenstraße	Aachen	Aachen-Soers	Combined sewer
Karl-Friedrichstr.	Aachen	Aachen-Horbach	Combined sewer
Dietrich-Bonhoeffer-Str.	Herzogenrath	Frelenberg	Combined sewer
Umkehr	Nideggen	Schmidt	Combined sewer
RRB Gewerbegebiet Zingsheim	Nettersheim	Urft-Nettersheim	Separate sewer
Akazienstraße	Nettersheim	Urft-Nettersheim	Combined sewer
Stadtwald	Zülpich	Bessenich	Combined sewer
Keldenich	Kall	Kall	Combined sewer
Hüttenstraße	Kall	Kall	Combined sewer
Heideweg/F6	Nettersheim	Marmagen	Separate sewer
T 3 Tondorf	Nettersheim	Urft-Nettersheim	Separate sewer
Wahlen Nord	Kall	Marmagen	Combined sewer
Harzheim	Mechernich	Mechernich	Combined sewer
Niederheid Ge-Gebiet	Geilenkirchen	Flahstrass	Combined sewer
Fürthenrode	Geilenkirchen	Flahstrass	Combined sewer
Tripsrath	Geilenkirchen	Flahstrass	Combined sewer
Hatterath	Geilenkirchen	Flahstrass	Combined sewer
Boscheln	Übach-Palenberg	Frelenberg	Combined sewer
Heidberg	Übach-Palenberg	Frelenberg	Combined sewer
Regenstapelbecken KA Dremmen	Heinsberg	Dremmen	Combined sewer
Gewerbegebiet Bocket	Waldfeucht	Waldfeucht Haaren	Separate sewer
Winkelhalde	Hückelhoven	Hückelhoven-Ratheim	Separate sewer
Wassenberg RRB Alt Holland (geplant)	Wassenberg	Wassenberg	Combined sewer

8 Appendix 7: Hydrological assessment on upper Geul basin: combined data-and model-based analysis (KU Leuven)

Authors: Ir. S.Moustakas and Prof.dr.ir. Patrick Willems

Rapid assessment
of the July 2021 flood
for the Geul basin

Ir. Sotirios Moustakas

Prof. dr. ir. Patrick Willems

October 2022

Contents

1   Introduction

This report is an annex report to the study "Rapid assessment study on the Geul river basin: floods and adverse consequences" by Deltares and partners. That study assessed the hydrological response of the basin to heavy rainfall, the associated floodings and their consequences in order to find measures that are potentially suitable for the prevention of future floods impacts. It is an extension of the three recently published reports from Klein, Natuurmonumenten and Deltares about this flood event in the Geul basin. That knowledge base is extended with an assessment based on a set of computer flood simulations, covering the entire basin of the Geul river. KU Leuven contributed to that study with catchment runoff modelling, data-based analysis of the runoff coefficients and their dependence on the soil saturation level, and statistical analysis of the river peak flows, in order to gain further insights in the catchment runoff conditions and processes during extreme flood events as the July 2021 flood.

The KU Leuven analysis described in this report focuses on the river flows recorded at the gauging stations of Kelmis, Sippenaeken and Meerssen (Figure 1). An effort was made to gain some insights on the behavior of their upstream areas (considered here to be about 75, 119 and 339 km^2, respectively). The discharge data were analyzed with respect to their different subflow components and the high flow values. All the data used for this task (river flows, rainfall and reference evapotranspiration) were provided to us by Deltares. In the following sections, the results are presented and discussed.
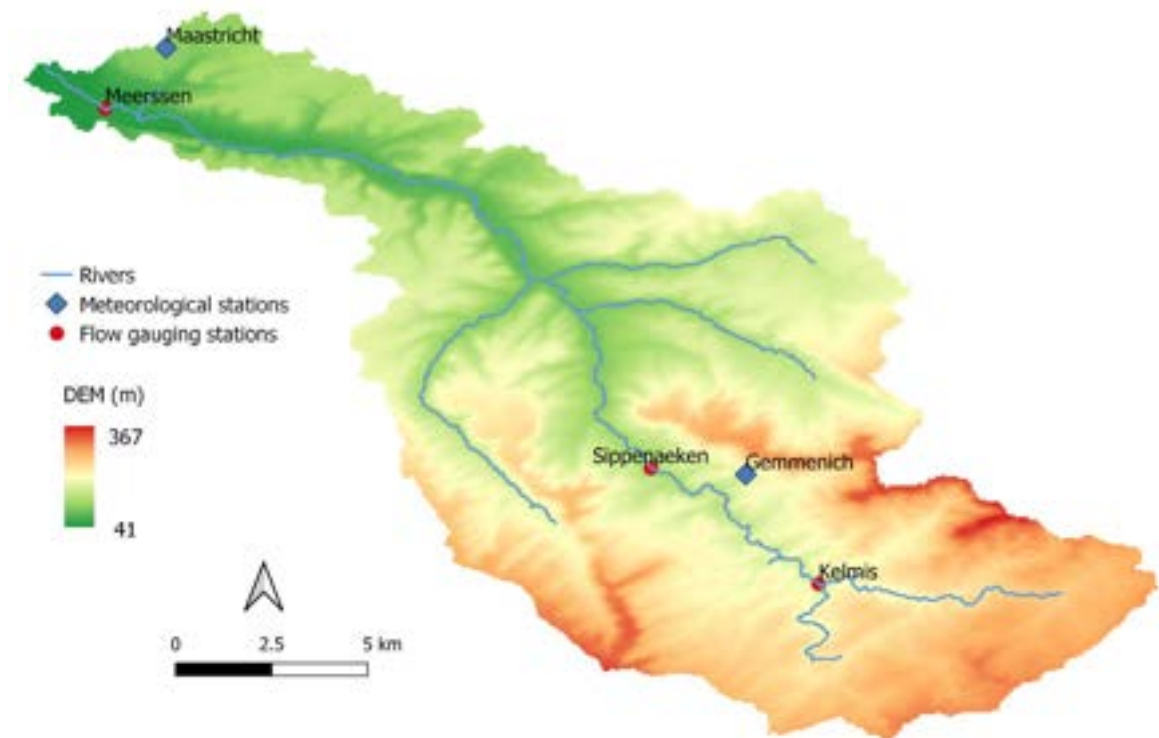

Figure 1. Study area.

2 Data-based approach

2.1 Separation of subflows

The observed discharge time-series were analyzed using the WETSPRO tool developed by Willems (2009). The tool has been used by several researchers (especially in Belgium) in data-based approaches for the investigation of river flows, while also for calibrating/evaluating the performance of hydrological models (e.g. Van Gaelen et al., 2017; Van Steenbergen and Willems, 2012; Vansteenkiste et al., 2014). Initially, the flows are separated in three subflow components: the quick flows (overland flow and interflow) and baseflow. This process is based on a generalization of the digital filter proposed by Chapman (1991). Assuming exponential recessions for each subflow, the methodology aims on the visual identification of the recession constant parameter and the fraction of each subflow. An example of subflows' separation for Kelmis can be seen in Figure 2. Subsequently, "nearly-independent" extreme high/low flow periods are identified via a number of criteria such as the length of the period between two extreme events.
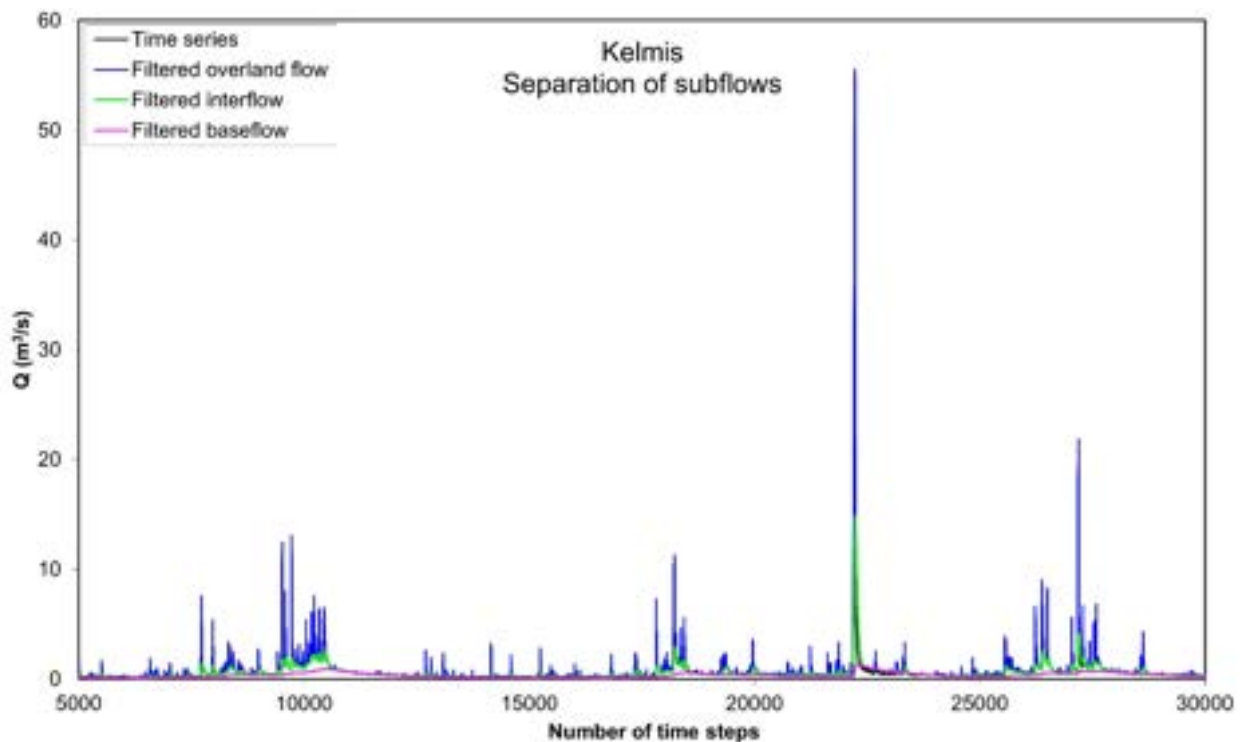

Figure 2. Example of sub-flow separation for Kelmis (January 2019 – April 2021) using WETSPRO.

Based on the subflows' separation, the quick flows (overland flow and interflow) for Kelmis, Sippenaeken and Meerssen were found to be about 55, 50 and 40% of the total flows, respectively. The larger fraction of quick flows in the upstream part of the catchment (draining to Kelmis and Sippenaeken) may be an indication that it reacts faster to rainfall in comparison to the downstream part.

2.2 Peak flows vs return periods

In Figures 3 and 4, the recorded peak flows are shown against their return periods (in a logarithmic x-axis) based on the discharge datasets for Kelmis and Sippenaeken. This was not done for Meerssen due to missing data, frequently during high flow periods (such as the event of July 2021). The period analyzed for Kelmis is 1 January 2009 to 12 July December 2022 (about 13.6 years), while the analysis period for Sippenaeken is 13 June 1996 to 31 December 2021 (about 25.7 years). The highest recorded flows for both stations correspond to the event of July 2021, which already suggests its severity.

In general, during high flow periods, the recorded river discharges might underestimate the runoff generated from their upstream areas due to flooding. This could allow (to an extent) to identify possible discharge values above which some flooding may occur via the recorded high flows. From the plot of Kelmis, we can visually distinguish a "break point" in the recorded high flows. Depending, of course, also on the distribution of the meteorological conditions that gave rise to the high flow events, this break point (about 20 m^3/s) could maybe be interpreted as a flooding threshold, or else a discharge value above which some flooding might occur.
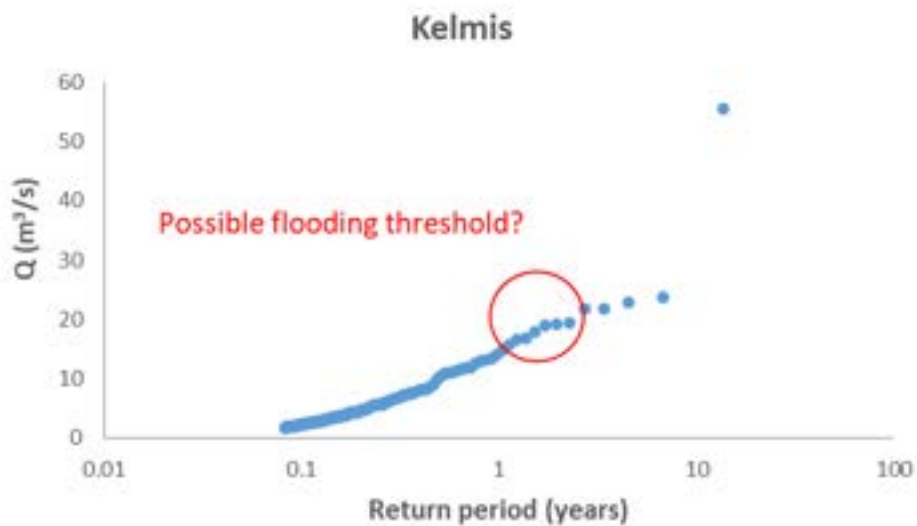

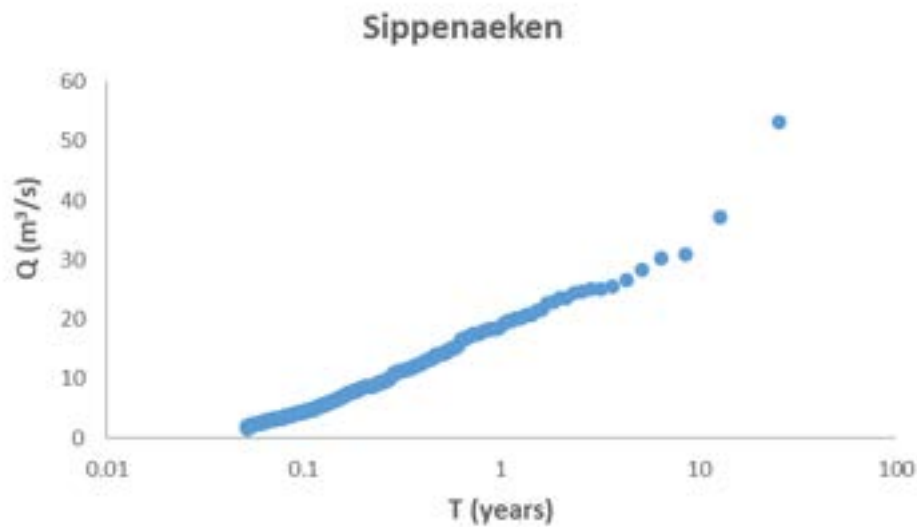**Figure 3.** "Nearly-independent" peak flows vs their return periods for Kelmis.

Figure 4. "Nearly-independent" peak flows vs their return periods for Sippenaeken.

2.3 Quick flow coefficients

The quick flow coefficient for each nearly-independent quick flow period identified with WETSPRO was here calculated as the ratio of the total quick flows (overland flow and interflow) to the total rainfall during the period. Those coefficients were plotted against a proxy for the mean relative soil moisture during each quick flow period. Due to lack of soil moisture data representative for the entire draining areas, the baseflow was used as its proxy as also described by Vansteenkiste et al. (2014). Essentially, this proxy was calculated as the ratio of the mean baseflow during the quick flow period with the largest baseflow value in the entire analysis period. This period was here 1 January 2015 to 1 October 2021.

Regarding rainfall, radar and reanalysis data were used from 1 January 2019 onwards. Before 2019 (when those were not available to us), data from the rain gauges were employed. For Kelmis and Sippenaeken, rainfall data from the Gemmenich station were used. For Meerssen, a weighted average rainfall series from the stations of Gemmenich and Maastricht were used. Based on the Thiessen polygons methodology, the weights of the two stations were roughly found to be 0.8 and 0.2, respectively. Those are summarized in Table 1.

Table 1. Meteorological stations' data used for rainfall data before 1 January 2019. From 1 January 2019 onwards, radar and reanalysis data were used for all stations.

Station	Rainfall data
Kelmis	Gemmenich
Sippenaeken	Gemmenich
Meerssen	0.8 * Gemmenich + 0.2 * Maastricht

In Figure 3, the plot of the quick flow coefficients against the relative soil moisture as reconstructed from the observations can be seen together for Kelmis, Sippenaeken and Meerssen datasets. Quick flow periods with less than 10 mm of total rainfall were not included in the plot to mitigate the appearance of very high coefficients due to imperfections in the temporal alignment of the rainfall and discharge data. It can be seen that Sippenaeken and Kelmis generally present larger quick flow coefficients than Meerssen. It should be noted that, since the subflows' separation methodology of WETSPRO is graphical, it inevitably includes a certain degree of subjectivity. Moreover, the discharge dataset of Meerssen includes several missing values, which might have affected the analysis.
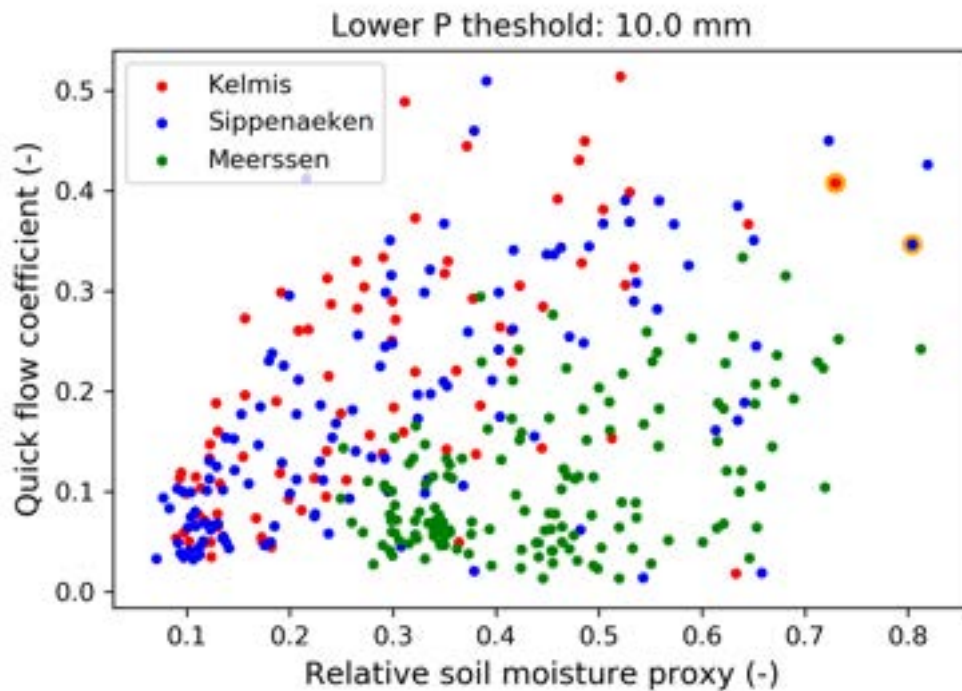

Figure 5. Quick flow coefficients vs the relative soil moisture proxy reconstructed from the observations. With orange, the main quick flow period of July 2021 is highlighted. It is not shown for Meerssen due to missing data.

3   Model-based approach

3.1   Setup of NAM models

The hydrological NAM model (DHI, 2004) was used to simulate the river flows at the Kelmis, Sippenaeken and Meerssen stations. NAM is a lumped conceptual model whose basic version comprises of nine parameters. The models were set up for the period of 1 January 2013 to 1 October 2021. Regarding rainfall, the methodology described in the previous section was followed here as well. In other words, radar and reanalysis data were used from 1 January 2019 onwards, while data from the rain gauges were used before (Table 2). Regarding the potential evapotranspiration, data from the Maastricht meteorological station were used for all models.

The simulation period was separated into a warm-up period (2013 and 2014) and the main simulation period from 2015 onwards. The models were calibrated via a combination of manual

and automatic methods for the second half of the main modelling period. Attention was given during calibration to the recorded extreme high flows. The effects of flooding on those recorded flows were not assessed. In reality, during high flow periods, the recorded river discharges might underestimate the runoff generated from their upstream areas due to flooding. Such flooding effects are not considered by the aforementioned calibration strategy.

The metrics used for evaluating the model performance are the Nash-Sutcliffe efficiency (NSE) (Nash and Sutcliffe, 1970), the Kling-Gupta efficiency (KGE) (Gupta et al., 2009) and the percent bias (PBIAS):

$$NSE = 1 - \frac{\sum_{t=1}^{t=N}\left(Q_m(t) - Q_o(t)\right)^2}{\sum_{t=1}^{t=N}(Q_o(t) - \overline{Q_o})^2}$$

$$KGE = 1 - \sqrt{(r-1)^2 + \left(\frac{\sigma_{model}}{\sigma_{obs}} - 1\right)^2 + \left(\frac{\overline{Q_m}}{\overline{Q_o}} - 1\right)^2}$$

$$PBIAS = 100 \times \frac{\sum_{t=1}^{t=N}\left(Q_m(t) - Q_o(t)\right)}{\sum_{t=1}^{t=N} Q_o(t)}$$

where: $Q_m(t)$ is the modelled flow at timestep t, $Q_o(t)$ is the observed flow at timestep t, $\overline{Q_o}$ is the mean observed flow, r is the Pearson correlation coefficient between the observed and modelled flows and σ is the standard deviation.

The values of the metrics for the simulation period are shown in Table 2. The worst performance is noted for Meerssen, while the best for Sippenaeken. In Figure 6, the observed and modelled hydrographs can be seen, while in Figure 7 the extreme high flows are shown. Note that the latter are not presented for Meerssen due to missing values in the observed flows (amongst others, also for the extreme event of July 2021). The return periods of those plots refer, of course, to the analysis period of 1 January 2015 to 1 October 2021 (and not the entire available dataset, as the ones in Figures 3 and 4). It can be seen that the modelled high flows follow the recorded ones closely. Nevertheless, as explained before, the recorded flows might actually underestimate the generated runoff if flooding occurred.

Table 2. NAM model performance metrics (1 January 2015 to 1 October 2021).

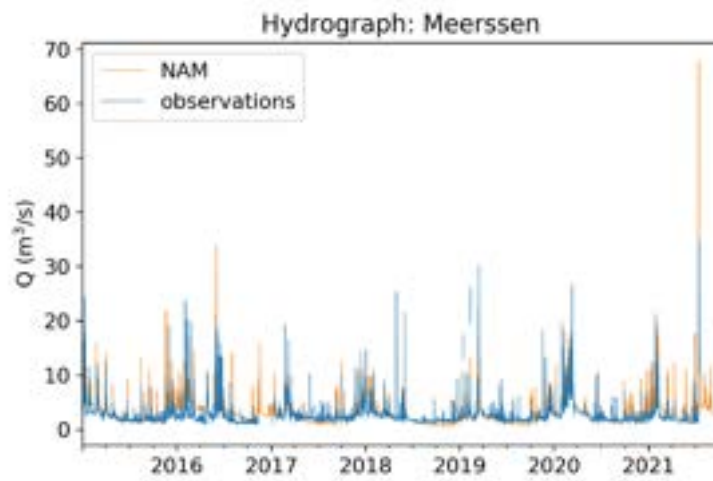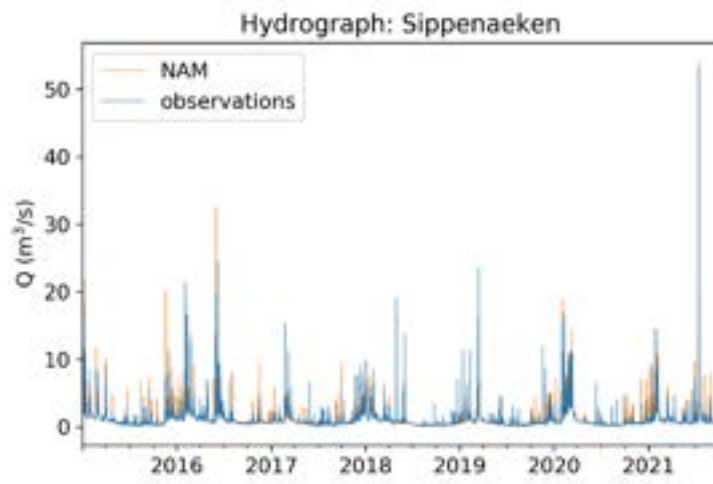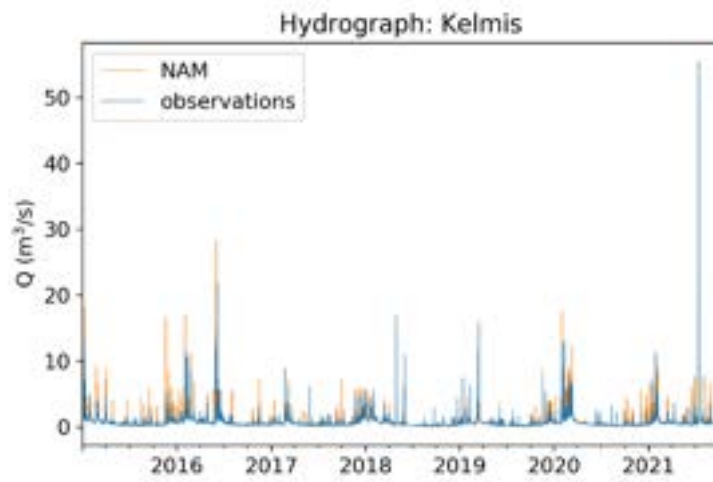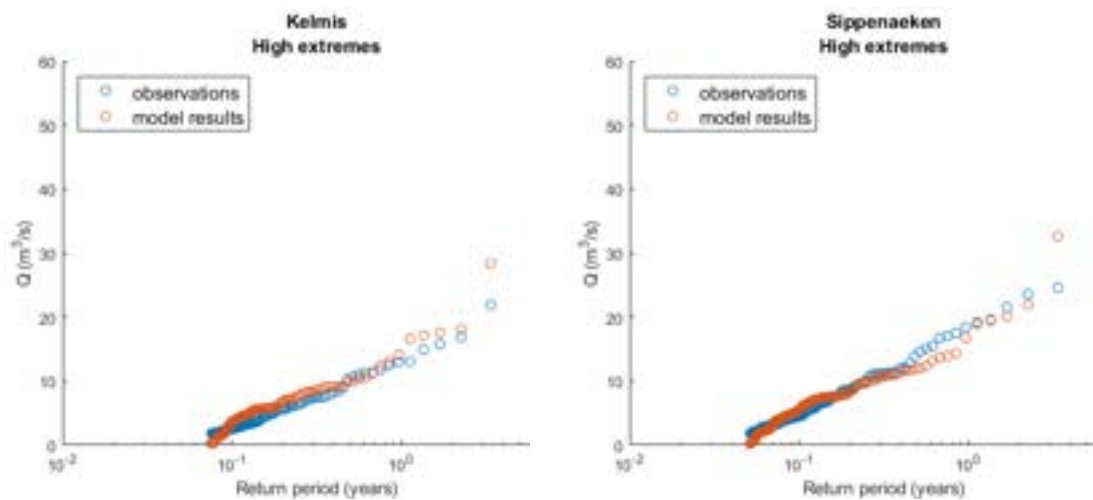| Station	KGE	NSE	PBIAS (%)
Kelmis	0.73	0.63	20
Sippenaeken	0.83	0.75	12
Meerssen	0.59	0.40	20

Figure 6. Observed and modelled hydrographs.

Figure 7. Observed and modelled high flows for Kelmis and Sippenaeken (1 January 2015 to 1 October 2021).

3.2 Comparison of NAM and wflow_sbm models

In this section, a comparison of the model results from the NAM and wflow_sbm models is carried out. The results of the wflow_sbm model from 1 January 2019 to 31 December 2021 were made available to us by Deltares. The comparison is, thus, based on the period from 1 January 2019 to 1 October 2021, which is common between the models. Furthermore, this period is covered by the radar and reanalysis rainfall data.

In Table 3, the performance metrics can be seen. The wflow_sbm model presents larger NSE value than the NAM model for Kelmis, while the opposite happens for Sippenaeken and Meerssen. Both models note their lowest NSE values for Meerssen. Moreover, both models overestimate the total flow volumes at the three stations for the aforementioned period. Those overestimations range between 16 and 47%. While those overestimation might partially stem from the calibration methodologies, further investigation may be needed to fully explain them.

Table 3. Performance metrics for NAM and wflow_sbm models (January 2019 to October 2021).

Station	KGE		NSE		PBIAS (%)	
	NAM	wflow_sbm	NAM	wflow_sbm	NAM	wflow_sbm
Kelmis	0.7	0.77	0.72	0.81	21	20
Sippenaeken	0.79	0.63	0.79	0.72	16	28
Meerssen	0.64	-0.18	0.44	-1.22	19	47

In Figure 8, the observed and modelled hydrographs are presented, while in Figure 9 the observed and modelled high flows for Kelmis and Sippenaeken are plotted against their return periods (in reference to the analysis period length). The NAM model results generally seem to be in line with the recorded high flow values for both stations. This can be explained by the calibration methodology for the NAM models, as attention was given to those recorded flows. For wflow_sbm, overestimations can be noted with respect to the largest return period for each station, which correspond to event of July 2021. For Sippenaeken, the wflow_sbm model seems to overestimates many of the flows larger than 10 m^3/s. The above do not mean that the NAM model is more accurate. As already mentioned before, the recorded river discharges might underestimate the runoff generated from their upstream areas when flooding occurs. Coupling with a river model capable to handle flooding could be an answer to such ambiguities.
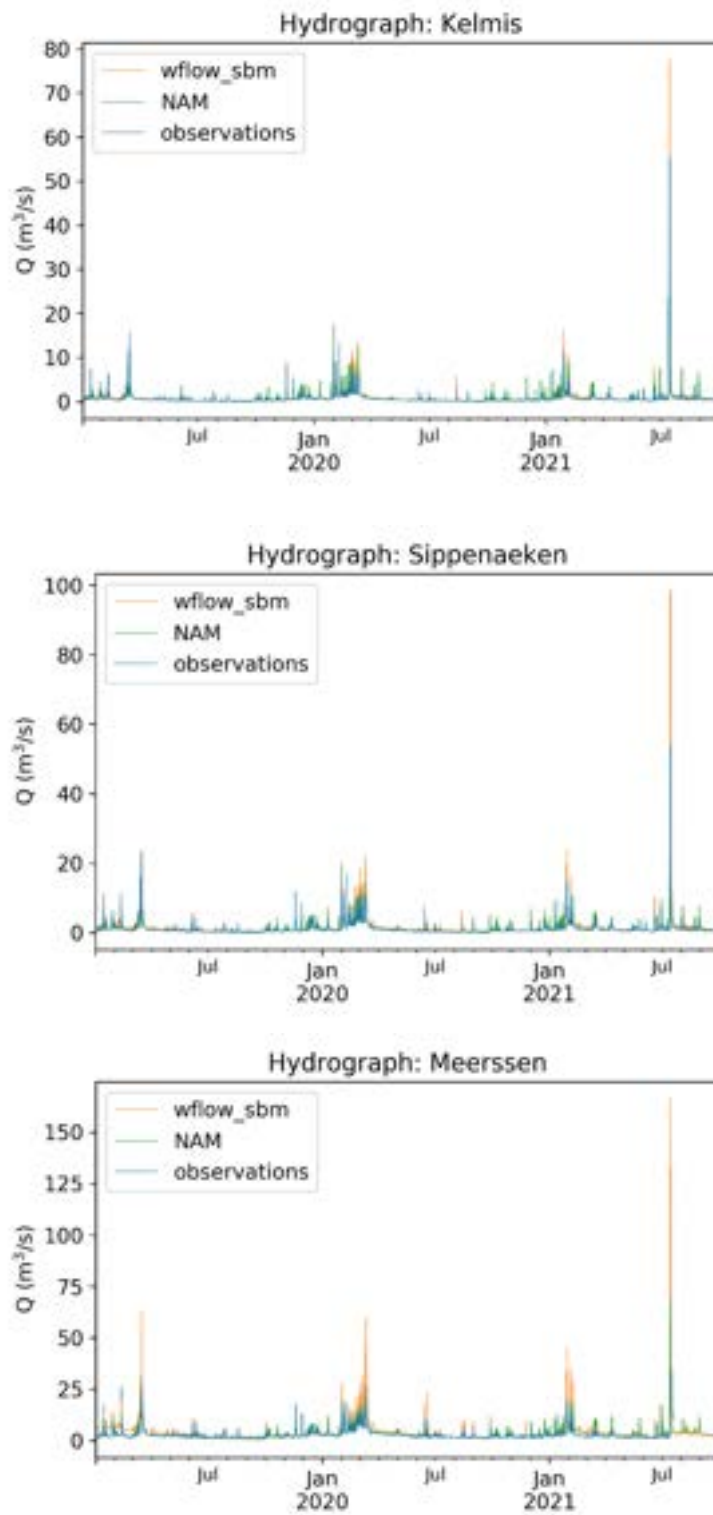
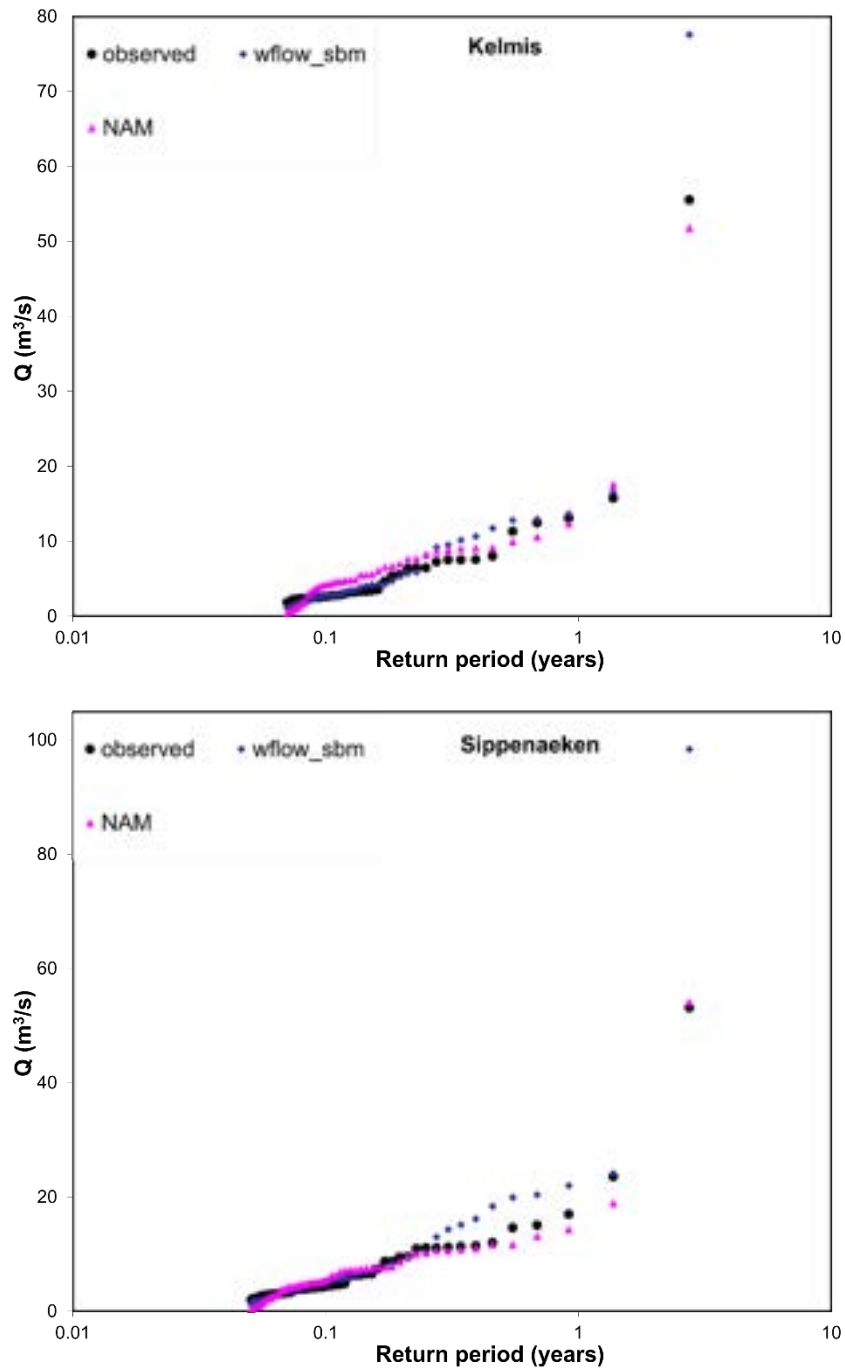**Figure 8.** Observed and modelled hydrographs from January 2019 to October 2021.

Figure 9. Observed and modelled high flows for Kelmis and Sippenaeken from January 2019 to October 2021.

The quick flow coefficients for two models were retrieved and compared to the ones reconstructed from the observations (Figure 10). The quick flow coefficients were retrieved from the models the same way as it was done for the observations. Essentially, for each quick flow period identified from the recorded time-series with WETSPRO, the coefficient was calculated as the ratio of the total modelled quick flows to the total rainfall. At the same time, the mean modelled baseflow value during each quick flow period was divided with the maximum baseflow value for the entire period (January 2019 to October 2021) and was used as a proxy for the soil saturation. Since the

results of the wflow_sbm model were provided to us as total flows, the baseflow in this case was estimated by filtering with WETSPRO. The quick flows were than calculated as the total flow minus baseflow. For the NAM models, the different subflows were directly retrieved as model results.

The models generally follow similar trends with each other and the observations. However, differences can be observed with respect to the event of July 2021. For this, it can be seen that the coefficients by wflow_sbm are closer to the observed ones (for both Kelmis and Sippenaeken). At the same time, the ones by NAM are lower than both the observed and the ones by wflow_sbm for this event. In other words, although the NAM models capture the highest recorded flow during the event of July better than the wflow_sbm model (Figure 9), the latter seems to better capture the corresponding total quick flow volumes.

To further investigate those, the observed and modelled hydrographs for the event of July 2021 are plotted (Figure 11). Apart from the NAM and wfow_sbm models, also the results from the hydraulic SOBEK model are shown. While the wflow_sbm model overestimates the recorded peak flows, those deviations are smaller for the SOBEK model. For Kelmis, the difference between the wflow_sbm and SOBEK models with respect to the peak flow is small, while it becomes more significant for Sippeanaekn and Meerssen. It can also be seen that the flow recession following the recorded peaks for Kelmis and Sippenaeken is not fully captured by the models as they generally present a more abrupt recession compared to the observations. The SOBEK model results seem to be somewhat closer to those recessions (especially for Sippenaeken). Given the severity of the events in July 2021, it could be hypothesized that the milder recession shown in the observed dataset is partially due to the delayed discharges from the water that escaped the rivers during the main rainfall events. As such, the wflow_sbm quick flow coefficients were closer to the observed ones compared to NAM (Figure 10) because wflow_sbm "compensated" for those flow volumes via the overestimated recorded peak flow. The above seem to support the theory that the overestimations presented by wflow_sbm with respect to the most extreme discharges could be partially explained by flooding (rather than a pure overestimation of the generated runoff during those events).
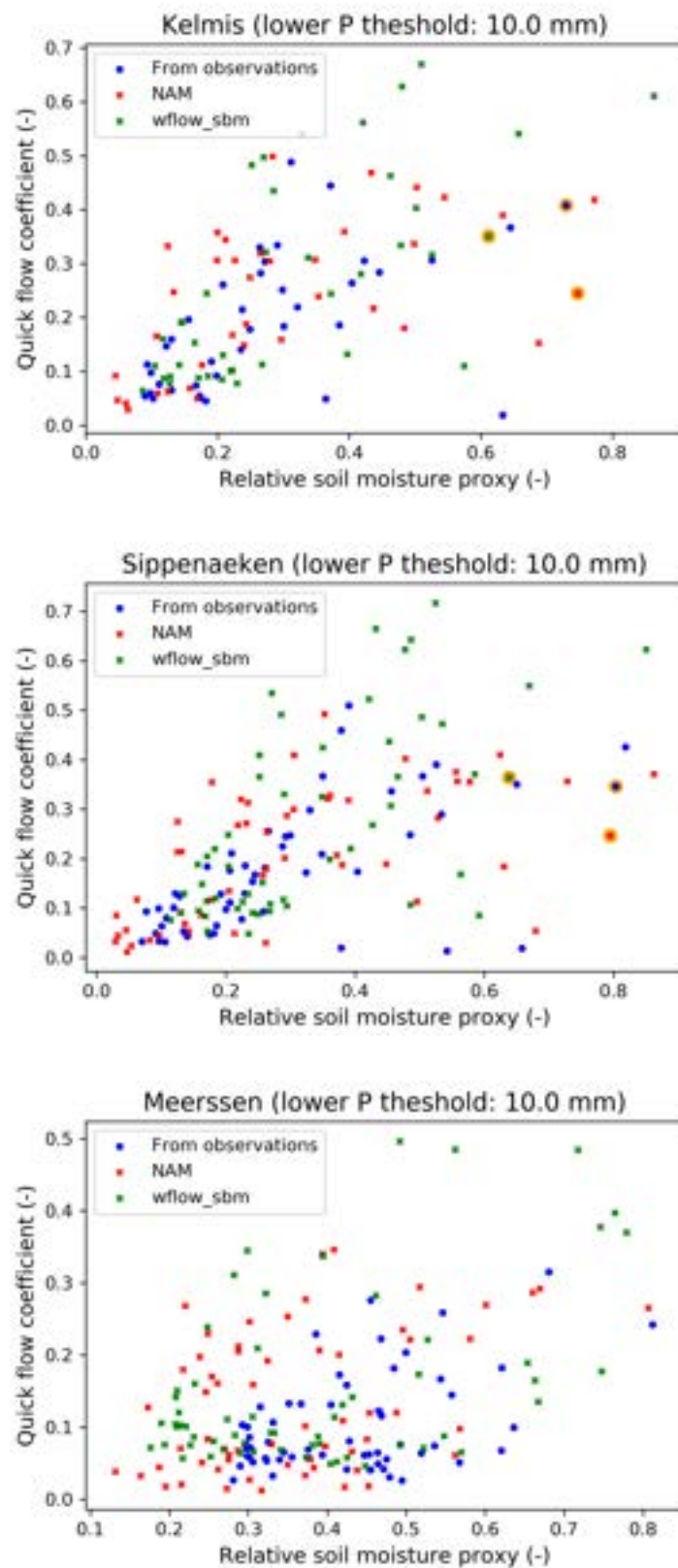
Figure 10. Modelled and "observed" quick flow coefficients. With orange, the main quick flow period of July 2021 is highlighted. It is not shown for Meerssen due to missing data.
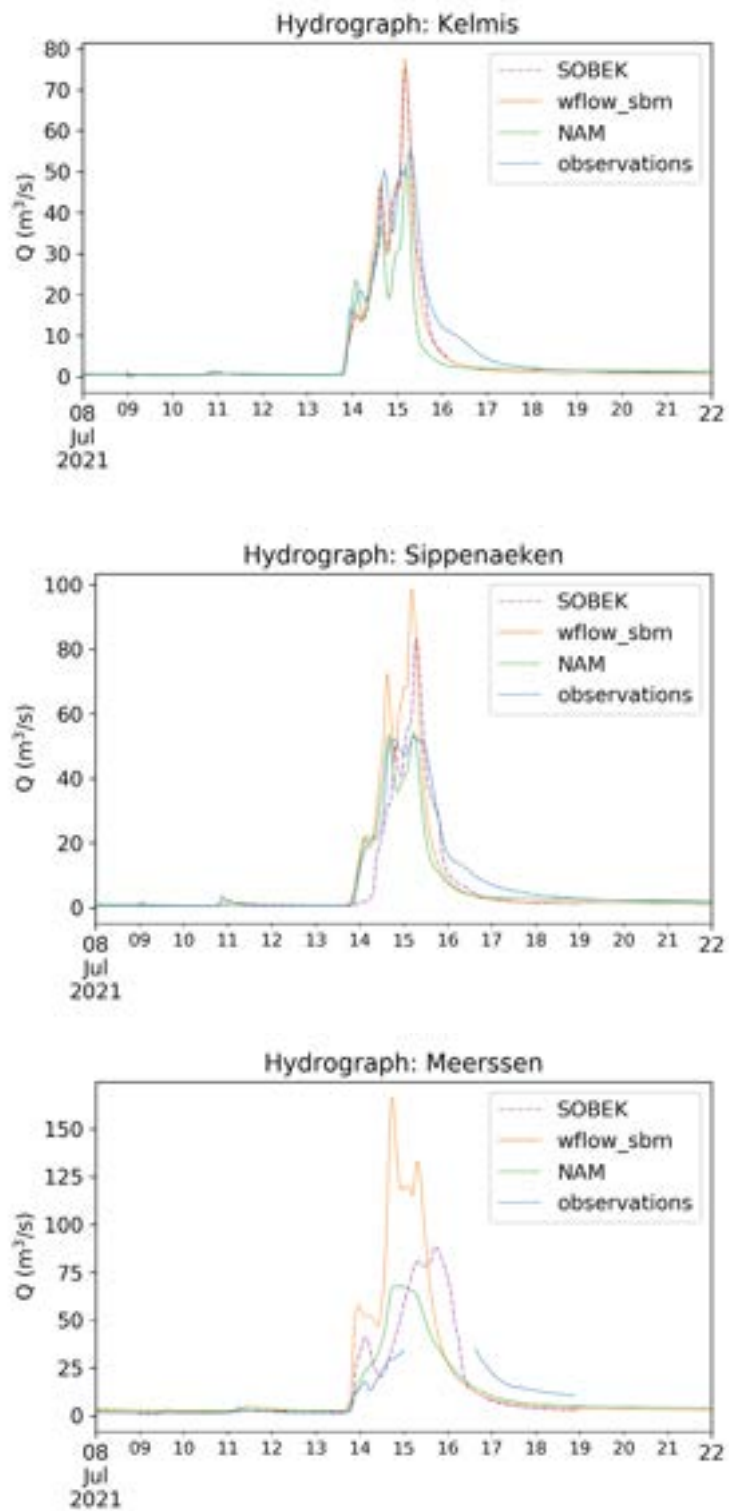
Figure 11. Observed and modelled hydrographs for the event of July 2021.

4 Conclusions and remarks

The main findings of our combined data- and model-based analysis are as follows; also some remarks are formulated:

- A data-based and a model-based approach were used to support the analysis of Deltares with respect to the investigation of the hydrological behavior of the Geul basin.

- The data-based approach indicates higher ratios of quick flows to the total flows while also higher quick flow coefficients at Kelmis and Sippenaeken compared to Meerssen. The runoff coefficients for the quick runoff are between 35% and 40% for the upstream stations Kelmis and Sippenaeken, which appear to be the typical runoff coefficients for the upstream part of the Geul basin when the soil is highly saturated as was the case during the July 2021 flood. For the more downstream station at Meerssen, the runoff coefficient is lower, around 20% for similar soil saturation conditions.

- Regarding the models, both NAM and wflow_sbm present acceptable NSE values for the flows at Kelmis and Sippenaeken, while both models note their worst performance at Meerssen. With respect to July 2021, the NAM models at Kelmis and Sippenaeken comply better with the recorded peak flows, while the wflow_sbm model complies better with the quick flow coefficients. In combination with the observed and modelled hydrographs for this event, it might be the case that the overestimations with respect to the recorded high flows noted by the wflow_sbm model are partially explained by flooding.

References

Chapman, T.G., 1991. Comment on "Evaluation of automated techniques for base flow and recession analyses" by RJ Nathan and TA McMahon. Water Resour. Res. 27, 1783–1784. https://doi.org/10.1029/91WR01007

DHI, 2004. MIKE 11, A Modelling System for Rivers and Channels, Reference Manual. DHI, Hørsholm, Denmark.

Gupta, H.V., Kling, H., Yilmaz, K.K., Martinez, G.F., 2009. Decomposition of the mean squared error and NSE performance criteria: Implications for improving hydrological modelling. J. Hydrol. 377, 80–91. https://doi.org/10.1016/j.jhydrol.2009.08.003

Nash, J.E., Sutcliffe, J.V., 1970. River flow forecasting through conceptual models part I—A discussion of principles. J. Hydrol. 10, 282–290. https://doi.org/10.1016/0022-1694%2870%2990255-6

Van Gaelen, H., Vanuytrecht, E., Willems, P., Diels, J., Raes, D., 2017. Bridging rigorous assessment of water availability from field to catchment scale with a parsimonious agro-hydrological model. Environ. Model. Softw. 94, 140–156. https://doi.org/10.1016/j.envsoft.2017.02.014

Van Steenbergen, N., Willems, P., 2012. Method for testing the accuracy of rainfall–runoff models in predicting peak flow changes due to rainfall changes, in a climate changing context. J. Hydrol. 414, 425–434. https://doi.org/10.1016/j.jhydrol.2011.11.017

Vansteenkiste, T., Tavakoli, M., Van Steenbergen, N., De Smedt, F., Batelaan, O., Pereira, F., Willems, P., 2014. Intercomparison of five lumped and distributed models for catchment runoff and extreme flow simulation. J. Hydrol. 511, 335–349. https://doi.org/10.1016/j.jhydrol.2014.01.050

Willems, P., 2009. A time series tool to support the multi-criteria performance evaluation of rainfall-runoff models. Environ. Model. Softw. 24, 311–321. https://doi.org/10.1016/j.envsoft.2008.09.005